
Analysis of stressed membrane structures

Implementation of non-linear material behaviour in structural analysis

Master's thesis
P.H. van Asselt
Student ID 1004212

Final project submitted in partial fulfilment for the Requirements for the Degree of Master of Science in Civil Engineering, Specialisation in Building Engineering, at the University of Technology Delft.

Graduation committee:
Prof. dipl. Ing. J.N.J.A. Vambersky
Ir. J.L.Coenders
Ir. P.A. de Vries
Dr.ir. P.C.J. Hoogenboom
Ir. R. Houtman (Tentech)

Delft University of Technology
Faculty of Civil Engineering and Geosciences
Structural Design Lab

November 2007

Acknowledgements

I would like to thank my graduation committee for the guidance and advices during this project. In addition I would like to thank R. van Leeuwen, C. van Beek and P. Vermeulen for their advice and assistance during the experimental stage of the research. The firm Verseidag (Germany) supplied the PTFE coated fibreglass used in this research. Mr. E. Moncrieff (Kurvenbau, Tess3D) contributed with his advices and interesting conversations about membrane engineering.

The fellow students who are involved in the Structural Design Lab made this graduation period a memorable experience.

Delft, November 2007

Cover: Image of hyperclastic shape, often used in membrane structures.
(source: <http://www.birdair.com/birdair/tech/design/images/graph1.gif>)

Summary

A growing use of tensioned membrane structures requires insight and understanding of the mechanical behaviour of the structure and the membrane material. In current practise the complex material behaviour is simplified due to the uncertainties that exist around the material behaviour. Testing and modelling the membrane material may provide a more accurate tool for structural analysis.

Research has been performed on PTFE coated fibreglass, a widely used architectural textile. Non-linear material properties have been identified as well as other material characteristics. Different aspects of bi-axial fabric testing have been researched. A bi-axial test protocol must provide accurate measurements that will provide insight in the non-linear stress-strain relation of PTFE coated fibreglass.

Various bi-axial tests have been performed in the Stevin Lab at the Faculty of Civil Engineering, Delft University of Technology. Accurate displacements measuring devices have been designed and created to record the strains of the fabric. These tests supplied insight in the non linear material properties. Bi axial tests at preset stress ratios have been performed on six identical cruciform test samples of PTFE coated fiber glass (Verseidag B18089).

Various approaches have been made to model the fabric's stress-strain behaviour. Modelling the stress strain relation by creating a best fit surface through the experimental data did not result in a useable model. A different approach where the nonlinear stress strain relation is linearized and where Hook's law was applied did not result in an accurate model. The best results were obtained by a non linear model based on the fibres' geometry. This model showed good resemblance with the experimental data. The model is calibrated by three parameters, fibre diameter, fibre spacing and Young Modulus of the fibres.

The material model is programmed in FORTRAN language and is linked to the general purpose finite element software Ansys. Several test cases have been analysed, based on the material model. It appears that non linear geometric behaviour combined with non linear material behaviour demands an accurate description of the Jacobian matrix for convergence purposes.

The performance of the model is not yet at the level of industrial application. Calculation times exceed the reasonable for desktop application. Various recommendations have been made in order to improve the model's performance. However, this research is a contribution to the second generation of stressed membrane analysis software. Additional tests on other fabric qualities may contribute to the applicability of the model. These tests must turn out whether the model can easily be adapted to other fabric qualities.

Table of contents

Analysis of stressed membrane structures	i
Acknowledgements	ii
Summary	iii
Table of contents	iv
1. Introduction	1
2. Problem definition	2
2.1 Problem description	2
2.2 Problem statement.....	2
2.3 Goal of the thesis	2
3. Material properties PTFE coated fibre glass	4
3.1 What is PTFE coated fibre glass.....	4
3.2 Structures of PTFE coated fibre glass	4
3.3 Production process	6
3.4 Mechanical properties.....	7
3.4.1 Non-linear properties.....	8
3.4.2 Anisotropy.....	8
3.4.3 Non-elasticity	9
3.4.4 Temperature dependency.....	10
3.4.5 Crimp interchange behaviour	10
3.4.6 Repetitive load cycles	12
3.4.7 Load history	12
3.5 Alternative for PTFE coated fibre glass	12
4. Current analysis methods for membrane structures	13
4.1 Geometric non-linearity	13
4.1.1 General geometric non-linearity	13
4.1.2 Dynamic Relaxation method	14
4.1.3 Force Density method.....	15
4.1.4 Transient stiffness method	17
4.1.5 Remarks on geometric non-linear calculation methods	18
4.2 Material representation for structural analysis	19
4.2.1 Model with two Young's moduli and one Poisson factor	19
4.2.2 Model with interaction moduli	19
4.2.3 Model with multi-step linearization	20
5. Bi-axial testing procedure	22
5.1 Other researchers.....	22
5.2 Various aspects of testing	22
5.2.1 Uni-axial and bi-axial testing	22
5.2.2 Types of bi-axial testing.....	23
5.2.3 Initial behaviour and <i>in-situ</i> behaviour.....	24
5.2.4 Applying different force ratios.....	26
5.2.5 Residual strain.....	27
5.3 Testing device.....	27
5.3.1 The bi-axial rig and its components	27
5.3.2 Preparing cruciform test specimen.....	28
5.3.3 Clamping the sample	29
5.3.4 Data output.....	31
5.4 Test procedure	31
5.4.1 Procedure	31
6. Testing validation	34
6.1 Sample analysis.....	34
6.1.1 Sample shape.....	34
6.1.2 Analysis of stress distribution	35
6.1.3 Material representation.....	36

6.1.4	Slits in the cruciform sample	36
6.1.5	Results of sample analysis	37
6.1.6	Sample configuration for the experiments	39
6.2	Potentiometers	40
6.2.1	Setting	40
6.2.2	Reproduction of identical tests	43
6.2.3	Repositioning of the potentiometers	45
7.	Test results	48
7.1	Conditioning of the sample	48
7.2	Test results of biaxial testing	50
7.3	Material representation.....	56
8.	Material model	58
8.1	What to represent in the model ?.....	58
8.2	Stress-stress-strain relation.....	59
8.3	Strain-strain-stress relation	62
8.3.1	Plane stress, isotropic	65
8.3.2	Plane stress, Orthotropic	69
8.3.3	Non-linear model including fibre interaction	70
9.	Ansys User Programmable Feature (UPF).....	74
9.1	Theory of the UPF 'usermat'	74
9.2	Setting up a UPF in Ansys	74
9.3	UPF Usermat for PTFE coated fibre glass	75
10.	Subroutine testing	77
10.1	Single element, homogenous stress	77
10.2	Multiple elements, homogenous stress	78
10.3	Multiple elements, non-homogenous stress	79
10.4	Membrane action	80
11.	Conclusions and recommendations	83
11.1	Conclusions.....	83
11.2	Recommendations	83
11.3	Future developments.....	84
11.4	Opportunities	85
	Literature and references	86
	List of Figures	87
	List of tables	88

Appendices

1. Introduction

The design of tensile membrane structures differs from the authentic approach of structures. In the authentic approach the structural designer needs to design the structure according to the architect's creation. For tensile membrane structures, the form is the structure and the structure is the form. This is caused by the properties of tensile structures, where the fabric surface needs to be double-curved in order to provide stability to the structure. Different techniques exist for finding this specific form and analysing the mechanical behaviour of the membrane structures.

Physical form finding helps the architect and engineer to find a shape that fits the demands of the architect, but also complies with the basic form properties of a tensile membrane design. By the use of a soap-film or panty-hose, combined with a steel wire frame, the obtained shape can easily be changed or adapted to acquire the desired result. The advantage of these methods is that it is very cheap, and easy to work with. On the other hand, it is impossible to get detailed insight in the structural behaviour of the design.

With the development and growing interest in tensile membrane structures in the late 60's, also the need for more advanced methods for form-finding and structural analysis arose. Computational pioneers designed tools to assist the engineer in parts of the design process. Computational tools for form finding were invented, as well as structural analysis tools and pattern cutting tools. These individual tools were later on merged into complete software packages, which could handle the complete process from form finding till pattern cutting. Widely used examples of these packages are Easy (Technet), and the fabric module of GSA (Arup's in-house software). Tess3D (in development by Mr. E. Moncrieff) is a new generation of membrane design tools, which is an easy to use program with a visual orientated user interface.

These integrated packages assist the engineer in the design process. On an iteration based manner the designer can switch between form-finding and structural analysis until the results are satisfactory. After this stage the patterns for the fabric can be designed for the cutting process.

During the structural analysis the engineer gains insight in the structural behaviour of the tensile structure. Various loads, such as wind and snow loads, are applied to the structure in different combinations, to produce a number of load scenarios the structure needs to resist.

The structural behaviour, as a result of the applied loadings, is depending on the mechanical properties of the material used in the design. Those mechanical properties are material characteristics and are thus material dependent.

The level of accuracy of the description of the material properties determines the accuracy of the outcomes of the structural analysis. In current structural analyses some of the mechanical properties of the material are simplified, because the exact properties are unknown. This counts in particular for the relation between stress and strain in the membrane material. A linear relation is assumed in current analyses, but the relation between stress and strain is actually non-linear. Due to these uncertainties in material properties, but also due to some other causes, the structural analyses are conservative.

The goal of this thesis is to research the material properties of PTFE coated fiber glass, an often used architectural textile, and to make a model that incorporates the researched properties. With this model a more accurate structural analysis can be made, using a general purpose finite element program.

2. Problem definition

In this section the problem will be described and the goal of the thesis will be formulated.

2.1 Problem description

In the current structural analysis of tensile structures, uncertainties exist on structural behaviour (deflections under external loads) and behaviour of the fabric.

In current analysis software for tensile structures, the non-linear relation between stress and strain of the material has not yet been taken into account. A linear relation is assumed and structural analyses are based on this assumption.

By assuming this linear stress-strain relation, structural analyses are conservative and do not represent the material's actual response. The purpose of solving this problem is acquiring insight in the material behaviour and making a reliable material model on which a structural analysis can be based on. It will take away some, but not all, of the current uncertainties in the structural analysis of membrane structures.

Accuracy in structural analysis depends on different aspects, such as load definition and the accuracy of the material model used in the analysis. In current practice, a linear stress-strain relation is assumed resulting in a constant Young's modulus for the glass fibre fabric. This can not be considered as accurate modeling of the fabric behaviour, because the actual fabric behaviour is non-linear.

This thesis' research provides in the need to a more accurate material model for structural analysis of membrane structures. By the use of a more accurate material model, a more accurate structural analysis can be made based on the model.

The purpose of a more detailed material model does not lie in the prevention of overstress, and thus failure, of the structure. Membrane structures almost never fail due to overstress in the fabric. However, failure of membrane structures can also be found in the non functionality of the structure. Understress, wrinkling, ponding and large deflections are all matters of great concern in designing membrane structures. A more detailed material model is capable of indicating these effects during structural analysis.

2.2 Problem statement

In structural analysis of membrane structures the biaxial non-linear relation between stress and strain needs to be described, in order diminish the uncertainties in fabric behaviour.

2.3 Goal of the thesis

The goal of this thesis is to develop a model of the biaxial stress-strain relation of PTFE coated fibre glass, and to implement this model in the structural analysis of stressed membrane structures with a general purpose FE program.

A number of sub goals of this final thesis can be identified as well.

- ▶ Perform a literature study on PTFE coated fibre glass
- ▶ Perform a literature study on methods of structural analysis used in current computational tools
- ▶ Research a bi-axial test procedure for testing samples of PTFE fabric on a biaxial test bench
- ▶ Develop a model for biaxial stress-strain relation of PTFE coated fibre glass

-
- ▶ Implement the stress-strain model in a general purpose FE program, called ANSYS, and perform structural analysis on a number of simple test cases
 - ▶ Compare the results of the new developed non-linear analysis with the results of the experiments performed in the laboratory

3. Material properties PTFE coated fibre glass

In this section an overview is given of the material that is researched in this thesis. Understanding of the material properties and characteristics is needed for making a proper model.

3.1 What is PTFE coated fibre glass

PTFE coated fibre glass is a widely used architectural textile (or structural fabric). The material consists of two different components with each of them having its own characteristics. The two components are a woven fibre glass fabric and a coating of PTFE. PTFE is the industrial name for poly-tetra-fluore-ethylene, but is also called Teflon. The name 'Teflon coated fibre glass' is therefore also a common used name.

3.2 Structures of PTFE coated fibre glass

PTFE coated fibre glass has been used in tensioned fabric structures since the revival of these types of structures in the late 70's. Large span structures like airport terminals, stadium and stage coverings for concerts are examples of structures built with this type of fabric. To illustrate the wide applicability of the PTFE coated fibre glass, some remarkable examples will be presented here.

Haj Terminal Jedda

Horst Berger, a well-known engineer in the field of tensile architecture, designed the Haj Terminal at the Jedda International Airport in Saudi-Arabia in the late 70's. The Haj Terminal is one of the largest roof span structures in the world. The structure consists out of square units with a canopy shape. Twenty-one of these units form a module, measuring 3 units wide and 7 units long, with an area of 43.000 square meters. The total Haj Terminal consists out of 10 of these modules, with a total area of 430.000 square meters. The PTFE coated fiberglass reflects large parts of the heat in this desert-like area. Therefore no additional mechanical systems are needed in the terminal to provide a comfortable indoor climate.



Figure 1: Haj Terminal, Jedda (www.geigerengineers.com)

Millenium Dome, Greenwich UK

One of the most famous stadiums, using a lightweight tensile structure, is the Millenium Dome in Greenwich. This structure was built in 1997 and completed in 1999, in order to celebrate the start of a new millennium. Engineering was performed by Buro Happold while the design was by the work of Richard Rogers Partnership. This large 80.000 square meters roof made of PTFE coated fibre glass in a spherical shape is supported by twelve 100 meter long masts. Steel cables attached to the mast support the fabric.



Figure 2: Millennium Dome, Greenwich (www.burohappold.com)



Figure 3: Detail of roof Millennium Dome, (www.greatbuildings.com)

Burj al-Arab hotel, Dubai

This hotel, completed in 1999, is the tallest building with a PTFE coated fiber glass facade. The fiber glass façade allows a comfortable amount of daylight into the hotel, and keeps the heat out for a large part. During nighttimes, colored lights are projected on the fabric, resulting in a dynamic appearance of the structure. Tensys was responsible for the engineering of the fabric facade.



Figure 4 : Burj al-Arab hotel, Dubai(www.wikipedia.org)

3.3 Production process

The glass fibre fabric is a woven fabric, and consists of threads of glass. Weaving is a process where threads in two opposite directions are converted into a fabric. This weaving process is a repetition of a procedure that consists out of 5 steps (Sen, 2001).

- ▶ The process starts with *shedding* of the warp threads. The threads are kept in a harness and are divided in an upper layer and a lower layer. These harnesses can switch where the lower layer becomes the upper layer and vice versa. The configurations of these harnesses determine the type of weave. With configuration is meant the sequence of threads in the upper and lower layer. This can be one up one down, or one up two down, or one up three down. Also two up two down, three up three down are possibilities for the configuration, see Figure 5.
- ▶ After the shedding a thread (weft) is passed through the enclosure between the upper and lower layer of warp threads.
- ▶ The new weft thread is pushed against the already made fabric. This is called *beating up*. The force that is involved in the beating process determines partly the density of the fabric.
- ▶ After the beating process the new weft thread is enclosed by the warp threads due to the position change of the warp harnesses. The lower harness becomes the upper one, and the upper harness becomes the lower one.
- ▶ At this moment the procedure repeats itself. A new weft thread is inserted in the enclosure between the upper and lower layer of warp threads.

The weaving process is a moving process. The completed fabric is winded on a roll at a certain speed. This speed is also depending on the speed of which the new warp threads are fed to the weaving machine. These speeds are closely monitored in order to obtain a uniform quality in the entire fabric.

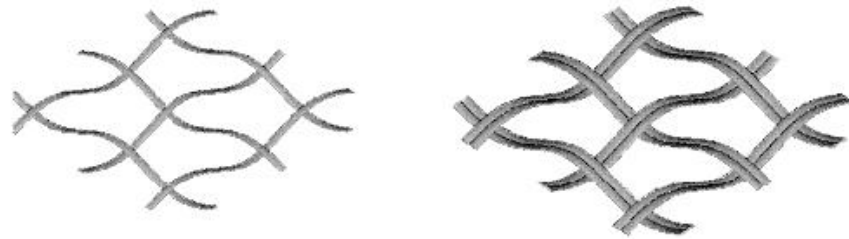


Figure 5: Two different configurations of a weave (Houtman,2000)

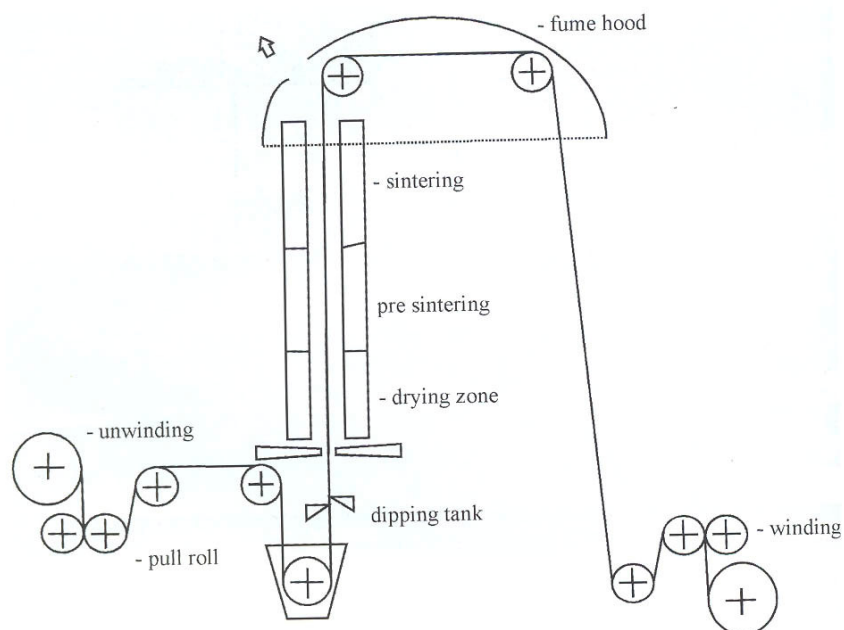


Figure 6: Application of PTFE onto the glass fibers (Mollaert,2002)

After the fabric has been woven, the material is coated with PTFE (Mollaert,2002). PTFE is applied on the glass fibre fabric by moving the fabric through a dipping tank, see Figure 6. To adhere the PTFE particles to each other and to the glass fibres, the fabric moves through a drying and sintering area. The coating adds a new set of characteristics to the fabric. The combination and interaction between these characteristics determine the characteristics of the coated fabric.

Due to the high temperatures of sintering, between 350 and 380°C, PTFE can only be applied to glass fibres which can resist these temperatures. Other synthetic fibres will melt or decompose at these temperatures.

3.4 Mechanical properties

The mechanical properties of PTFE coated fibre glass are different from the traditional used building materials like steel and concrete (Blum,1990). The coated woven fabric is non-linear, anisotropic and non-elastic. These characteristics will be discussed here separately.

3.4.1 Non-linear properties

Non-linear behaviour of the fabric refers to the relation between stress and strain of the fabric. Stress is the force acting on the fabric, measured per length unit for membrane materials. Strain is the amount of elongation of the fabric, due to the acting force (or stress), compared to the original length before stressing. On linear materials, the increase in stress in the material corresponds to a linear increase of the strain in the elastic range. That means that a doubling of the stress results in a doubling of the strain. When the stress strain relation is non-linear, a doubling of the stress will result in a less or more than doubling of the strain. This is shown in Figure 7.

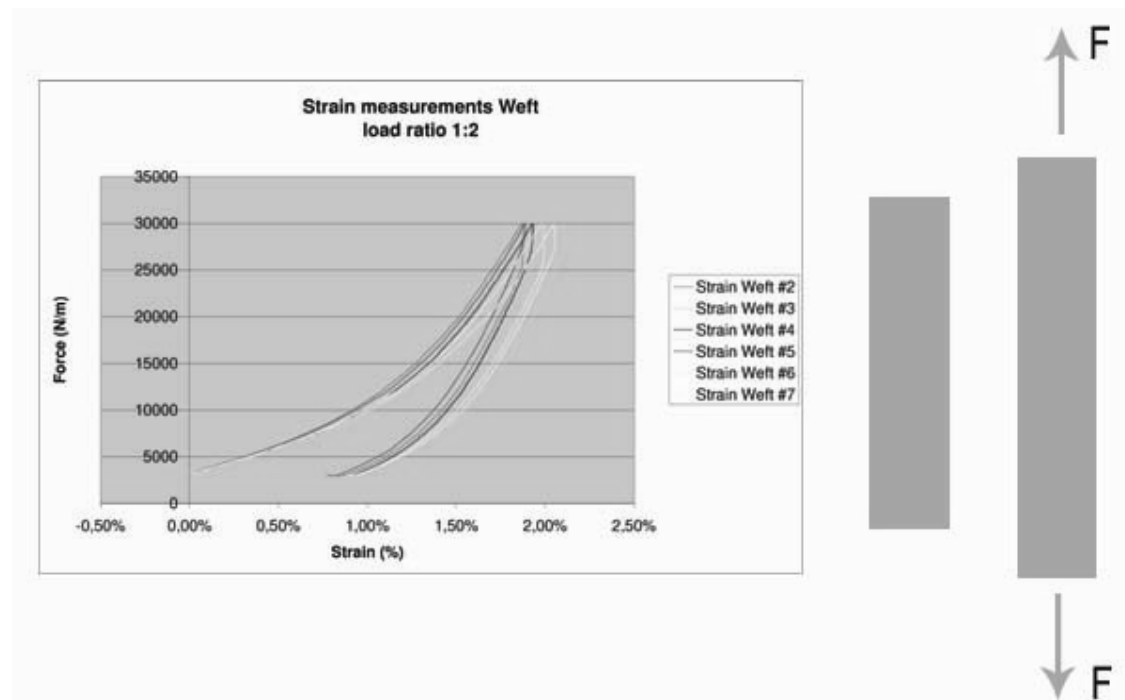


Figure 7: Fabric shows non-linear force-strain behaviour

3.4.2 Anisotropy

In Section 3.2 the production process of the fabric is described. As a result of the specific configuration of the fabric, the material is anisotropic. This means that material characteristics depend on the orientation of the fabric.

The warp-direction of the fabric is the direction in which the threads run straight. In the weaving process these threads are kept under a certain tension, and in the final product these threads remain straight. When the fabric is stressed in the warp direction, the warp threads are almost immediately stressed. The resulting strain behaviour is significantly different from the weft direction.

The weft threads are running in a wave pattern through the fabric, going under and over the warp threads. When the fabric is stressed in the weft direction, the threads first stretch out and lose the wave pattern. This goes together with an elongation of the fabric. After the situation is reached where the threads are straight, the threads are stressed by the acting force.

The described behaviour of the warp and weft threads is based on a uni-axial loading of the fabric. That means that the fabric is loaded in one direction only. When the fabric is loaded at two perpendicular directions, corresponding to the warp and weft direction of the fabric, interaction between the two directions occurs.

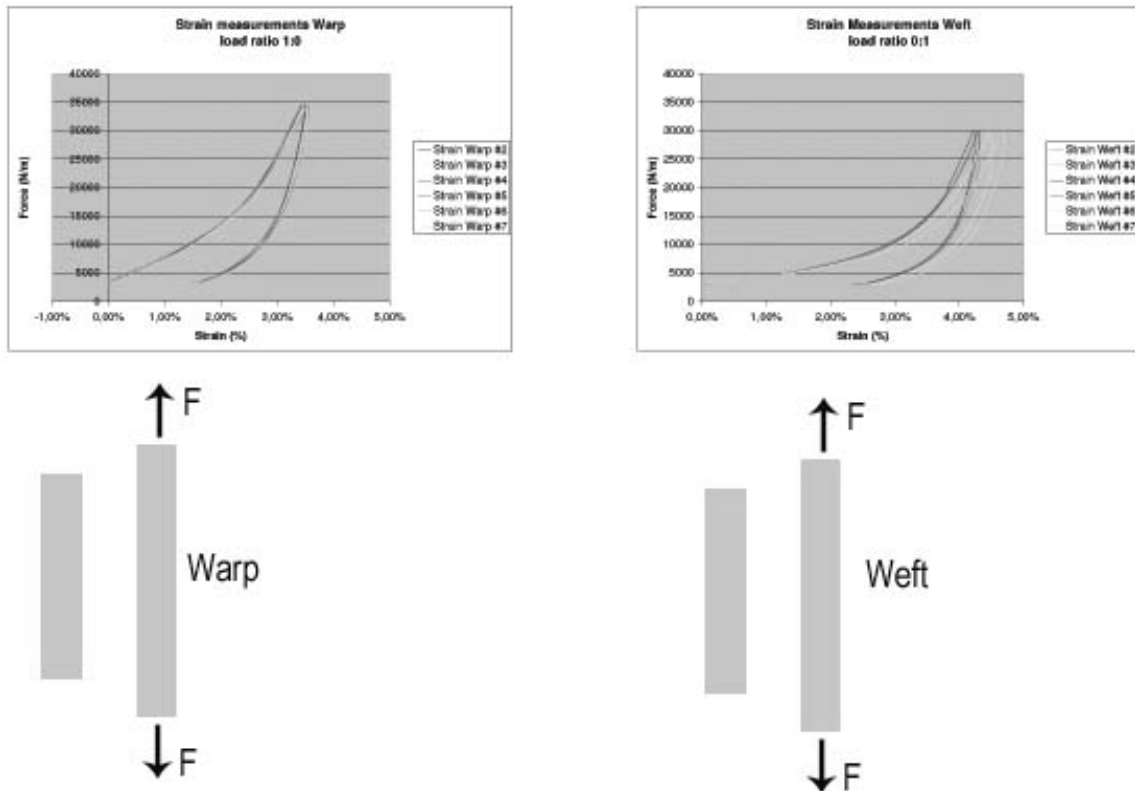


Figure 8: Fabric response is depending on the fiber orientation

3.4.3 Non-elasticity

When elastic materials are loaded and unloaded, the unload path coincides with the load path. That means that after the unloading no residual strain is present in the material.

Woven fabric is non-elastic. The unload path does not coincide with the load path. After a load cycle a permanent strain is present in the fabric. When the load cycles are repeated, the additional permanent strain becomes smaller. A certain maximum permanent strain in the fabric can be reached.

The non-elasticity is closely related to the hysteretic properties of fabric. Both symptoms act simultaneously, which makes it difficult to visualize the effect of both symptoms. The hysteresis is caused by the changing geometry of the glass fibre matrix, due to loading. This effect has been taken in account in the testing procedure.

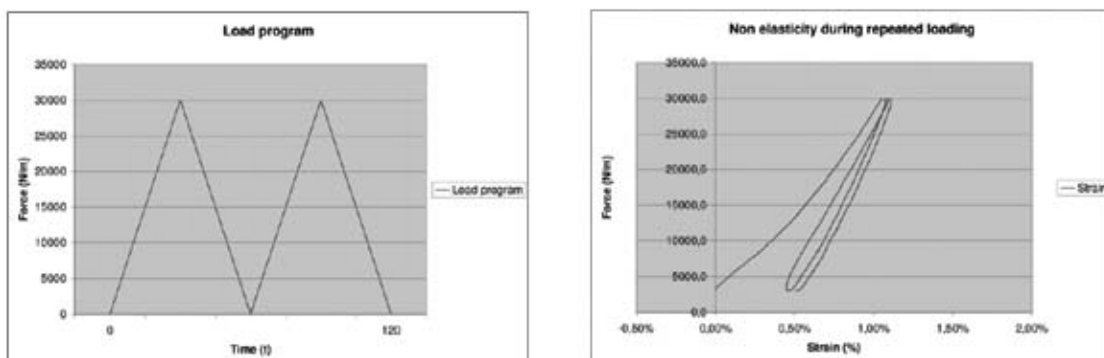


Figure 9: The fabric shows a non-elastic response under repeated loading

3.4.4 Temperature dependency

The coating on both sides of the fabric is a polymeric solution. The PTFE coating has a service range between -200°C and 260°C (Mollaert, 2002). Even at low temperatures the PTFE will keep its flexible properties.

Research performed by C.A.G. Nederpelt (Nederpelt, 2004) on silicone coated fibre glass showed a relation between material breaking strength and the temperature of the surrounding area on which the tension tests were performed. Although silicone coated fibre glass is not the same material as PTFE coated fibre glass, both materials contain a glass fibre woven fabric coated with a polymeric substrate coating. Therefore the temperature dependant behaviour is comparable. An increase in breaking strength was measured when performing the tension tests at 70 °C compared to tests performed at 23 °C. The stiffness of the material remained constant in both cases.

In Nederpelt's case it is shown that for an increasing temperature, the material behaviour becomes favourable with regard to the breaking strength properties. What not has been shown is the material behaviour at low temperatures.

Due to technical feasibility no tests will be performed at low temperatures. The focus of this thesis will be at tests performed at 22°C ($\pm 2^\circ\text{C}$).

3.4.5 Crimp interchange behaviour

Due to the configuration of threads created in the weaving process, the fabric shows an interchange between the crimp of the two main directions of the fabric (warp and weft direction). Crimp is the specific curved shape of the warp and weft threads.

To illustrate this phenomenon a cross section of a PTFE coated fibreglass fabric shows the crimp shape of a yarn, with a view on the cutting face of the perpendicular crossed yarns, see Figure 10.

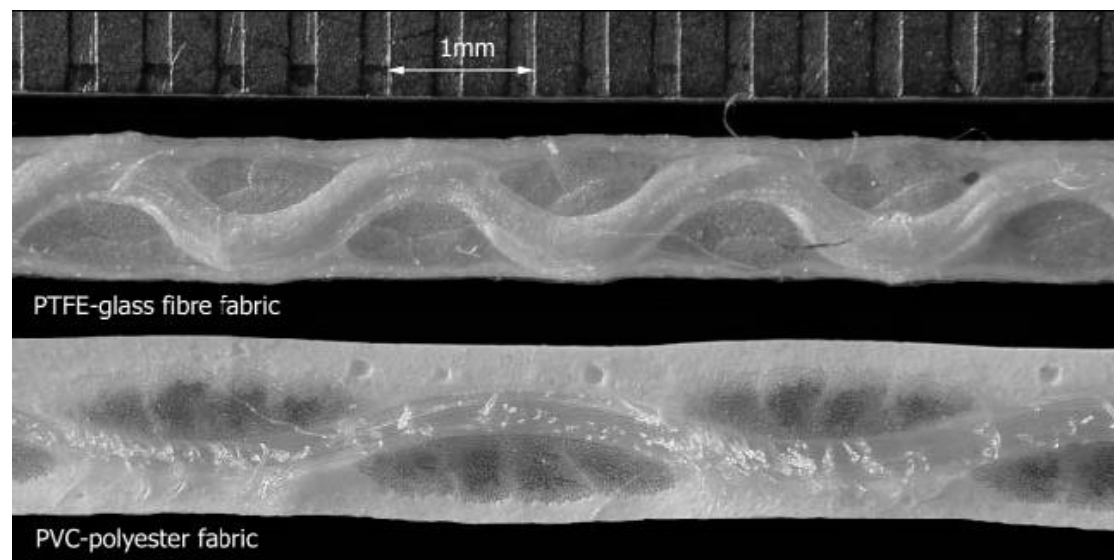


Figure 10: Cross section on a PTFE coated fiberglass fabric and a PVC coated polyester fabric (Bridgens et al, 2004)

It must be stressed that the warp threads are not exactly straight, but are also not as crimped as the weft yarns.

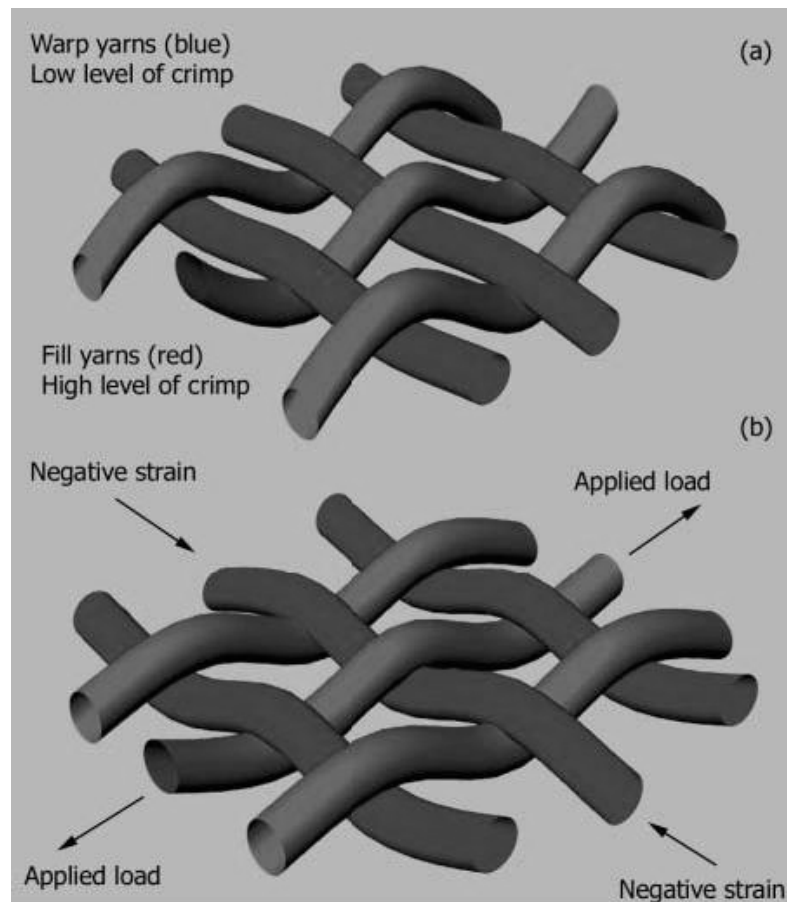


Figure 11: Schematic representation of the crimp interchange effect in a fabric (Bridgens et al, 2004)

The crimp interchange can best be explained by the schematic illustration of a part of woven fabric, see Figure 11. A load on the fabric in one direction (warp) increases the crimp of the threads in the perpendicular direction (weft) of the load direction. However, the amount of additional crimp of these weft threads depends on the amount of loading on these weft threads. The ratio of loading between warp and weft determines the crimp interchange between both directions. Negative strain is a result of an increasing amount of crimp in the threads.

Due to the coating with a layer of PTFE the glass fibres are locked in their initial position. After loading however, the fibres can rearrange themselves into a new equilibrium, which results in a material deformation. This phenomenon needs to be taken into account when testing the material on its stress-strain behaviour.

In practise the permanent strain is taken into account in the design stage of pattern cutting. Due to the limited width of the role of fabric, and the required orientation of the yarn direction, different parts of fabric are seamed together to form the required shape. The expected permanent strain is already taken into account when cutting the patterns. The patterns are cut smaller than they should be *in situ*, but after tensioning the fabric, the designed shape is reached due to the strain of the material. This phenomenon is also called *compensation*.

3.4.6 Repetitive load cycles

Due to the non-elastic properties of the PTFE coated fibreglass, repetition of load cycles has an effect on the permanent strain of the material. It was mentioned in Section 3.3 that the repetitions of load cycles result in a decreasing addition of permanent strain after each cycle of loading and unloading. Eventually this will lead to an equilibrium situation at which no, or only small additional permanent strain is measured after performing a load cycle.

This equilibrium state of the fabric is called a *conditioned state* of the fabric (Bridgens et al, 2004). This represents the situation of *in situ* fabric. For obtaining a realistic stress-strain relation of the fabric, this conditioned state of the fabric is used when performing tests on the fabric.

3.4.7 Load history

The history of loading on the fabric also has an effect on the stress state in the fabric (Bridgens et al, 2004). Bridgens chose a reference state of stress in the fabric, and approached it from different stress states. It appeared that the previous stress state influences the new stress state.

In order to take this load history into account, Bridgens proposes to spread high loads throughout the tests. If one load path contains a high warp load and low weft load, the next load paths should contain a low warp load and a high weft load.

3.5 Alternative for PTFE coated fibre glass

Architectural fabrics are available in various types and qualities, but the two most applied types of fabric are PVC coated polyester and PTFE coated fiber glass. Some characteristics of the each of the fabrics are stated below (Mollaert,2002).

PVC coated polyester

- Easy to work with (transporting and mounting)
- High elongation up to fracture
- "friendly" crack propagation
- Small shear resistance, and therefore low accuracy of analysis and dimensioning required
- Lifespan of approximately 10-20 years
- Tends to get dirty

PTFE coated fiberglass

- Difficult to handle due top high bending stiffness of the fabric
- Can be damaged easily during transport or mounting
- Small disturbances in the coating can lead to crack propagation
- High mechanical strength
- High lifespan of approximately 30 years

From the different characteristics it seems that PTFE coated fiberglass has some major disadvantages. However, the choice for PTFE coated fiberglass is made when applied in large scale projects with large spans. The high strength of the fabric is an important feature of the fabric, which makes it a good product for membrane applications.

Due to the flexibility and long elongation of the PVC coated polyester, this fabric tends to be more 'forgiving' than the stiff fiberglass fabric. Therefore high accuracy in detailing and calculating is essential when working with PTFE coated fiberglass.

4. Current analysis methods for membrane structures

In this section an overview is given of various methods for structural analysis of tensile membrane structures. Different methods will be presented on calculating non-linear geometric structures. Also, different approaches to fabric material representation will be given. Insight in these methods must provide a better understanding of dealing with geometric non-linear calculations and structural analysis of tent structures.

4.1 Geometric non-linearity

4.1.1 General geometric non-linearity

Tensioned membrane structures behave in a geometric nonlinear way. This means that due to external loadings, the structure deforms in such a way, that the original geometry is not valid anymore to base the structural calculations on. In the next calculation step, a new geometry caused by the applied external loading, must be adapted in the calculations.

To illustrate this non-linear phenomenon, a small example is included (Lewis, 2003)

The sample is based on a two bar system, hinged on the sides and at the centre. The bars are elastic and have a length L_m . The elongation of each bar is called e_m , and the current length of a bar is then $L_m + e_m$. The system is loaded at the centre joint with a force P .

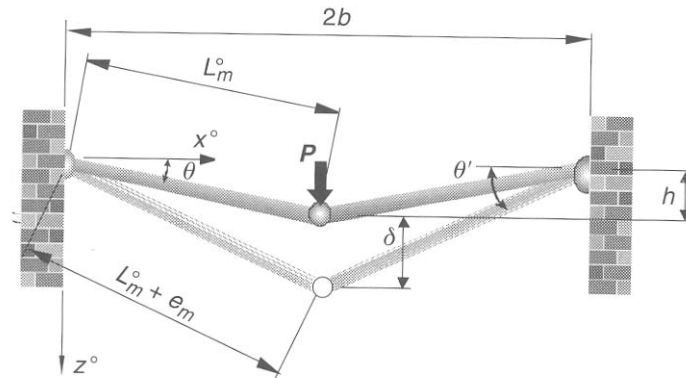


Figure 12: Example of a geometric nonlinear two-bar system (Lewis, 2004)

For the system to be in equilibrium, the vertical components must equal the external applied load P . Thus,

$$P = 2Ke_m \sin \theta' \quad (4.1)$$

where $K = \frac{EA}{L_m}$

After rewriting $\sin \theta'$ to

$$\sin \theta' = \frac{\sqrt{(L_m + e_m)^2 - b^2}}{L_m + e_m} \quad (4.2)$$

The equilibrium situation can be formulated as

$$P = 2Ke_m \frac{\sqrt{(L_m + e_m)^2 - b^2}}{L_m + e_m} \quad (4.3)$$

After rewriting and manipulating on gets

$$P = 2K \left(\delta + h - \frac{L_m(\delta + h)}{\sqrt{(\delta + h)^2 + b^2}} \right) \quad (4.4)$$

This shows that the relation of load P and displacement δ is nonlinear. From this equation it becomes clear that only for small displacements, the relation of P and δ is linear. The second order term containing the displacement becomes small enough for small displacements to be neglected, resulting in a linear relation of P and δ .

In tensioned membrane structures the displacements are not negligibly small, resulting in non-linear relations between the loading and the displacements. Different methods exist to solve these non-linear problems. The preference of which method is used seems to be geographical determined. In the next sections, each of these methods will be described.

4.1.2 Dynamic Relaxation method

A method that is commonly used in Anglo-Saxon countries is the dynamic relaxation method. This method is based on the principle where the nodal masses oscillate about the equilibrium position of the node. This oscillation damps out due to viscous damping, until the equilibrium point is reached (Lewis, 2003).

The method uses the equation of motion. It states that the nodes move around the equilibrium position, driven by the difference of internal and external forces. As long as the internal and external forces are not equal, the motion of the node continues. The motion stops at the point where internal forces in the elements equal the external applied load.

The equation of motion, where the dynamic relaxation method is based on, is given by

$$P_{ji} = \left[\sum K \delta \right]_{ji} + M_{ji} \ddot{\delta}_{ji} + C \dot{\delta}_{ji} \quad (4.5)$$

In this equation j stands for the node number and i is the direction in a discretized system. P is the external applied load and $\left[\sum K \delta \right]_{ji}$ is the internal load. K is the stiffness matrix and δ is the nodal displacement. Note that in a static situation, these two terms must equal in order to form an equilibrium situation. If not, there is a residual force, called

$$R_{ji} = P_{ji} - \left[\sum K \delta \right]_{ji} \quad (4.6)$$

For now, the situation is not in its equilibrium situation but the node is oscillating around the equilibrium position. This causes a nodal acceleration ($\ddot{\delta}_{ji}$) and a nodal velocity ($\dot{\delta}_{ji}$). These nodal acceleration and velocity cause internal forces.

From the equation of residual forces it follows that

$$R_{ji} = M_{ji} \ddot{\delta}_{ji} + C \dot{\delta}_{ji} \quad (4.7)$$

where M is the nodal mass and C is the damping coefficient. This equation shows that the motion of the node is caused by the out of balance force, or residual force. In order to reach a static equilibrium, this out of balance force must become zero.

In order to solve this equation, the nodal displacement must be found, in which the residual force is zero. By using an iterative process, this displacement can be found.

Using centered finite differences, where the acceleration is represented by the average velocity over time interval Δt , and the velocity is represented by the average on the same interval, the residual force can be written as

$$R_{ji} = M_{ji} \frac{\dot{\delta}_{ji}^{n+\frac{1}{2}} - \dot{\delta}_{ji}^{n-\frac{1}{2}}}{\Delta t} + C \frac{\dot{\delta}_{ji}^{n+\frac{1}{2}} + \dot{\delta}_{ji}^{n-\frac{1}{2}}}{2} \quad (4.8)$$

This can be rewritten as a term of the velocity

$$\dot{\delta}_{ji}^{n+\frac{1}{2}} = \left\{ \dot{\delta}_{ji}^{n-\frac{1}{2}} \frac{\frac{M_{ji}}{\Delta t} - \frac{C}{2}}{\frac{M_{ji}}{\Delta t} + \frac{C}{2}} \right\} + \frac{R_{ji}^n}{\frac{M_{ji}}{\Delta t} + \frac{C}{2}} \quad (4.9)$$

The velocity on its turn is used to predict the displacement at time $n+1$

$$\delta_{ji}^{n+1} = \delta_{ji}^n + \dot{\delta}_{ji}^{n+\frac{1}{2}} \Delta t \quad (4.10)$$

This dynamic relaxation method uses a damping factor. In the description above, the viscous damping factor is demonstrated. The kinetic damping factor can also be used in this method. This damping factor is based on a process where the iterations stop at the point of maximum kinetic energy in the system. From that point, calculations restart with the structural configuration of the stopping point, but resetting the nodal velocities to zero. This repeated process continues till the nodal velocities eventually become zero. The residual forces then become also zero, resulting in a static equilibrium of the node. The disadvantage of the kinetic damping factor is that it needs more calculation time caused by a higher amount of iterations, compared to the viscous damping method.

4.1.3 Force Density method

This method is based on a cable net system, where the cable elements represent a part of the tensioned membrane. The force density method is based on the mathematical assumption that the ratio of tension force to the length of each cable element is constant (Lewis, 2003).

By assuming this constant force-length ratio, the set of non-linear equations that describe the equilibrium situation transform into a set of linear equations. This new set of equations can be solved easily. This method was proposed by Linkwitz and Schek in 1972 and was used in the computational modelling of the Olympic stadium in Munich.

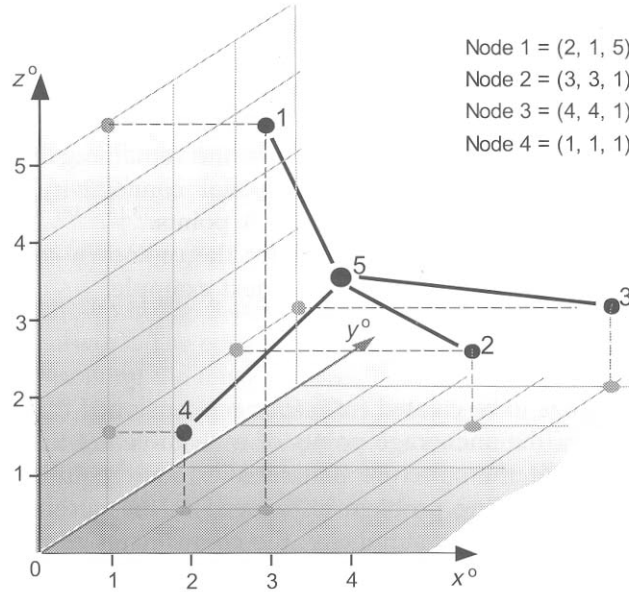


Figure 13: Example of a cable structure with unknown coordinates for node 5 (Lewis, 2003)

The method can be illustrated with a small example of a cable structure, see Figure 13. The boundaries of the cables are known coordinates, while the connecting node is unknown. With the force density method these coordinates can be derived from a set of linear equations.

For this method all tension forces in the cable elements are resolved into their global components. This is achieved by multiplying the axial tension forces with their direction cosines. Direction cosines are the ratio between the projected length and the actual cable length. Each cable has a start node i and an end node k . In the end node the cable elements are connected. The general equation for direction cosines is:

$$\frac{x_i - x_k}{L_m} = \frac{L_{mx}}{L_m} \quad (4.11)$$

$$\frac{y_i - y_k}{L_m} = \frac{L_{my}}{L_m} \quad (4.12)$$

$$\frac{z_i - z_k}{L_m} = \frac{L_{mz}}{L_m} \quad (4.13)$$

In the unknown node 5 the internal forces must equal the external applied load P at node 5 in order to achieve an equilibrium situation. This leads to the following set of equations.

$$\begin{aligned} \frac{T_1(x_1 - x_5)}{L_1} + \frac{T_2(x_2 - x_5)}{L_2} + \frac{T_3(x_3 - x_5)}{L_3} + \frac{T_4(x_4 - x_5)}{L_4} &= P_x \\ \frac{T_1(y_1 - y_5)}{L_1} + \frac{T_2(y_2 - y_5)}{L_2} + \frac{T_3(y_3 - y_5)}{L_3} + \frac{T_4(y_4 - y_5)}{L_4} &= P_y \\ \frac{T_1(z_1 - z_5)}{L_1} + \frac{T_2(z_2 - z_5)}{L_2} + \frac{T_3(z_3 - z_5)}{L_3} + \frac{T_4(z_4 - z_5)}{L_4} &= P_z \end{aligned} \quad (4.14)$$

This system is now non-linear, caused by the unknown coordinates of node 5. This non-linear system can be made linear by assuming a constant ratio between force and

length in each cable element. This ratio is also called the *force density* of a cable element, what explains the name of this method.

The force density is expressed as

$$q_m = \frac{T_m}{L_m} \quad (4.15)$$

where m denotes the member number. The set of equations now becomes linear

$$\begin{aligned} q_1(x_1 - x_5) + q_2(x_2 - x_5) + q_3(x_3 - x_5) + q_4(x_4 - x_5) &= P_x \\ q_1(y_1 - y_5) + q_2(y_2 - y_5) + q_3(y_3 - y_5) + q_4(y_4 - y_5) &= P_y \\ q_1(z_1 - z_5) + q_2(z_2 - z_5) + q_3(z_3 - z_5) + q_4(z_4 - z_5) &= P_z \end{aligned} \quad (4.16)$$

This set with only 3 unknown variables (coordinates of node 5) can be solved now. The coordinates of the boundary nodes are known, in this case nodes 1 through 4. A value for the force density q_m can be set at any value, for example 1. In case of no external applied load, the values for P_x , P_y and P_z are set at zero. By filling these known variables in the formula, the coordinates of node 5 can be calculated.

4.1.4 Transient stiffness method

The transient stiffness method is derived from the assumption that if the displacement is small enough, the force-displacement relation can be called linear. The 2nd and higher order terms in the equation, containing the displacement parameter, become insignificant and are thus truncated. This results in a linear load-displacement relation (Lewis, 2003). The actual structural behaviour shows large displacements, causing some adjustments on the equations.

The transient stiffness method, for now linear, is based on a linear load-displacement relation. This equation describes the relation

$$K\delta = P \quad (4.17)$$

Where K is the stiffness (N/m), δ is the displacement and P is the applied force. Since this system is only valid in a uni-axial system, the relation can be re-written for a global Cartesian coordinate system. Each of the components of the equation becomes a vector or matrix. The equation becomes:

$$[K]\{\delta\} = \{P\} \quad (4.18)$$

$$\text{with } K = \begin{pmatrix} a_{11} & a_{12} & a_{13} \\ a_{21} & a_{22} & a_{23} \\ a_{31} & a_{32} & a_{33} \end{pmatrix}$$

$$\{\delta\} = \begin{bmatrix} u \\ v \\ w \end{bmatrix}$$

$$\{P\} = \begin{bmatrix} P_{x^0} \\ P_{y^0} \\ P_{z^0} \end{bmatrix}$$

The equation has to be valid on every node of the structure. The internal forces ($K\delta$) have to equal the external applied force P on the particular node. This equation can be used in structures with small displacements. The relation of force and displacement is linear and is therefore not suitable for membrane structures. A modification must be made on this equation in order to make it useable for membrane structures.

The stiffness matrix K is based on the initial geometry of the structure. The displacements are assumed to be small, so that the changed geometry with displacements is almost similar to the original geometry. The stiffness matrix is therefore still valid. However, in membrane structures the displacements under external loads are large. The stiffness matrix based on the original geometry is therefore not valid anymore for the changed geometry. This condition asks for a different approach.

The new approach is based on an iterative process, where the displacements are taken into account when calculating the stiffness matrix. The internal forces that can be calculated, using the displacement vector and the modified stiffness matrix, will not match with the external applied load. The difference between internal forces and external applied load represents a residual load vector. This residual load forms the basis for an update of the displacements. The updated displacements create a new geometry and its corresponding stiffness matrix. Based on these updated displacements and stiffness matrix a new residual force can be calculated. The iterative process repeats itself until the internal load equals the external applied load.

The process can be written in equations. Due to the iterative process, a parameter is added, called k . This stands for an iterative step in the process. The next step is then called $k+1$. The geometry in the k^{th} step of the process is called $\{X\}_k$, and the corresponding stiffness matrix $\{K\}_k$. Now the displacements can be calculated

$$\{\delta\}_{k+1} = [K]_k^{-1} \{P\} \quad (4.19)$$

The new geometry can now be derived using

$$\{X\}_{k+1} = \{X\}_k + \{\delta\}_{k+1} \quad (4.20)$$

From this new geometry a new stiffness matrix is constructed, $[K]_{k+1}$. With the updated stiffness matrix and the updated displacement vector, the internal loads can be calculated:

$$[K]_{k+1} \{\delta\}_{k+1} = \{\tilde{P}\}_{k+1} \quad (4.21)$$

The calculated internal load does not equal the external applied load, causing a residual load. This vector is called $\{R\}_{k+1}$. With this residual load, it is now possible to calculate a correction on the displacement vector.

$$\{\Delta\delta\}_{k+1} = [K]_{k+1}^{-1} \{R\}_{k+1} \quad (4.22)$$

This process can now be repeated until the residual load becomes zero, meaning that the internal loads equal the external applied load.

4.1.5 Remarks on geometric non-linear calculation methods

As stated in the introduction, application of these methods seems to be geographical determined. Advantages and disadvantages of these methods are found in the field of

computational efficiency and CPU usage. The number of iteration steps and the corresponding total calculation time are main criteria in comparing these methods.

In stressed membrane structures displacements under external loading are usually of a magnitude where geometric linear calculations are not appropriate. For accurate structural analysis of stressed membrane structures the geometric non linearity should be taken in account.

4.2 Material representation for structural analysis

In the preceding sections different methods are described how to calculate the geometry of membrane structures, and how external applied loads influence this geometry. The last step in a structural analysis is to determine the stresses in the fabric, and to verify if these stresses are acceptable. The changed geometry of the structures gives information about strains in the fabric material. A proper fabric model should be able to provide the corresponding stresses, given the material strains.

In the past, different attempts have been made to model the strain-stress behaviour of architectural fabric. However, one never succeeded in an accurate representation of the fabric behaviour. Bridgens (2004) researched these different attempts and pointed out the weaknesses of each of these models.

4.2.1 Model with two Young's moduli and one Poisson factor

The classical representation for a material, with two Young's moduli for both warp and weft direction and one Poisson factor does not hold for fabric material. The Young's moduli are derived from the secant modulus of warp and weft stress-strain curves. A constant stress ratio is assumed and the Young's moduli are based on this ratio. However, the stress ratio remains constant during the structural analysis, which is not appropriate. Under external applied loading the stress ratio will vary, and thus will the Young modulus not be a constant.

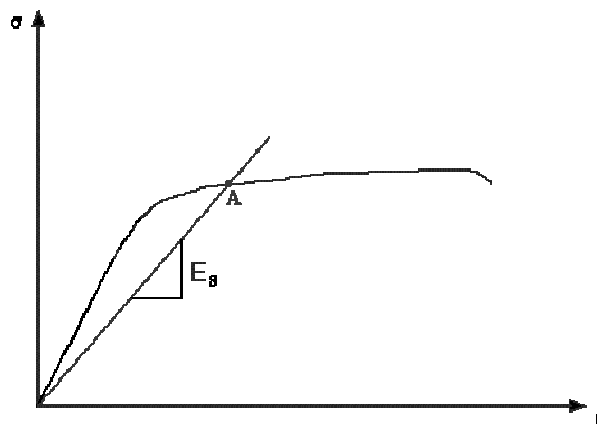


Figure 14: Principle of determining the secant modulus (www.ae.msstate.edu)

4.2.2 Model with interaction moduli

Another representation for fabric behaviour can be made by Young's moduli and interaction moduli. The interaction moduli represent the interaction between warp and weft threads, and also between weft and warp threads. Combined with two Poisson's factors for warp-weft and weft-warp, the following equation is defined:

$$\begin{bmatrix} \sigma_{11} \\ \sigma_{22} \end{bmatrix} = \begin{bmatrix} E_{1111} & E_{1122} \\ E_{1122} & E_{2222} \end{bmatrix} \begin{bmatrix} \varepsilon_{11} \\ \varepsilon_{22} \end{bmatrix}$$

The subscripts 11 and 22 represent the warp and weft direction, while 1122 is representing the interaction between warp and weft.

In this method, particular areas in the non-linear stress-strain curve are linearised in order to obtain the values for E. The area of interest is usually the part between prestress state and an upper stress limit expected to occur for external loading such as wind and snow load.

Bridgens (2004) attempted to verify this system of equations for fabric material, but concluded that these equations do not hold for fabric material. By manipulating the equations Bridgens managed to get results that matched the experimental data. However, this system of equations does not provide an accurate representation of the material behaviour.

Nederpelt (2004) also concluded that these equations are not valid for woven fabric material. The Poisson's factors do not represent the actual interaction between warp-weft and weft-warp. Nederpelt explains this by the fact that the woven fabric does not follow the physical laws of homogenous materials, and therefore is the Poisson's factor not valid.

4.2.3 Model with multi-step linearization

Minami (Bridgens et al, 2004) tested fabric at different stress ratios. From the test data Minami produced a surface in the stress-stress-strain system. Different parts were linearized in order to derive the Young's modulus from the surface. Data points from areas which were not tested are derived by interpolating the known test data. To illustrate this method, a surface generated from a tested fabric is given in Figure 15.

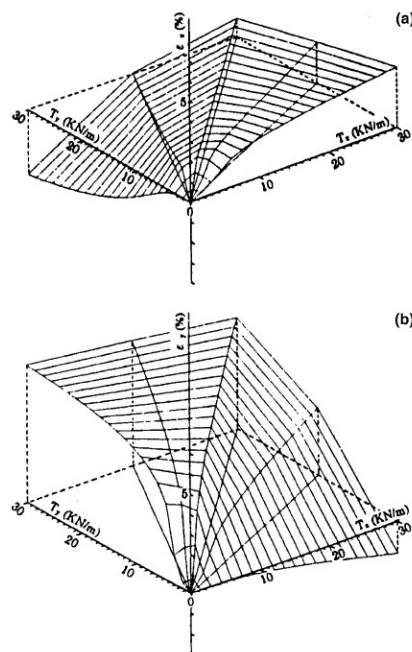


Figure 15: Response surface created by Minami (Bridgens et al, 2004)

According to Bridgens (2004) Minami's model is an approximation of the fabric behaviour. The snapshots from the stress-strain curve, or the linearized parts of a

nonlinear curve, providing the Young's modulus, are not suitable for an accurate representation of the fabric behaviour.

5. Bi-axial testing procedure

This chapter gives an overview of the different aspects that have to be taken into account when performing bi-axial tests on PTFE coated fibreglass. No European standard exists yet for bi-axial testing. Therefore different earlier researchers will be examined in order to describe a test method that will be used for testing the PTFE coated fibreglass.

5.1 Other researchers

One of the main current actors in the field of material research on membrane fabrics is Ben Bridgens, from the Newcastle University. Bridgens, under supervision of Dr P.D. Gosling, researched different aspects of the material properties of woven based architectural textiles. The aim was to model the material behaviour in order to provide a predicted relationship between the stress and strain for each warp and weft direction (Bridgens, 2005). The work of Bridgens is the most recent on the field of material testing, and has a high level of detail.

The work of Bridgens is relevant due to the method he described in order to find data that is comparable with the in-situ conditions of the fabric. There is a difference between the virgin material and the in-situ material that is found in build constructions. In order to find material properties which are comparable with the in-situ conditions, he described a method for testing the fabric.

At the Delft University of Technology research on fabrics has been performed by C. Nederpelt and J. de Vries. Both have been using the bi-axial tests bench that will be used in this thesis' research as well. De Vries performed research on ETFE foil, used as a single sheet membrane construction material (De Vries, 2003). Nederpelt researched the possibility of silicon coated fibreglass being an alternative for the PVC coated polyester. The advantage of silicon coated fibreglass over PVC coated polyester is the reduced influence on the ecological environment. Material properties of the silicon coated fibreglass had to be found through experiments and were compared to properties of PVC coated polyester (Nederpelt, 2004).

The work of Nederpelt and De Vries is relevant due to the specific experience they have gathered with the bi-axial test bench that will be used in this thesis. Their recommendations on test procedures and sample preparing need to be considered.

5.2 Various aspects of testing

In order to gather test data that is useable for the purpose of this thesis, some aspects of testing need to be considered. This section will go over these aspects in order to set the right conditions for gathering the desired test data.

5.2.1 Uni-axial and bi-axial testing

Membrane fabric can be tested on both uni-axial as on biaxial manner. Uni-axial testing gives insight in the stress-strain behaviour until the breaking point of a fabric. This type of test is intended to determine the breaking strength of the fabric. The bi-axial interchange effect is not included in this way of testing. Therefore uni-axial testing is not appropriate for acquiring the fabric response. When the fabric is tested bi-axial, the crimp interchange is included in the fabric behaviour, which makes bi-axial testing essential.

A remark must be made on the response of the fabric in bi-axial testing. Due to the shape of the test samples, the fabric response will not be tested until the breaking

point. The fabric will tear earlier in the process in the corners of the cruciform shape of the sample. However, the response area acquired through bi-axial testing is the area of interest.

5.2.2 Types of bi-axial testing

Bi-axial tests can be performed in three different manners: bursting test, cylinder test and plain bi-axial test. Only the plain bi-axial test is suitable for testing architectural fabric (Bridgens, 2004).

In a bursting test, the fabric is clamped on a ring shaped element. By increasing the air pressure under the ring, the fabric is tensioned. Due to the test device, it is not possible to vary in different force ratios in either warp or weft direction of the fabric. In that way it is not possible to monitor the crimp interchange in warp and weft direction, because there is only one and also unknown ratio of forces on which the sample is tested.

In the cylinder test, a cylinder is made out of a piece of fabric by seaming the piece together, see Figure 16. The cylinder is put in a uni-axial test bench and is inflated. Strain of the sample is measured by using a digital imaging system. This method is not useful for architectural fabric caused by limiting seam strength of the sample (Bridgens, 2004). Besides that, Nederpelt (2004) recommended that this method is less suitable due to the low force range that could be carried out during the tests. The samples slipped out of the clamps under low stresses, making the test data useless. Therefore this method is not suitable for testing PTFE coated fiber glass.



Figure 16: Cylinder test (Nederpelt, 2004)

The plain bi-axial test is a widely used method in the industry (Bridgens, 2004), see Figure 17. A cruciform shaped sample is stressed in the two main fibre directions of the fabric. The size of the applied forces and the ratio between these forces can manually be set. By monitoring the applied forces and measuring the displacement of the sample, a stress-strain relation can be derived for various force ratios. This method will be used in this thesis to acquire the stress-strain data of the PTFE coated fibre glass.

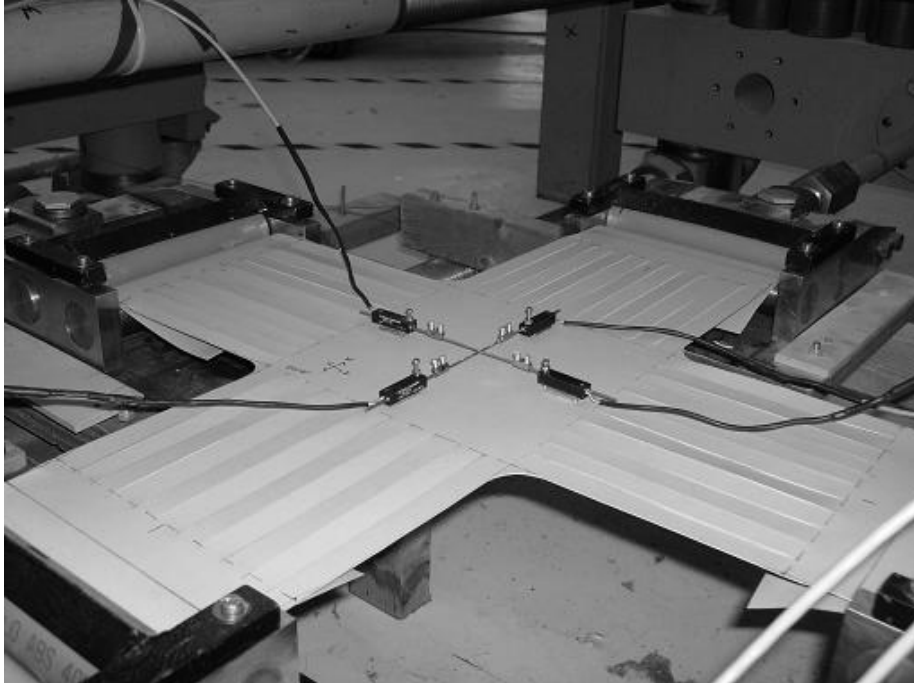


Figure 17: Plain bi-axial test

5.2.3 Initial behaviour and *in-situ* behaviour

Due to the woven structure of the woven fibreglass fabric, there is a difference between initial and *in-situ* fabric response. In Section 3.3 the production method of the fibre glass fabric is explained. The initial tensioning, or load cycle, of the fabric results in a rearrangement of the fibres in the fabric. A large permanent deformation, up to 7%, of the fabric is the result of this rearrangement of fibres (Nederpelt, 2004). A second load cycle results in a smaller additional permanent deformation, up to 1%. This process can be repeated until the additional strain becomes a negligible proportion of the total strain.

Figure 18 shows the behaviour of a silicon coated fibreglass fabric. This fabric behaviour is the results of a biaxial test on an unconditioned fabric sample (see Section 3.6 for *conditioning*). It becomes clear that repeated tests give results that are not comparable with each other. These results are therefore not usable for the purpose of this thesis. This thesis focuses on the fabric behaviour of *in-situ* material.

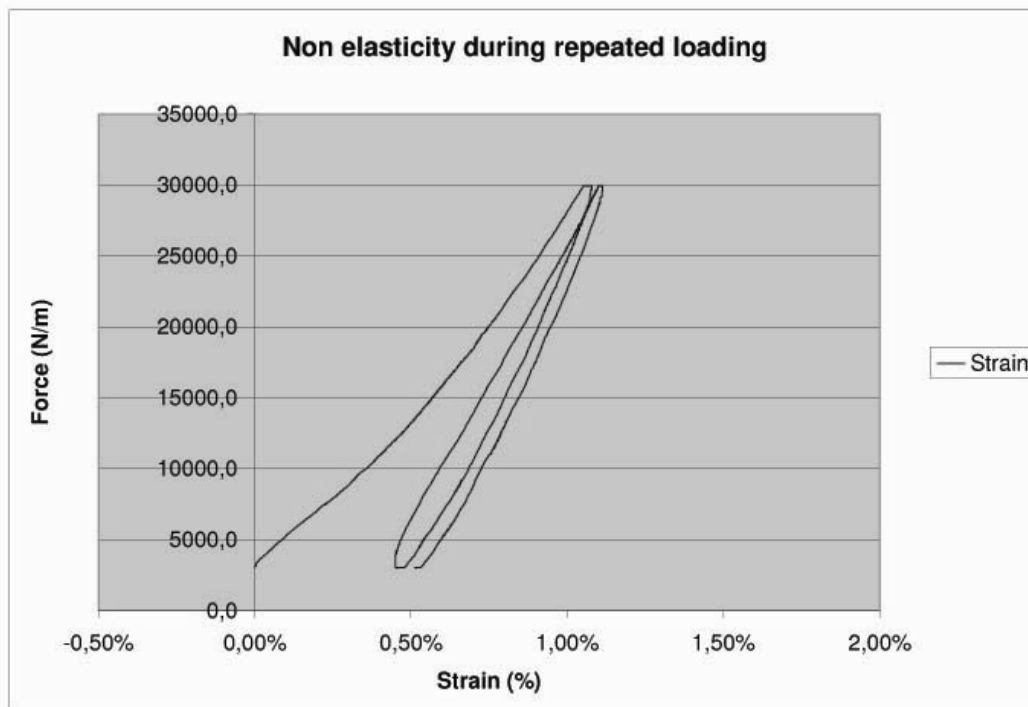


Figure 18: PTFE coated fiber glass, initial behaviour and a decreasing additional strain

Permanent strains of initial loadings are taken into account in the design of a membrane structure by a process called *compensation*, see also Section 3.5.

In order to acquire the desired fabric response through testing, the fabric should be conditioned first. By conditioning the fabric, the *in-situ* conditions are simulated. The fabric response after conditioning is then comparable with the *in-situ* conditions (Bridgens, 2004). Repeated tests on the fabric sample will then show similar results for a given stress state.

Bridgens (2004) proposed a protocol for conditioning the fabric, in order to prepare the fabric for testing. This protocol describes a 17-hour lasting prestress state and a number of load cycles performed on the test sample, until the point is reached where the additional strain is less than 5% of the total strain. At this point the test sample is considered to be *conditioned* and ready to perform the tests on. Figure 19 shows this principle in a schematic way.

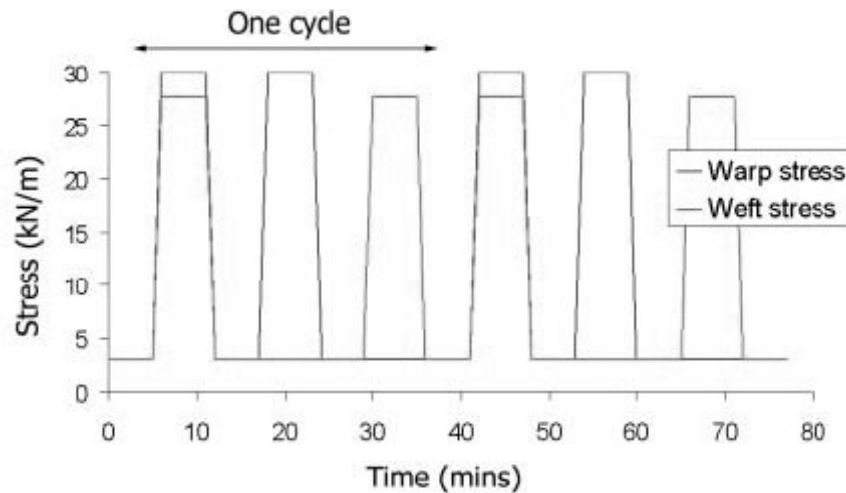


Figure 19: Conditioning process to prepare the fabric sample for testing (Bridgens, 2004)

5.2.4 Applying different force ratios

After the fabric has been conditioned, Bridgens (2004) proposes that the fabric is then tested by applying forces in different ratios. Different ratios are essential to include the bi-axial crimp interchange in the mechanical behaviour of the fabric. The crimp interchange is not a constant, but varies with the different applied ratios.

The amount of ratios to be performed depends on the required accuracy of the fabric response. The more ratios are applied, the more accurate the response model can be predicted.

Earlier research performed by A.S. Day (1986) proved that 3 ratios, namely 1:1, 1:5 and 5:1, are not sufficient to produce a fabric response model. More extensive research by Bridgens (2004) showed that 8 ratios offer a wider range of data, to produce a more reliable response model.

Each load cycle remains in the preset ratio of forces in both warp and weft direction. The point of return, where the unloading of the test sample starts, needs to be described. Bridgens defines this point as a percentage of the strip Ultimate Tensile Strength (UTS). Mono-axial tests provide data on the breaking strength of the fabric. This breaking strength of the fabric is defined as the UTS. Tear propagation does not occur until approximately 25% of the UTS. This point is chosen as the maximum loading during testing. For example, when the UTS is 100 kN, the test load will not exceed 25 kN.

In this illustration, see Figure 20, a number of load paths are described. Note that the load paths start from the level of pre-stress. The load paths can be extended with additional paths at different ratios in order to provide data with a larger range.

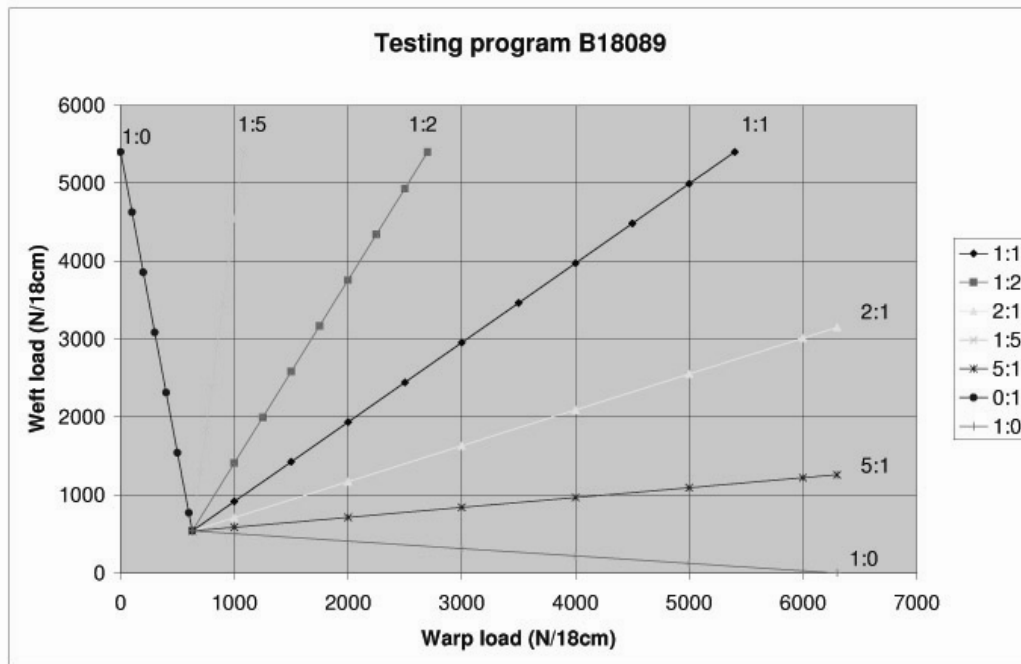


Figure 20: Different load paths in preset warp-weft ratios produce a wide range of stress states of the fabric

5.2.5 Residual strain

The fabric will show residual strains during the test procedure. Due to rearrangements of the fibres after a load path, the strain rate will be increased after unloading. The loading program is set up in such way, that the effects of these residual strains are minimised. In Section 8.1 it is discussed in what way these effects have to be taken in account when modelling the material behaviour.

5.3 Testing device

The bi-axial tests will be performed on the bi-axial test rig, at the Stevin Laboratory of the faculty of Civil Engineering and GeoSciences, Delft University of Technology. Previous research has been performed with this machine on silicon coated fibre glass and ETFE foil. Researchers in these fields were C.A.G. Nederpelt (2004) and J.W.J. de Vries (2003). Their experiences and recommendations will be used to use the bi-axial tests in an efficient way.

5.3.1 The bi-axial rig and its components

The bi-axial rig consists of two independent structures. Each of these structures can apply a force on the test specimen. These forces are applied on one side of the cruciform specimen, while the opposite side is fixed in place. By placing displacement sensors on the centre part of the test specimen, the displacement of the test specimen can be monitored. Combined with the monitored forces that are applied, a computer gives the combined output of forces and strain of the test specimen.

Due to the asymmetrical application of the forces, the centre part of the specimen moves away from the centre of the test rig, according to De Vries (2003). In order to avoid undesired stresses in the test specimen, caused by prohibited displacement, special measures need to be taken. De Vries invented a solution, in which the rig can be moved along with the centre displacement. In this way the opposite rig stays in line with the centre of the specimen. This is necessary at high strain rates.

However, the strains expected for this thesis' research are less than the strains De Vries experienced. The PTFE coated fibre glass is much stiffer than the ETFE foil, which makes the use of the centre-tool not necessary.



Figure 21: Test rig for bi-axial testing

The sample is placed in 4 clamps (C). Two hydraulic cylinders (A) apply forces on the fabric sample in the two main directions. The applied forces are logged through a load cell (B). The fabric sample is placed on a supporting table (E). The area of interest is the central square of the fabric sample (D). At this square the fabric strain in 2 directions is logged.

5.3.2 Preparing cruciform test specimen

The test specimen has a cruciform shape, with a central test area. The four 'arms' of the cruciform shape are clamped into the test bench. The clamps are attached to a hydraulic force generator. In the central part of the specimen, the two force directions cross over and bi-axial interchange can be monitored on that location. In order to get useful measurements, the following aspects must be considered:

- Uniform stress distribution along the width of the sample
- Size of the stress acting on the area of interest

Bridgens (2004) researched four different types of configurations of the cruciform shape, see Figure 22. His study focussed on the most efficient way of introducing the applied forces in the fabric. Bridgens varied the amount and the size of slits in the force application zone. By doing so, Bridgens reduced the influence of lateral contraction in the cruciform arms. The result is a uniform stress distribution in the central test area of the cruciform sample. Bridgens concluded that the configuration with 11 slits of 150 mm each provides the best transfer of stresses in the material. The stress distribution in the area of interest showed the least variation along the width of the square, compared with the other three configurations.

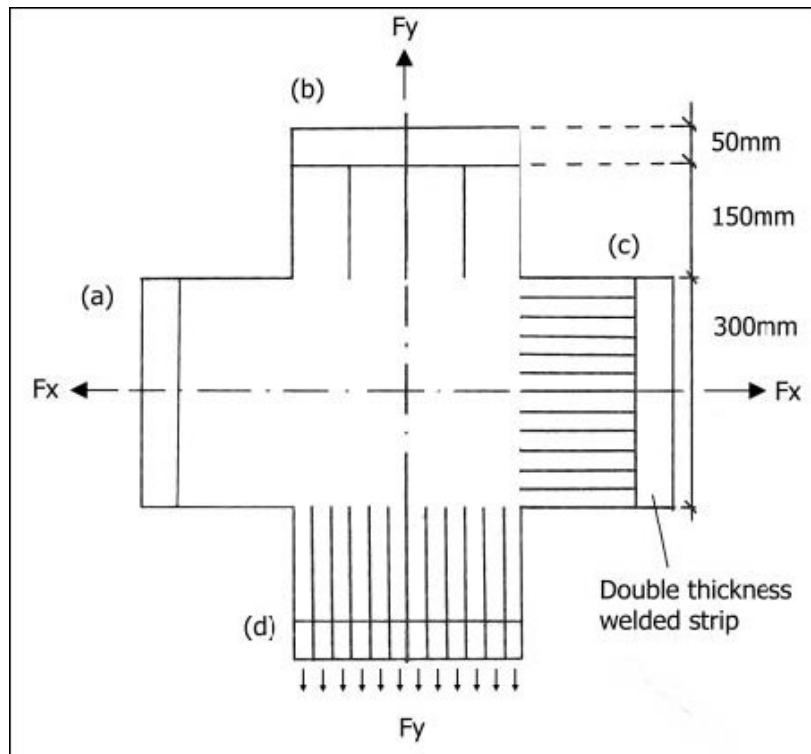


Figure 22: Four different configurations for slits in the cruciform sample (Bridgens, 2004)

Bridgens measured a difference in the applied load on the sample, and the measured stress in the central square. Therefore Bridgens introduced a reduction factor of 0.95. The motivation for this reduction factor is found in the transfer of a part of the force into the arms of the sample. The force acts on a wider area than the 300mm width of the square of interest.

In the case of this thesis' research a different size sample is used, due to a limited size of the clamps at the Stevin laboratory. The clamps have a width of 180mm instead of 300mm in Bridgens' case. A new test must be carried out in order to determine the most efficient way of introducing the forces, see Section 6.1. The configuration of the slits in the cruciform arms will be determined. In order to determine the reduction factor, a test must be carried out to determine the effective width of the central square of the sample.

The test sample will be modelled in Ansys. By applying forces on the cruciform arms, stress distributions in the central square can be visualized. A slit configuration resulting in the most uniform stress distribution in the central square can be determined in this way. Known stresses over a known width will result in determining the reduction factor.

5.3.3 Clamping the sample

Proper attachment of the sample in the clamp is essential to derive accurate measurements of strains in the material. If the material slips in the clamp, the measurements contain errors. The displacement measured during testing will then contain both strain and slipping of the fabric. Slipping of the fabric is not desired.

Nederpelt (2004) used a pvc pipe in the clamp, to prevent the fabric from slipping in the clamp. The elastic properties of the PVC pipe are used to cancel out any irregularities in the fabric material. These irregularities cause an unevenly spread pressure on the clamp and the sample. By using a PVC pipe a constant pressure in the

clamp on the sample can be reached. In this way, Nederpelt was able to get results without slipping of the sample.

This method was mainly used in a mono-axial test, using the biaxial clamps. Due to an applied stress up to the UTS, the sample slipped in the clamp. However, on lower stresses the sample did not show any forms of slip when using the regular clamp, according to Nederpelt. A sample of the clamp is shown in Figure 23.



Figure 23: Clamping the sample (Nederpelt, 2004)

The fabric tested for this thesis is much stiffer than the silicon coated fibre glass tested by Nederpelt (2004). Forces acting on the pvc pipe cause the tube to deform, resulting in slipping of the fabric. A tube with a thicker wall deforms less, but the steel clamp can not be tightened sufficient in order to generate sufficient pressure. A strengthening of the steel clamp is necessary to be able to fasten the clamp and prevent fabric from slipping in the clamp, see Figure 24.



Figure 24: Enforcement on the clamp

5.3.4 Data output

The test sample is equipped with two displacement measuring devices, positioned in line with the two acting forces. These devices record the displacement of the sample, caused by the strain of the material. The strain of the material on its turn is caused by the acting controlled forces. The size of these forces is recorded simultaneous with the recording of the strain. Note that the ratio between the two forces remains constant during one particular load cycle.

The results of these measurements are plotted in a diagram, with the stress on the vertical axis, and the material strain on the horizontal axis. These results can either be plotted in two diagrams, or in one diagram. By plotting the response in one diagram, it provides a quick overview in the response of both warp and weft direction.

An example of the desired data output is given in Figure 25.

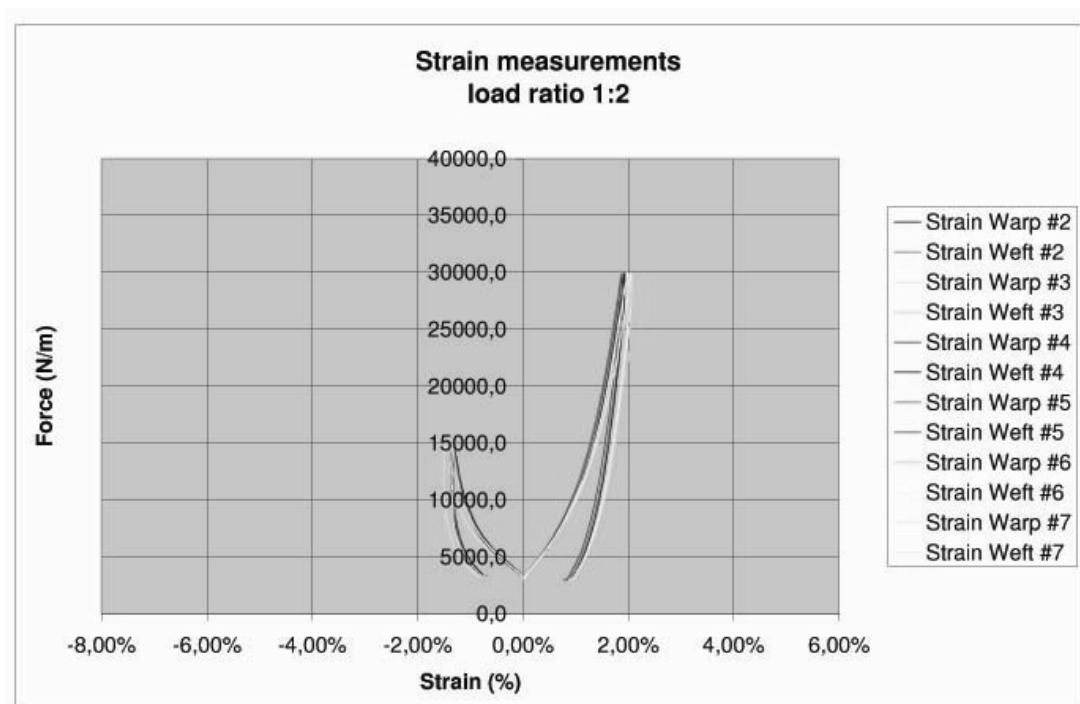


Figure 25: Example of the data gathered from the experiments

5.4 Test procedure

After going over various aspects of the bi-axial testing of fabrics, a procedure can be set for testing the fabric. This will give a clear overview of the different actions to be taken in the testing. This overview will also improve the efficiency during testing.

Note that this procedure is invented by Bridgens (2004) and is adopted for this thesis. A more detailed description of the experiments is included in the Appendix B3.

5.4.1 Procedure

Material

The material to be tested in this thesis is Verseidags B18089. This is a glass fiber based fabric, with a PTFE (or Teflon) coating. Additional technical data of this type of fabric is added in the Appendix B1.

Samples

The samples need to be cut out of the role of fabric, according to the sample properties discussed in Section 5.3.2. A certain variation in fabric properties is expected (see

Section 3.2 Production process). Samples cut out of the side of the role are expected to be different than the samples cut out of the centre part of the role. Markings on the sample will make it possible to identify the origin, and make it possible to explain possible deviance in the outcomes.

Prestress

The test specimen will be put in the bi-axial test bench. In order to prepare the specimen for the conditioning and testing, a 17 hour during state of prestress will be applied on the sample. The prestress level is set at 2,5% of the ultimate tensile strip strength (UTS). The UTS will be derived from the manufacturer’s data sheet of the B18089 PTFE coated fibre glass, see appendix B1.

Conditioning

The fabric will now be conditioned. In a number of loading cycles, the fabric will be stressed up to 25% of the UTS. One cycle contains three different loadings. One loading with both warp and weft at 25% UTS, then two with either the warp or weft loaded at 25% of the UTS. This cycle lasts for 30 minutes, and must be repeated up to 3 times in order to condition the fabric. The total conditioning time will take up to 90 minutes.

The exact conditioning program is stated below in Table 1 (Bridgens, 2005). The corresponding graph of the conditioning program is stated in Figure 27.

Table 1: Conditioning program

Time (minutes)	Warp load	Weft load
0-5	Prestress	Prestress
5-10	Conditioning Load	Conditioning Load
10-15	Prestress	Prestress
15-20	Conditioning Load	Prestress
20-25	Prestress	Prestress
25-30	Prestress	Conditioning Load

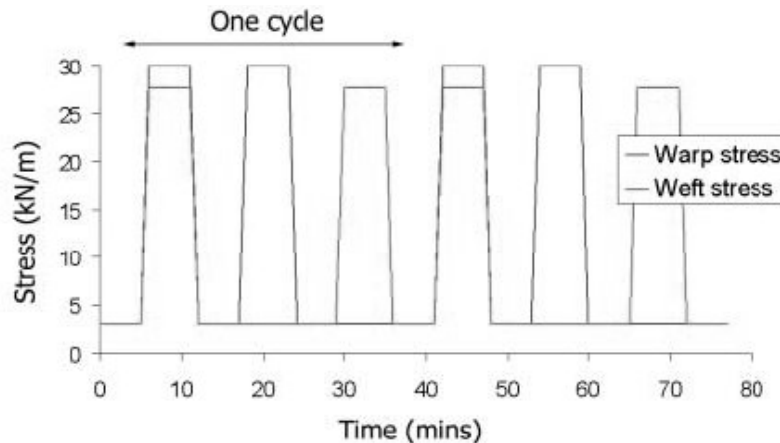


Figure 26: Conditioning program (Bridgens, 2005)

Testing

After the fabric has been conditioned the actual testing begins. The fabric is tested with different force ratios. The maximum loading may not exceed the 25% UTS to prevent the sample from tearing. The force is applied stepwise. Each step will be held for 1 minute. During each step, the strain will be measured every 5 seconds. The average of 5 consecutive readings will be taken as the data point for the strain. The data will be logged on the loading path as on the unloading path as well. The total testing time will last up to 6 hours. A complete testing procedure, from prestress until testing will take

up to 25 hours. During 8 hours of this process attendance is required and data needs to be logged.

An example of a testing program is given in Figure 27.

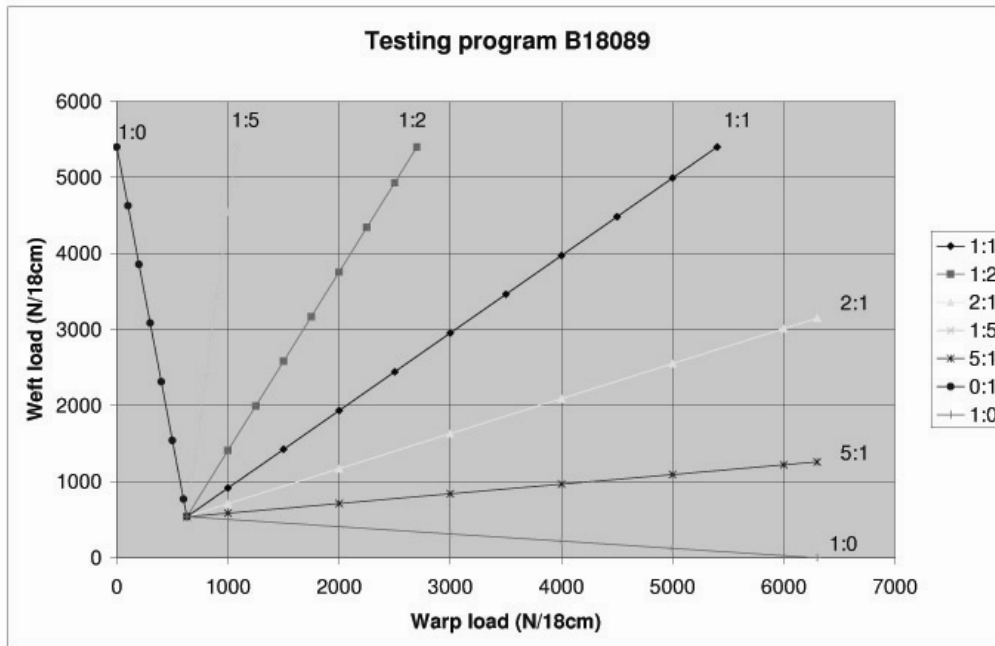


Figure 27: Testing program with applied load in both warp and weft direction

A manual for testing is included in the Appendix B2.

6. Testing validation

One quality type of PTFE coated fibreglass has been tested in the Stevin Laboratory of the Delft University of Technology. The procedure for testing is described in Section 5.4. It is essential to validate some aspects of testing in order to eliminate errors from testing. First the test sample is analyzed in order to determine the correct slit configuration and effective width factor of the sample. Also the potentiometers, used for displacement recordings, are researched.

6.1 Sample analysis

When testing the cruciform sample, strains of the fabric are measured together with the corresponding stresses that are applied to the fabric. It is essential to have insight in the stress distribution in the measuring area of the cruciform shape. It is desired to have a uniform stress distribution in the area over which the strain is measured. Besides the distribution of the stress, also the magnitude of the stress is important to know. An analysis is performed to acquire insight in these aspects.

6.1.1 Sample shape

The cruciform sample's dimensions are defined by the bi-axial test bench's clamps. The width of these clamps is 180mm, resulting in a cruciform with 180mm wide arms. Uni axial loads are applied at the arms, resulting in a square area where the loads overlap. In this area a bi-axial loading is present. In this area the strains are measured in an orthogonal way, corresponding with the yarn directions.

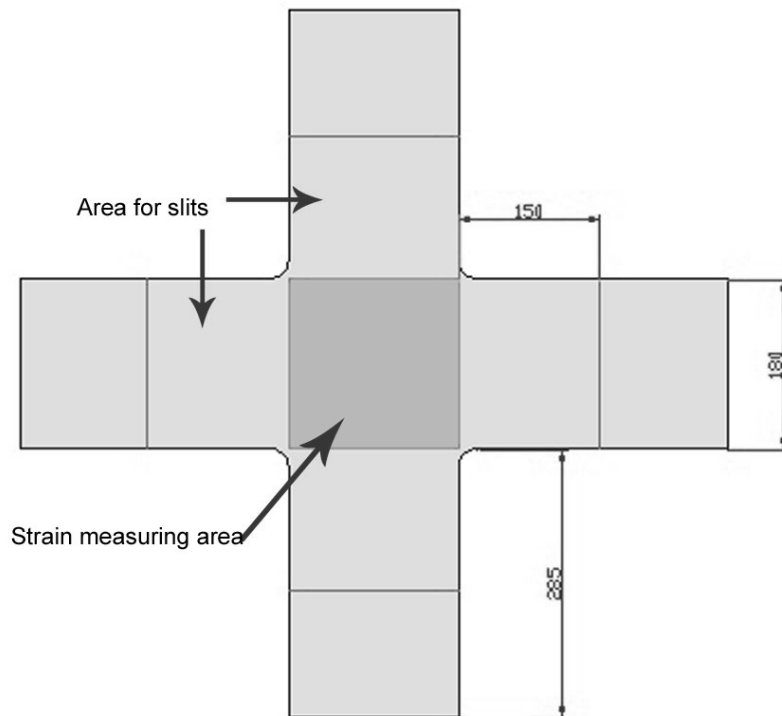


Figure 29: Dimensions of the cruciform sample

6.1.2 Analysis of stress distribution

The cruciform sample is modeled in a finite element program, called Ansys. The conditions similar to the testing conditions are simulated in the analysis. This means that from each arm, one side is constraint while the other side is loaded. The clamps are modeled by pieces of steel, causing a uniform introduction of the applied load to the fabric.

An example of a model is given in Figure 30. The sides with a constraint degree of freedom are indicated as well as the applied loading at the opposite ends of the cruciform arms. This configuration is similar to the test configuration in the test bench.

The purpose of the analysis is to determine the stress distribution in the central square. Besides the distribution, the stress magnitude is also essential to know. It is desired to acquire a uniform stress distribution, because strains measured over a uniform stress result in a proper stress-strain relation. By making slits in the cruciform arms, a more uniform distributed stress is generated. To determine the slits configuration, an analysis is performed by using Ansys (see Section 6.1.3-6.1.6).

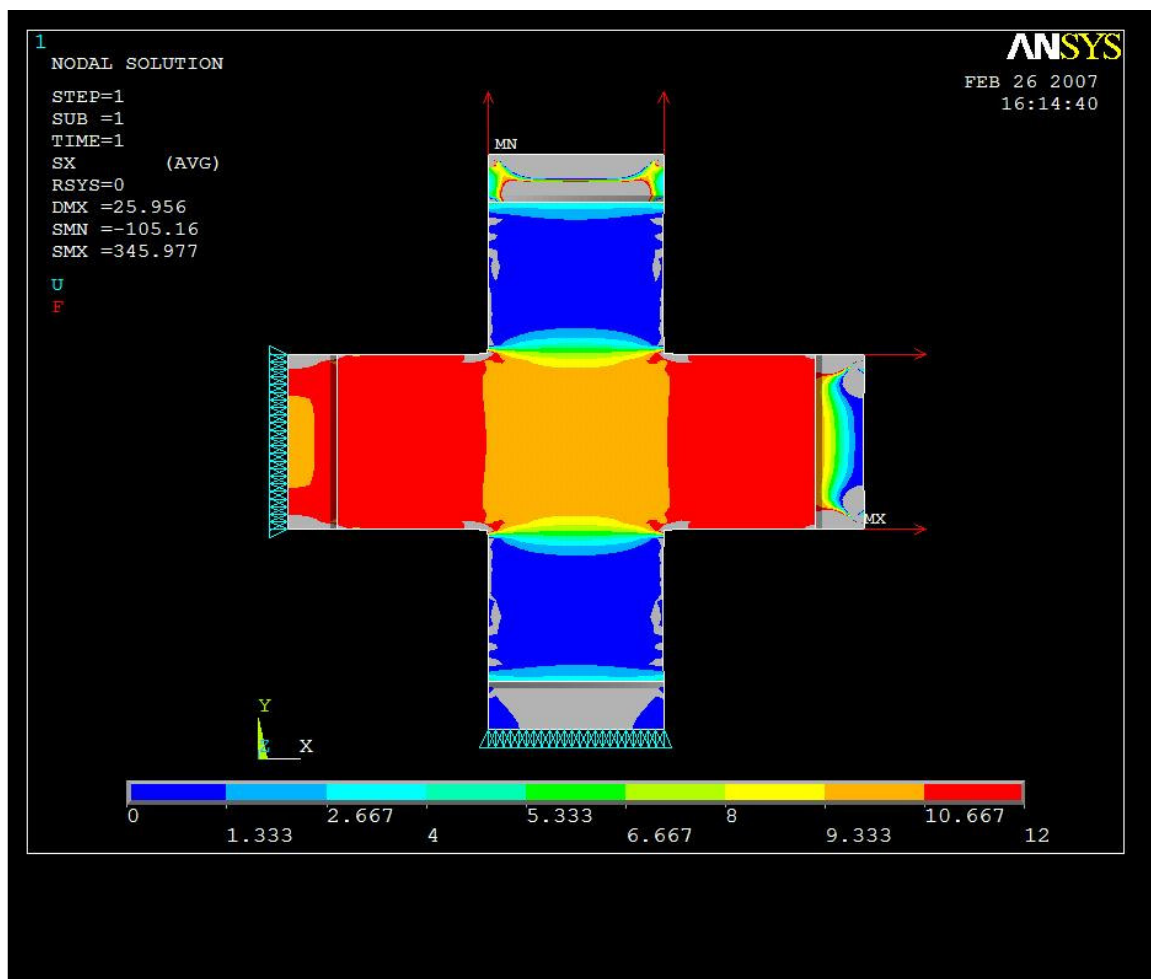


Figure 30: Stresses in x -direction in the sample

6.1.3 Material representation

In the analysis, the material properties have to be described as well as the element type. For the element type either a membrane or shell element can be used. The material properties however seem a bit contradictorily. The exact material properties are researched through the biaxial tests that are performed later on, and are thus not available yet.

Therefore an assumption has to be made in order to be able to perform the analysis. Comparable research has been performed by Bridgens (2005). Bridgens used an anisotropic material with the properties:

$E_{\text{warp}} = 600 \text{ kN/m}$
 $E_{\text{weft}} = 600 \text{ kN/m}$
Poisson's ratio = 0,3
Shear modulus = 30 kN/m

Unlike the realistic modulus of elasticity (E), the used modulus is a constant throughout the analysis. Besides that, a Poisson's ratio is used to take the bi-axial interchange into account. This, however, has been contradicted earlier, see Chapter 4.2.1. However, for a first estimation of stress distributions these assumptions are sufficient. Values for material properties used by Bridgens are adopted in this thesis' analysis in order to be able to compare results.

6.1.4 Slits in the cruciform sample

Stresses are applied in a uniaxial manner on the cruciform arms. These stresses are uniform introduced in the fabric. Following the direction of the stresses along the length of the cruciform arm, the stresses remain uniform distributed. However, when crossing the transverse arm, the stresses tend to act on a wider area than the 180mm width of the arm. This results in a decrease of the magnitude of the stress level in the central square. Eventually the stress magnitude will increase again when arriving at the end of the transverse arm. From there the stresses are uniform distributed again, up to the constraint end of the arm.

The decrease of the magnitude of the stresses in the central square is an undesired effect. The decrease of the stresses at the sides of the central square causes a non-uniform distributed stress around these areas. The aim is to minimize these effects in order to obtain a uniform distributed stress with a magnitude as close as possible to the applied stress. Because the magnitude will eventually not match the magnitude of the applied stress, a reduction factor can be derived from an analysis.

By applying slits in the transverse arm, the effect mentioned above can be reduced. Theoretically the effect is reduced maximally when making the amount slits infinitely large. However this is practically not possible. An analysis must be made to research slit configurations anywhere between zero and 20 slits.

Bridgens (2005) researched a cruciform sample with a different geometry. Due to this different geometry, it is not possible to use the same slit configuration without analyzing. Similar material properties are used in an analysis on a geometry used for this thesis. A new reduction factor will result from this analysis.

The corners of the cruciform sample are curved, to prevent sudden tear propagation. A rounded corner is less sensible for tearing. This rounded corner has a negligible effect on stress distribution in the central square of the test sample.

6.1.5 Results of sample analysis

Different analyses have been performed with various slit configurations:

- No slits
- One slit
- 5 slits
- 10 slits
- 19 slits

On each cruciform arm a load is applied of 2kN. Theoretically this results in a stress magnitude of 11,11 N/mm on a width of 180mm. Paths have been set out along the width of the central square. On different points on these paths, the stresses have been listed. By plotting these stress values in a graph (over the location), the effect of the slits was visualized.

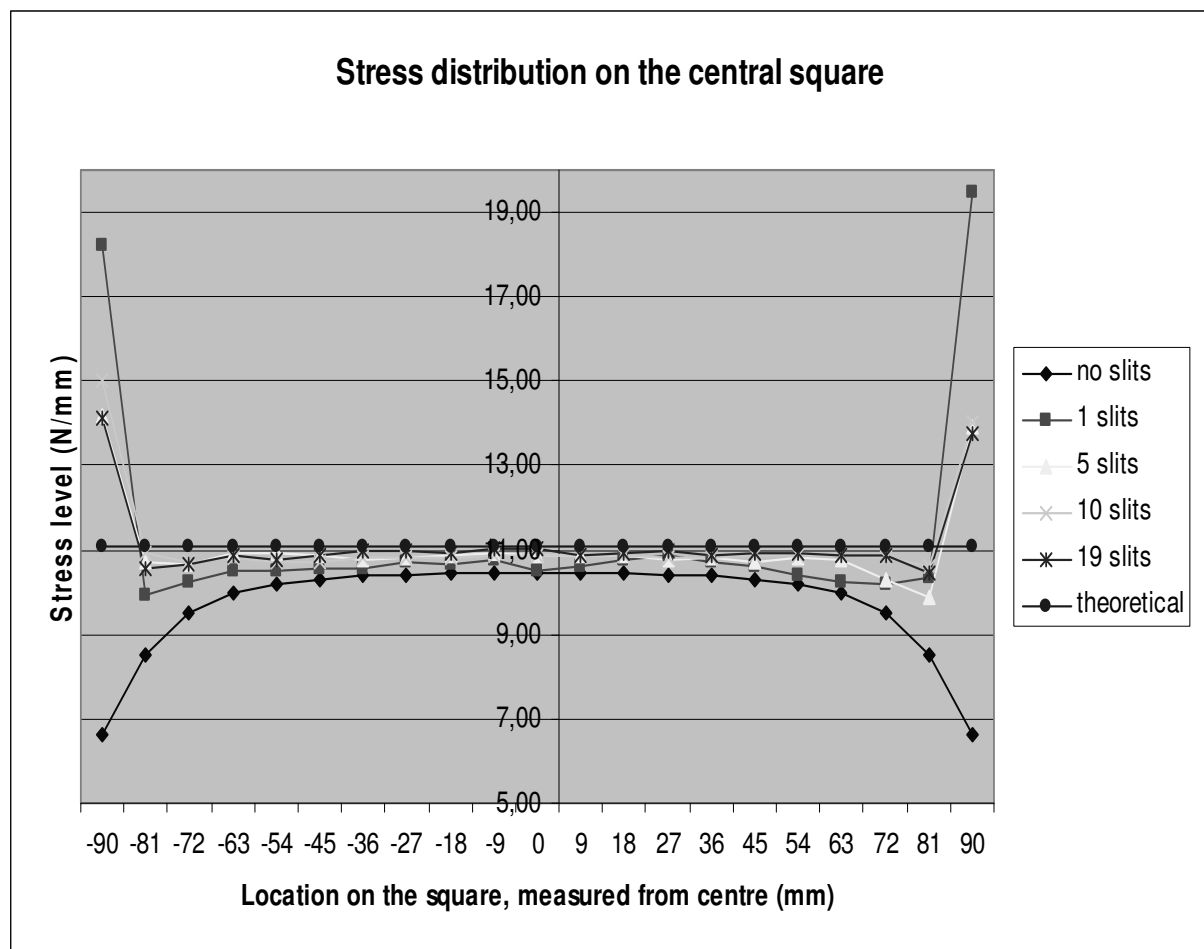


Figure 31: Stress distribution on the central square

As expected, the uniformity of the stress distribution improved when increasing the amount of slits, see Figure 31. Close to the edge of the square, side effects occurred. The influence of the side effects on the stress distribution decreased at a higher amount of slits. The sudden increase in stress magnitude at the edge of the central square is probably caused by a stress concentration around the end of a slit. The location of the path can be shifted, in order to remove these sudden increases of stress. The overall stress distribution is uniform over the central part of the square, with a decrease to zero at the end. The zero point of the stress distribution line lies outside the 180mm width of the central square. Therefore the plotted lines in the graph do not end at zero. To illustrate this, a plot is included from the no-slit configuration, measured on a larger width than the central square. It becomes clear that the stress magnitude eventually becomes zero, at approximately 50mm from the edge of the central square, see Figure 32.

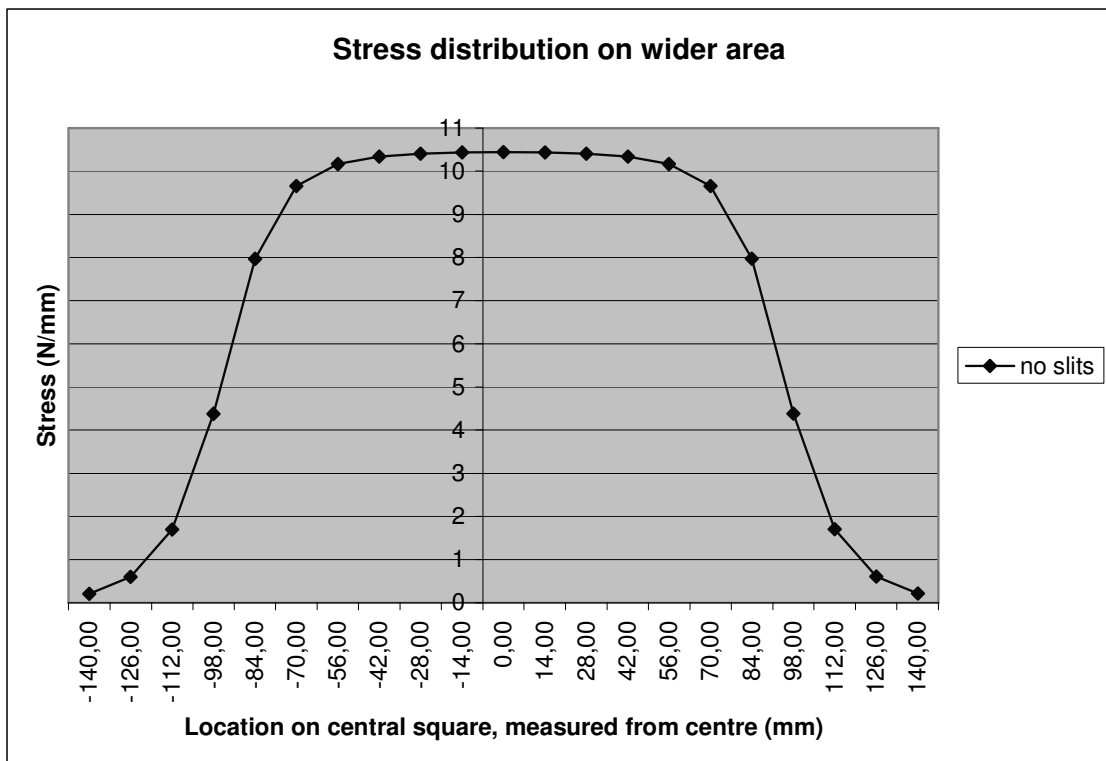


Figure 32: Stress distribution on a wider area than the central square

6.1.6 Sample configuration for the experiments

The aim of applying slits is to acquire a uniform stress distribution as well as an optimal stress magnitude in the central square. It is clear from the results that these two effects are closely related to each other.

By applying 10 slits in the cruciform arm, a uniform stress distribution is acquired in the central square. When taking the edge effects out of consideration, the average stress is 10,815 N/mm. With a theoretical stress magnitude of 11,11 N/mm, a reduction factor of 0,973 should be applied. The result is a uniform stress distribution with a known magnitude.

Ignoring the edge effects is justified when measuring the displacements on a smaller area with uniform distributed stresses.

The 19-slits configuration differs only slightly, and hardly noticeable, from the 10-slits configuration. Therefore it is more practical to apply only 10 slits in the cruciform arm, instead of 19 slits.

Comparable research from Bridgens (2005) resulted in a reduction factor of 0,95, which gives confidence in the used method.

An example of the sample with 10 slits is shown in Figure 33.

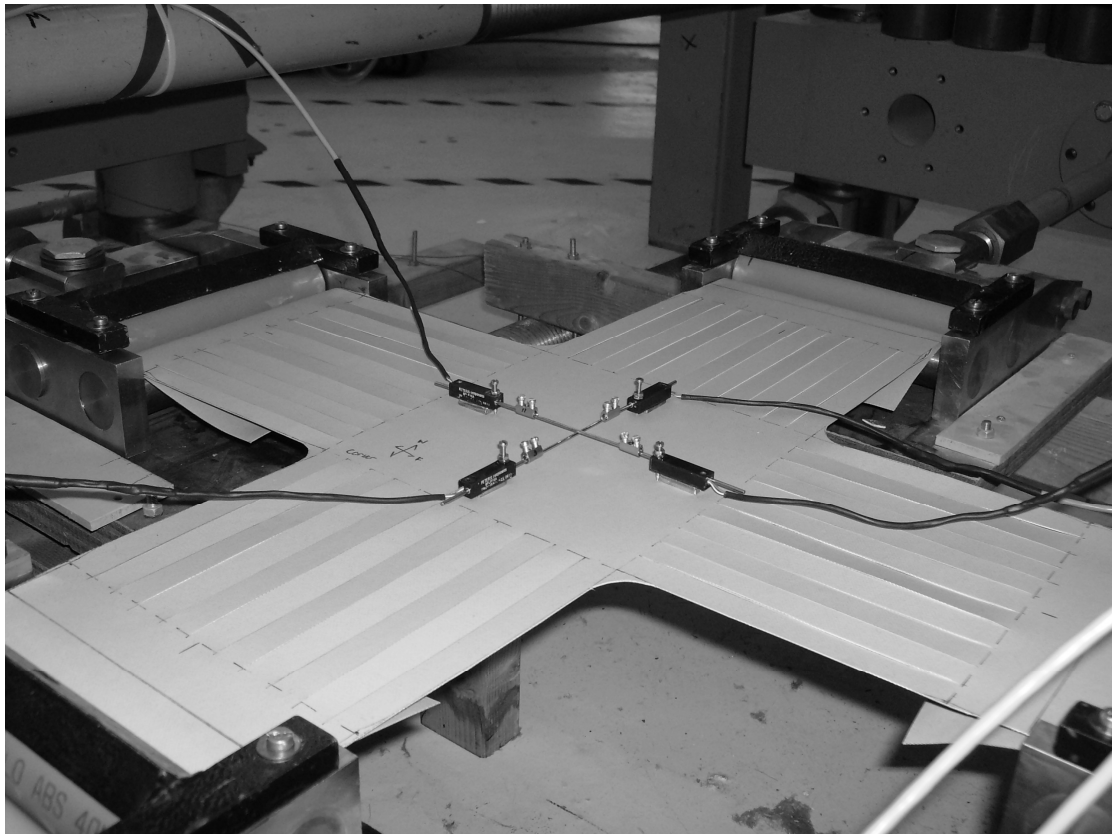


Figure 33: Sample with 10 slits in the cruciform arms

6.2 Potentiometers

In order to validate the potentiometers, different tests have been performed. A test with repeated loading cycles gives insight in the stiffening behaviour of the fabric. A test with repositioning the potentiometers gives insight in the sensitivity of the placement of the potentiometers on the fabric.

6.2.1 Setting

Potentiometers are used to record the displacement on the measuring square of the sample. In the previous section it has been shown on which part of the measuring area the stresses are uniform distributed. Anywhere on this area the displacements can be measured. From the original distance between the potentiometers and the recorded displacements, the strain of the fabric can be derived using the following relation.

$$\varepsilon = \frac{l_0 + \Delta l}{l_0}$$

where ε = strain, l_0 = original length and Δl = elongation of the fabric. This setup is shown in Figure 34.

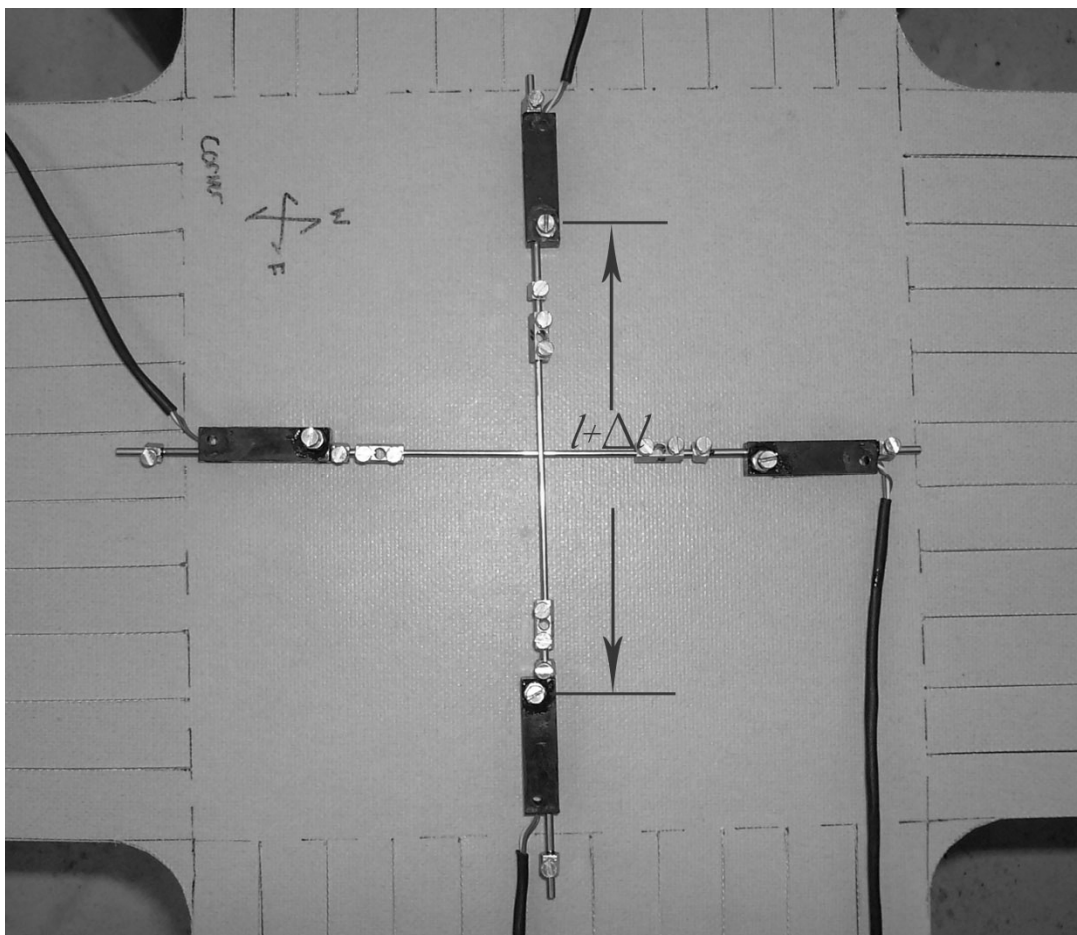


Figure 34: Potentiometers on the measuring area

The potentiometers are connected through a small rod. The range of both potentiometers added together gives a sufficient range to record the expected fabric strain. To avoid the potentiometers to access the non-linear, and at a point even non-

recording zone, some small mechanical devices are attached to the potentiometers. These devices are attached to the sliding rod, and prevent it from accessing the non-linear zone of its range.

The potentiometers are connected to the fabric by using a magnet and a small steel plate. The steel plate is glued to the bottom side of the potentiometer. The magnet is applied on the bottom side of the fabric, keeping the potentiometer in place. To avoid sliding of the sensor, a small medical needle is driven into the fabric. Damage to the fibres is minimized by applying a medical needle with a diameter of 0,3mm. This configuration is shown in Figure 35. The magnet is not shown.

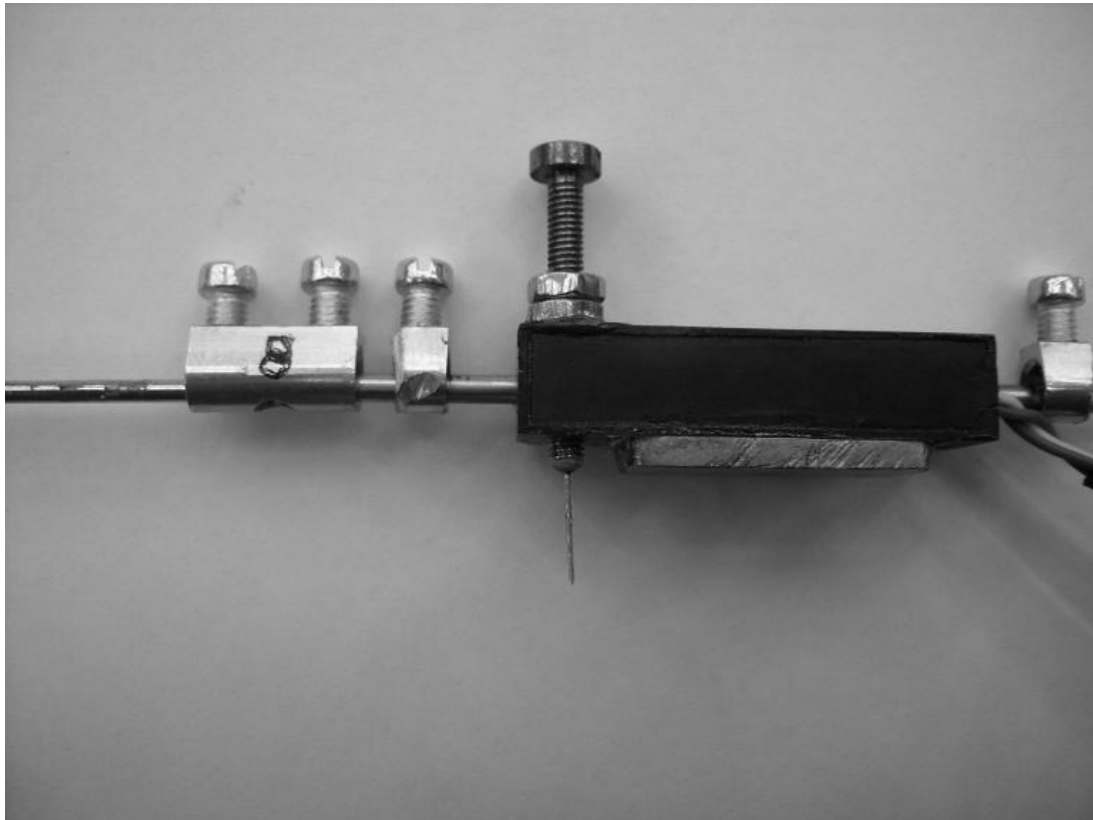


Figure 35: A medical needle ensures a fixed position of the potentiometer

The setting of the potentiometer is shown in Figure 36. It is plausible to state that the medical needle can be considered as the fixed point of the potentiometer. Although there is a reasonable amount of friction between the steel plate and the fabric, this friction is by far not as much as the friction of the needle into the fabric. To diminish any uncertainties about friction and fixed points, a rolling support is added to the potentiometers, to minimize friction between the steel plate and the fabric.

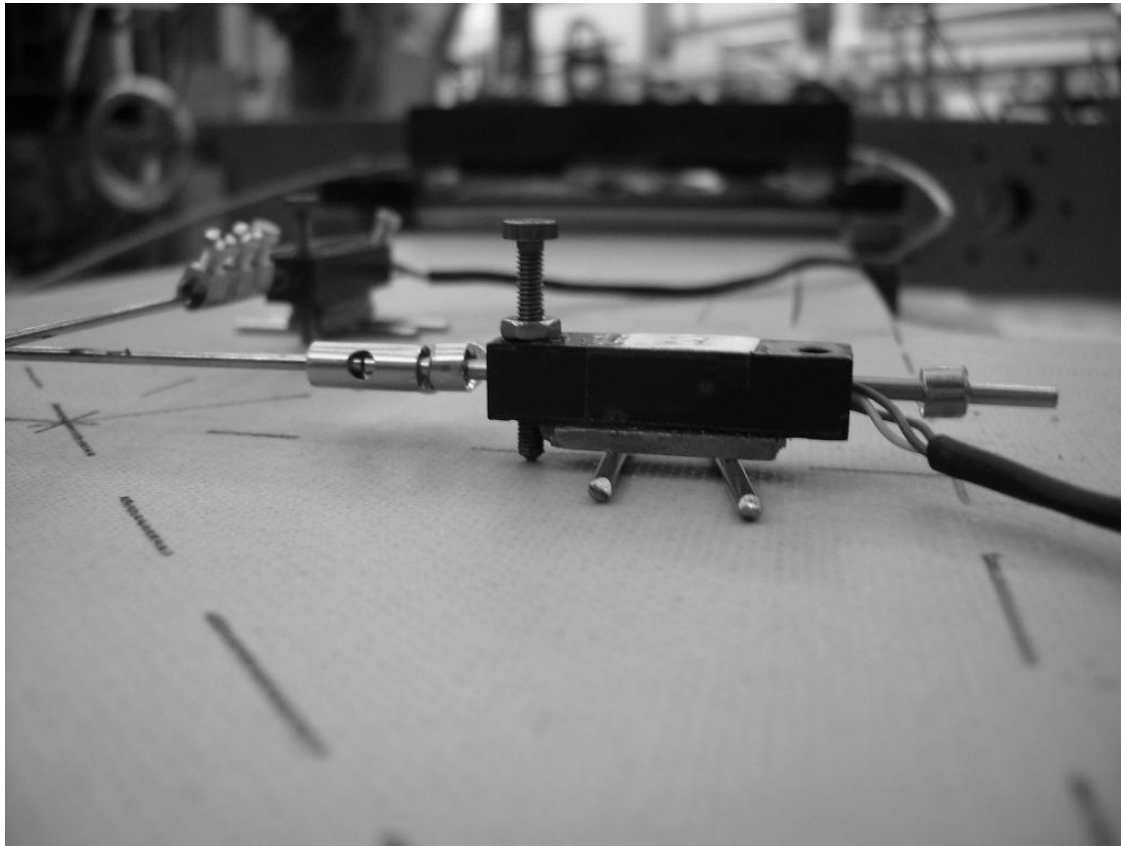


Figure 36: Potentiometer with rolling supports

The soundness of the potentiometers however must be proven by a test. In this test, both sets of potentiometers are placed parallel and next to each other on the fabric. This setup must result in identical strain data for both sets of potentiometers.

6.2.2 Reproduction of identical tests

A large set of repeated identical tests have been performed on the fabric to show the time dependant stiffening behaviour of the fabric. The fabric has been relaxed over night. After setting the fabric to prestress state, 10 tests have been performed on the fabric with the following characteristics.

Table 2: Test characteristics

Number of tests	10
Prestress state	500 N/18cm
Max applied force	5400 N/18cm
Speed	20 N/s
Load ratio warp:weft	1:1

The potentiometers are placed parallel, and symmetrical to the centre of the fabric, as shown in Figure 37.

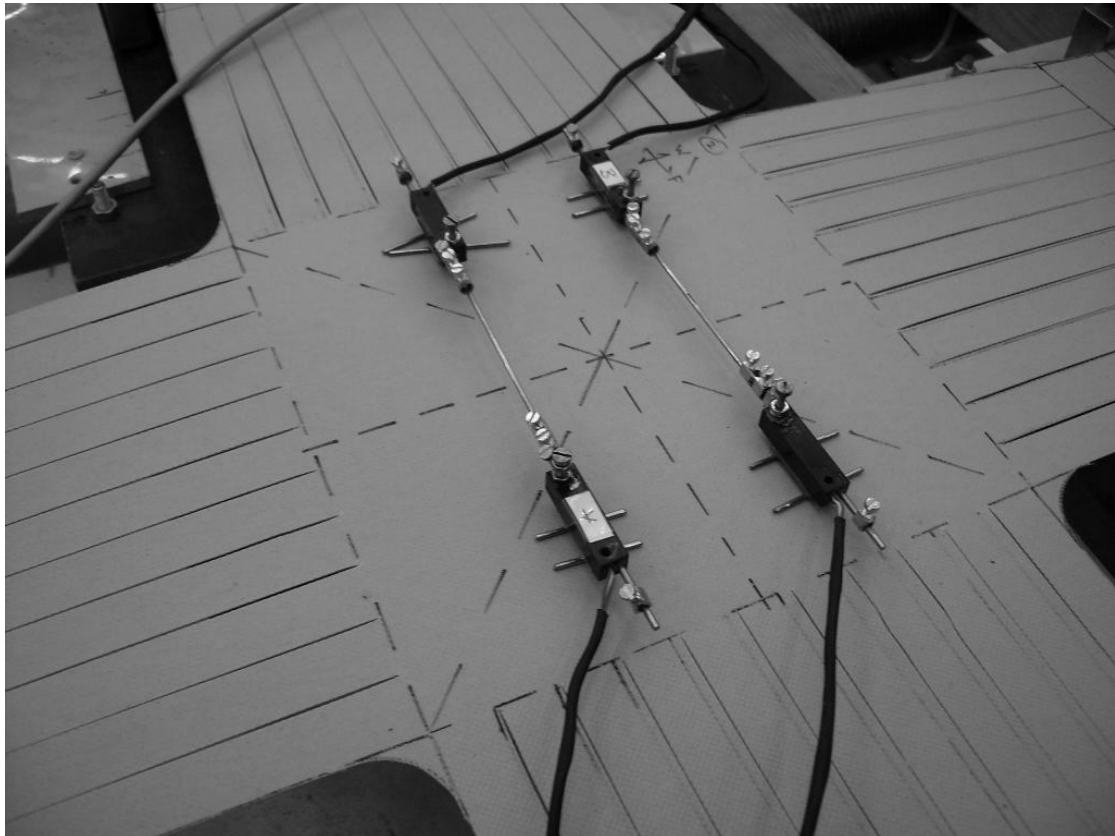


Figure 37: Parallel setup of the potentiometers

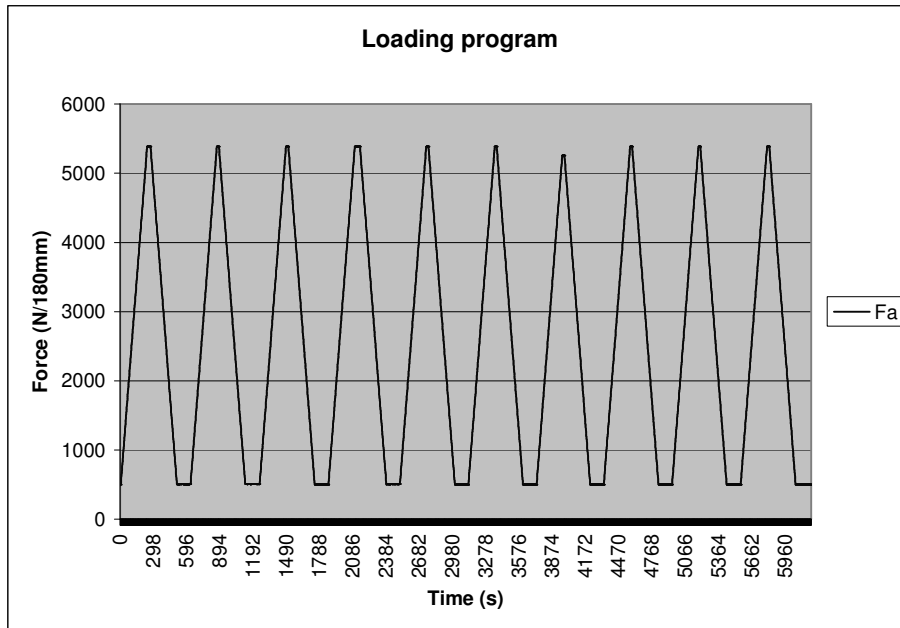


Figure 38: Loading program for repeated tests

The stiffening effect over time of the fabric can best be illustrated by a plot showing the Young's modulus of the fabric. The Young's modulus of the fabric is derived from strain-force relations. The Young's modulus is derived on 4 particular zones in the fabric. In other words, the non-linear stress-strain relation has been linearised on four parts of the plot. These parts are arbitrary chosen, and are parts of the loading path from prestress up to 5400 N. The Young's modulus is derived between 1000N and 2000N, between 2000N and 3000N, 3000N-4000N and 4000N-5000N. An example of a stress strain relation is shown in Figure 39.

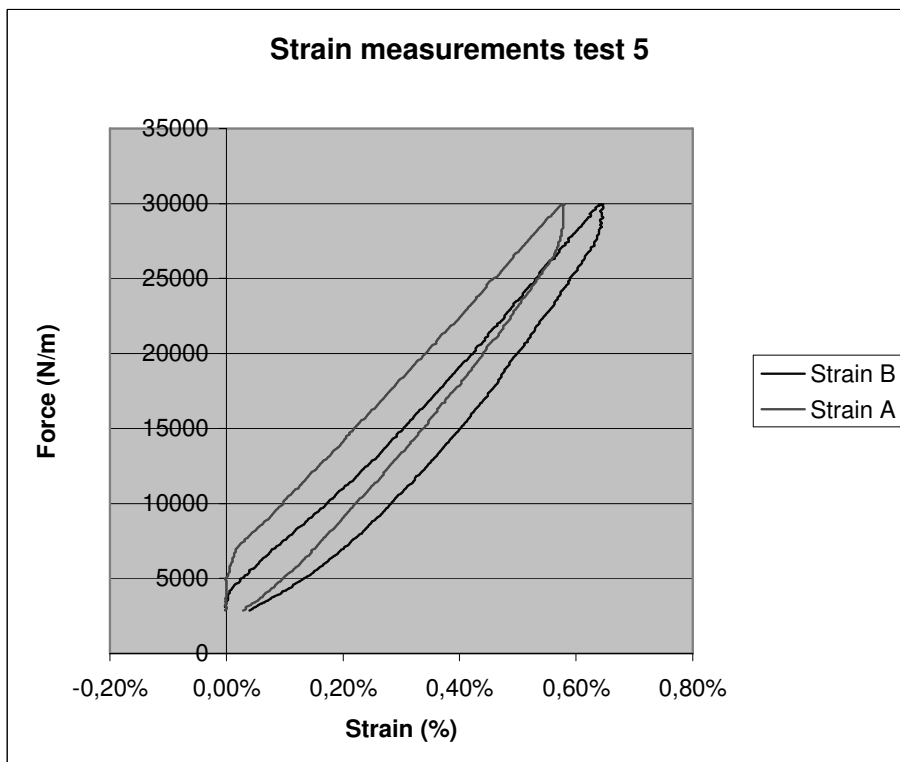


Figure 39: Force strain results for 5th test

It must be noticed that the potentiometer set A shows recording errors. The potentiometer reacts not immediately on the strain of the fabric. This error has been solved later on, before the real tests were performed. Figure 40 is based on the correct readings of potentiometer set B.

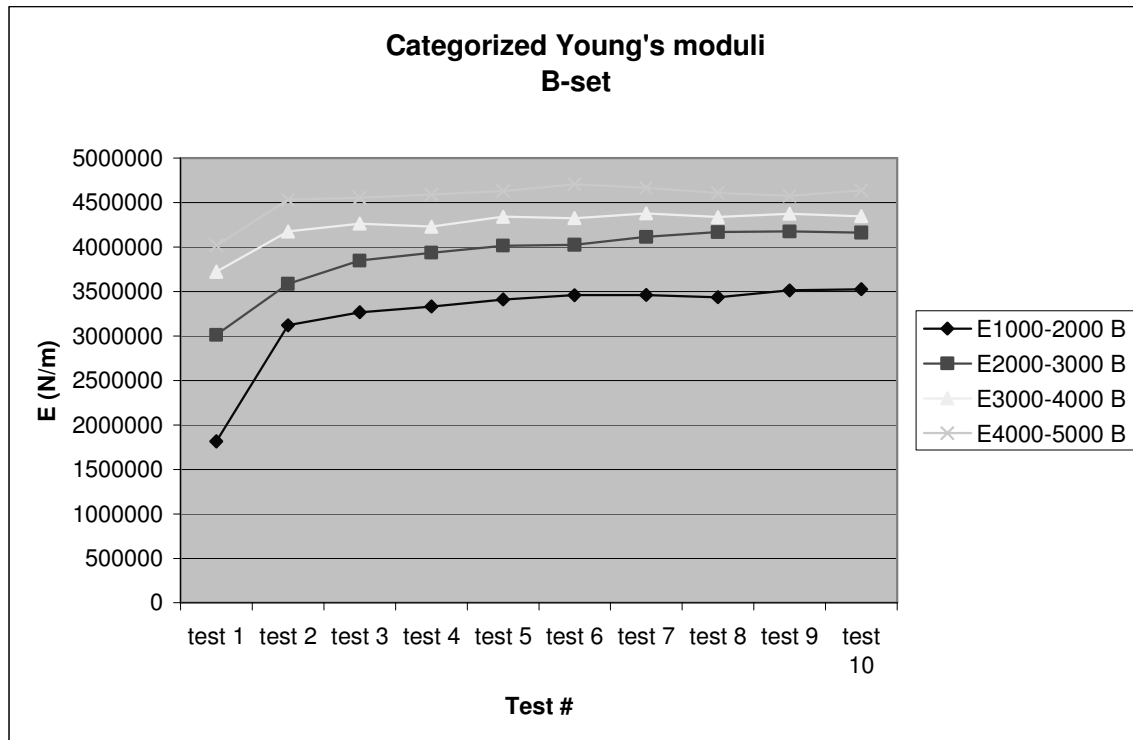


Figure 40: Young's moduli categorized

From this plot in Figure 40, it becomes visible that the fabric stiffens after the first tests, while the stiffness reaches a constant level, after about 4 repeated tests. This is an expected behaviour. The fibres tend to rearrange after the first tests. This rearranging of fibres involves large strains, resulting in a low Young's modulus. After the rearranging, the fabric tension is caused only by fibre stretching. The Young's modulus is increased, compared to the first tests. This behaviour is diminished with the conditioning protocol, which will be applied in the actual tests.

The plot in Figure 40 also shows that tests are not comparable and thus reproducible when tests are performed on a non-conditioned fabric. The conditioned state is reached after the third test. From that point the fabric is in a state where results are reproducible.

6.2.3 Repositioning of the potentiometers

During testing, the potentiometers are placed on the symmetry line of the cruciform sample. In order to determine the sensitivity of the positioning, a test is performed. Repetitive load cycles are applied to the fabric. The potentiometers are then picked up and replaced on the fabric on a slightly different position ($\pm 5\text{mm}$). This must give insight in the sensitivity of the positioning of the potentiometers.

As shown in Section 6.2.2, it must be considered that there is a stiffening effect in the first four repetitive load cycles.

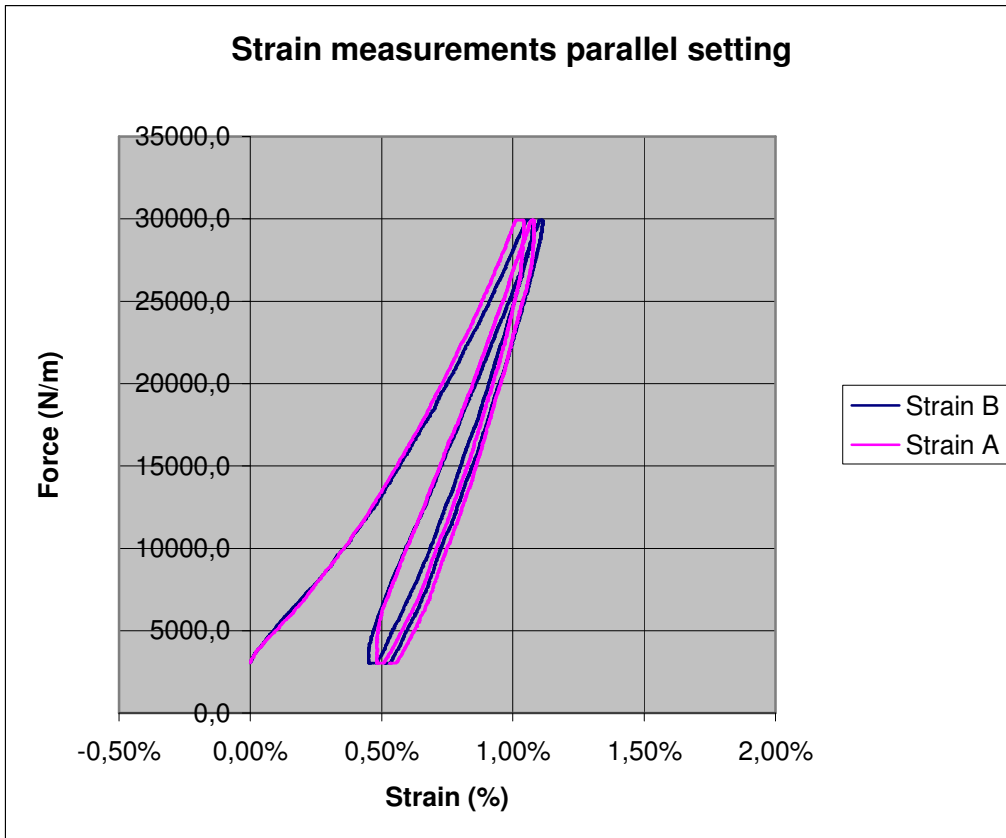


Figure 41: Strain measurements

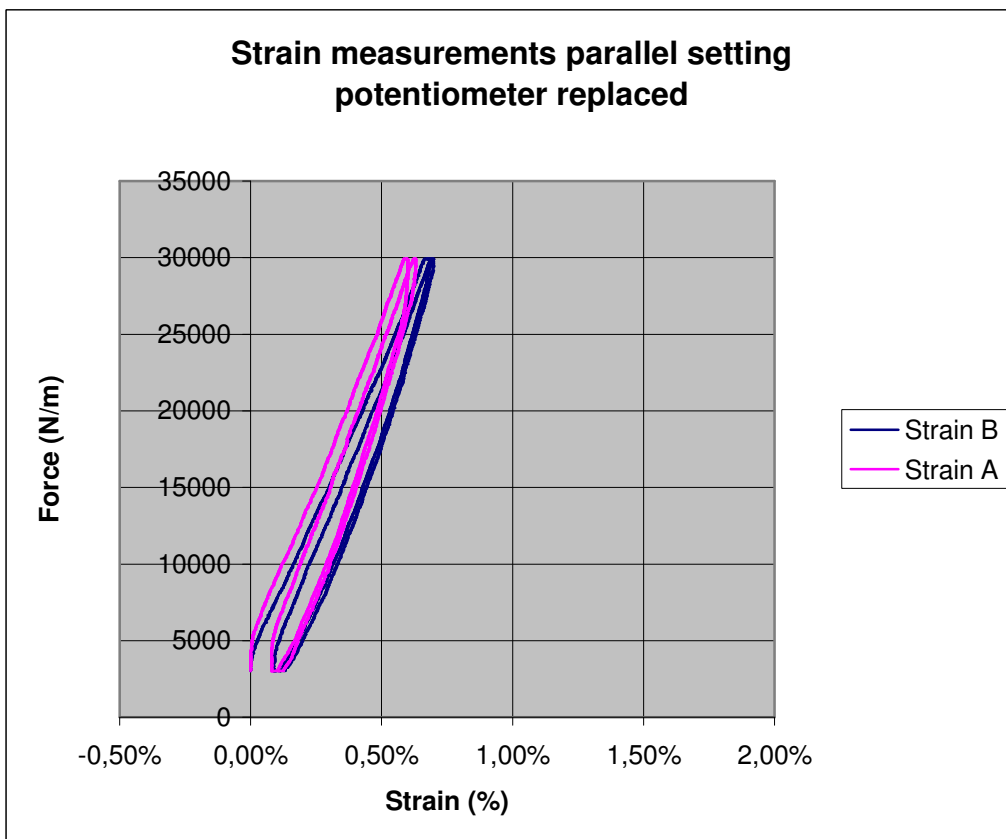


Figure 42: Strain measurements with potentiometers replaced

The plots in Figures 41 and 42 show that repositioning of the potentiometers has no significant effect on the strain recording. The permanent strain in Figure 41 should be neglected. This is caused by the rearranging of the fibres for this particular load ratio. After this rearrangement, the strain behaviour is elastic and reproducible. After changing the position of the potentiometer set, the strain recordings are similar with the previous setting. The conclusion is that the positioning of the potentiometers is not critical, as long as the positioning stays within the limits of around 5mm from the objected position.

7. Test results

In Chapter 6 the test method has been validated. From this point, tests are performed on a test square with known stresses that are uniformly distributed. The strain measurement devices are validated. The objective of the tests is to acquire data on the relation between bi-directional stresses and their corresponding strains. Tests are performed according to the test regime that is described in Chapter 5.4. The results of the bi-axial tests are presented here. A theoretical setup for a material model is also presented in this chapter.

7.1 Conditioning of the sample

The test samples are cut out of a role of fabric. The width of a role is 2450 mm. The samples are coded, according to Figure 43. Unused fabric samples are also coded, in order to be able to analyze possible abnormalities in the test results. Future references to fabric numbers can be derived from Figure 43.

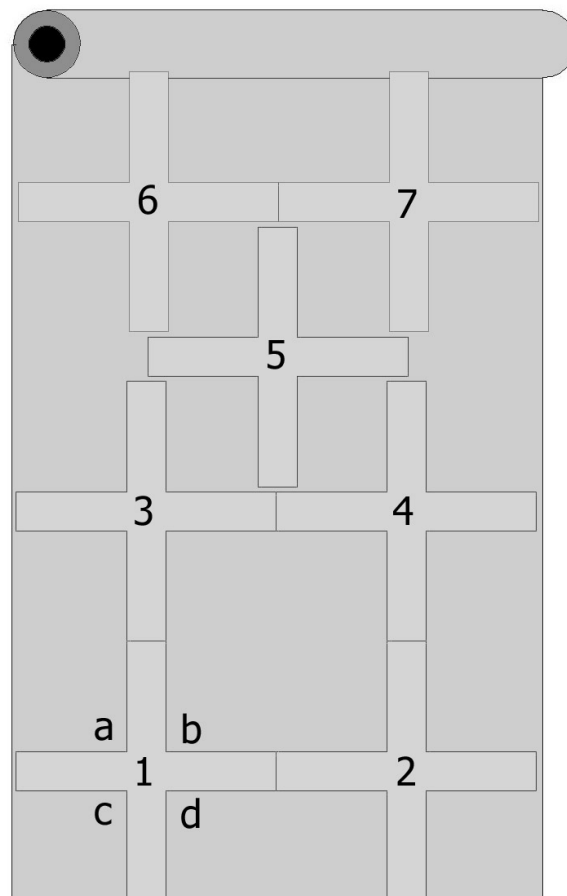


Figure 43: Fabric codes

The test pieces are kept under prestress in both warp and weft direction for a period of 17 hours. The prestress is set at 2,5% of the strip Ultimate Tensile Strength (UTS). UTS values are derived from the manufacturer's datasheets. After the 17 hour during prestress, the test samples are conditioned. The conditioning process consists out of a number of loading cycles. The objective of the conditioning process is to remove permanent strain from the test piece.

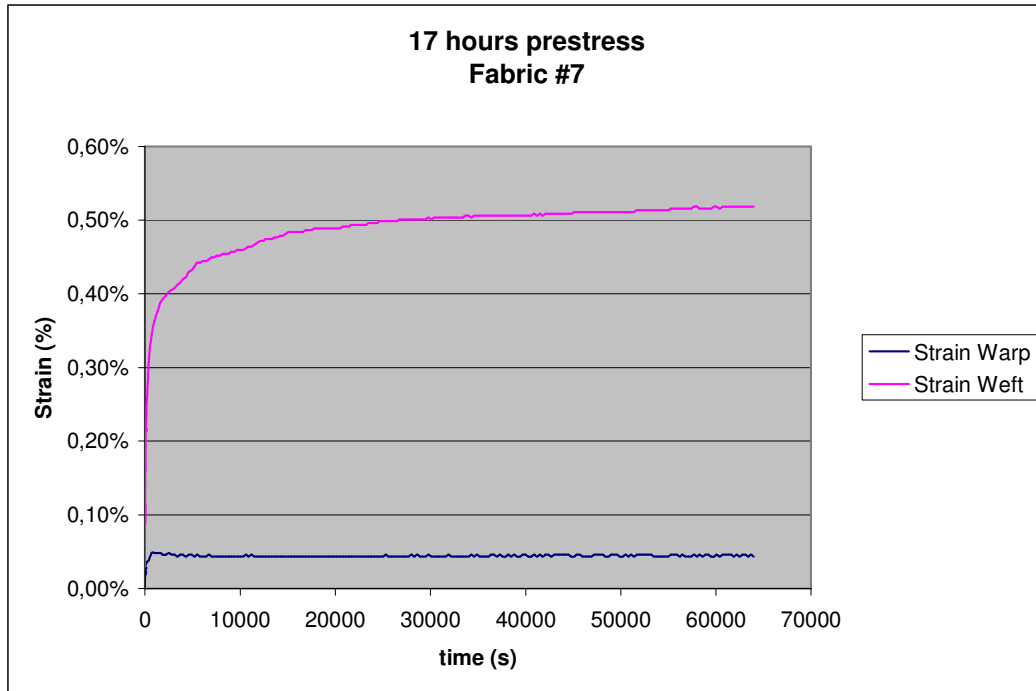


Figure 44: Example of 17 hours prestress

The conditioning procedure consists of a number of repeated loading cycles, see Chapter 5.2.3. The purpose of these load cycles is to remove permanent strain from the fabric. With the permanent strain removed, the fabric behaviour is similar to the *in-situ* condition of fabric.

In table 2 the conditioning procedure is shown.

Table 3: Conditioning procedure

Time (minutes)	Warp	Weft
0-5	Prestress	Prestress
5-10	Conditioning Load	Conditioning Load
10-15	Prestress	Prestress
15-20	Conditioning Load	Prestress
20-25	Prestress	Prestress
25-30	Prestress	Conditioning Load

The results from the conditioning process show that the fabric does not show large additional strains in the fabric. The strain measuring devices are set to zero strain at the start of a conditioning process on a test piece. Therefore all plots start at zero strain.

The loads from the conditioning process are programmed manually in the control software. Therefore it is possible that small errors are made. The duration, at which loads are kept constant, is not always exactly as prescribed. An error in activating the hydraulic actuators occurred during the conditioning of fabric sample 5.

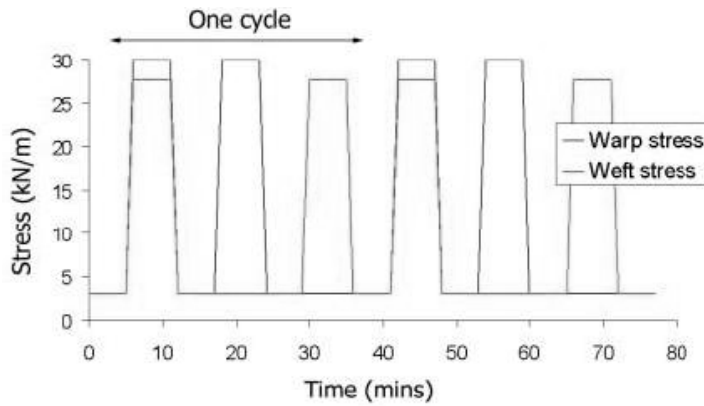


Figure 45: Conditioning program (two cycles)

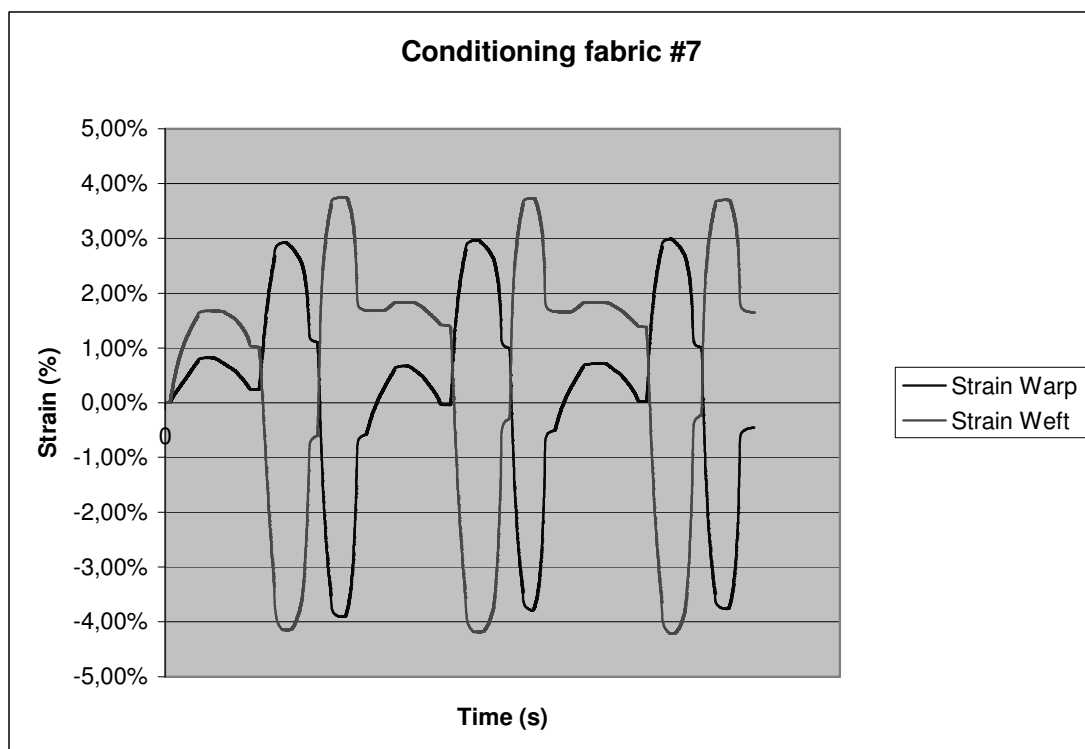


Figure 46: Conditioning fabric 7

7.2 Test results of biaxial testing

With permanent strains removed from the fabric, the fabric behaviour is comparable to *in-situ* conditions. Therefore the results obtained from fabric testing on conditioned fabric are useable for structural analysis of membrane structures.

The fabric is tested according to the test regime described in Chapter 5.4. The fabric is tested in a biaxial way, at various preset force ratios between the two fibre directions. Testing in a biaxial way includes biaxial interaction between the fibres in the test results. This can not be achieved by uniaxial testing, see also Chapter 5.2.

The reference state from which the tests are performed is the prestress state. This is the state from which structural analyses are performed. Loads are applied to the structure (and thus geometry), as it is *in-situ*. Only prestress stresses act in the fabric.

This state is also considered to be the reference state at which no strains are present in the fabric.

The preset stress ratios at which the biaxial tests are performed are stated in Figure 23. These load paths are the theoretical load paths. Strains are measured continuously during a load path. The actual performed load paths are stated in Figure 24. The plots indicate the accuracy of the independently controlled hydraulic actuators of the biaxial testing machine.

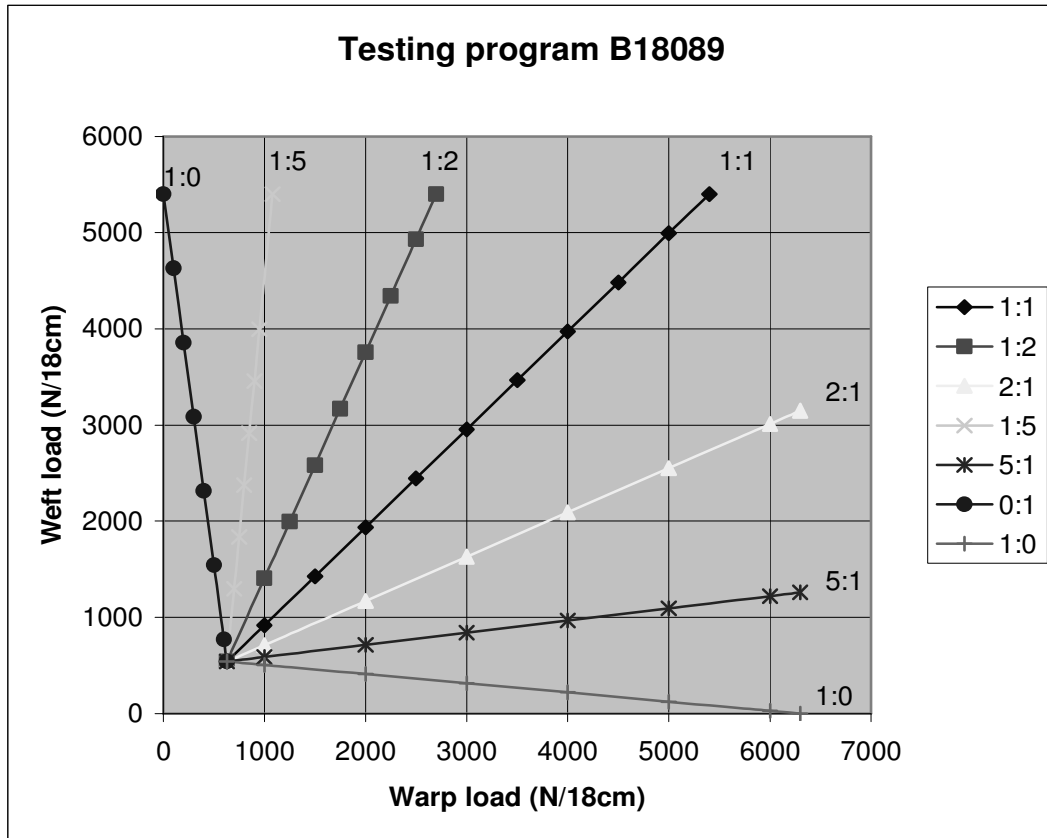


Figure 47: Theoretical load paths for fabric quality B18089

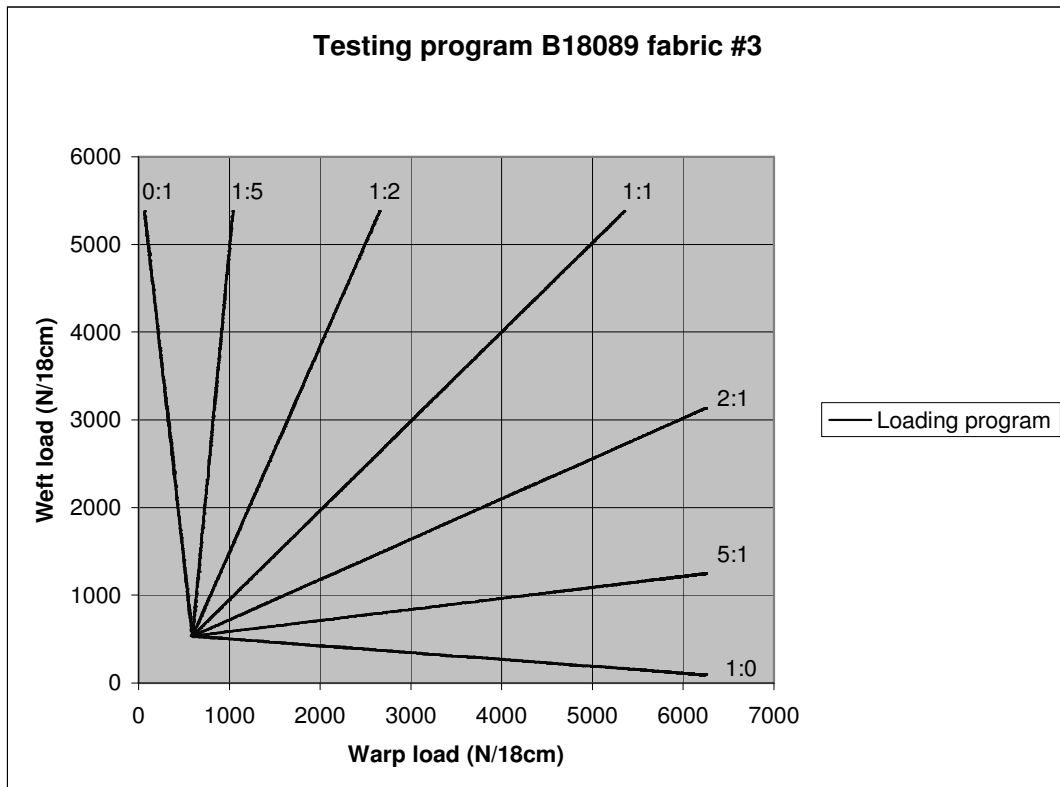


Figure 48: Actual load paths performed during testing

Representing the results can be done in various ways. However, for the purpose of comparing results from different fabric samples it is sufficient to plot the results in a 2 dimensional graph. This way of representing the test result gives a quick overview of the fabric strains in the various tested force ratios. It enhances comparison between fabric samples. Representation of the results, suitable for application in the material model is explained in Chapter 7.3.

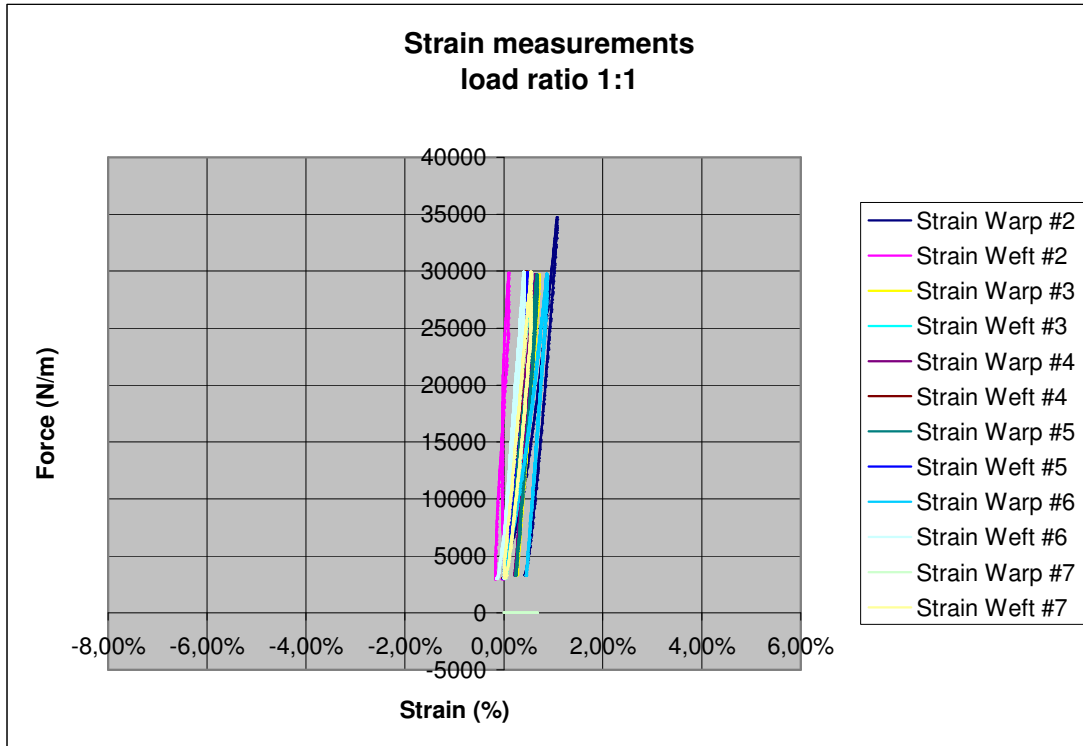


Figure 49: Strain measurements for load ratio 1:1

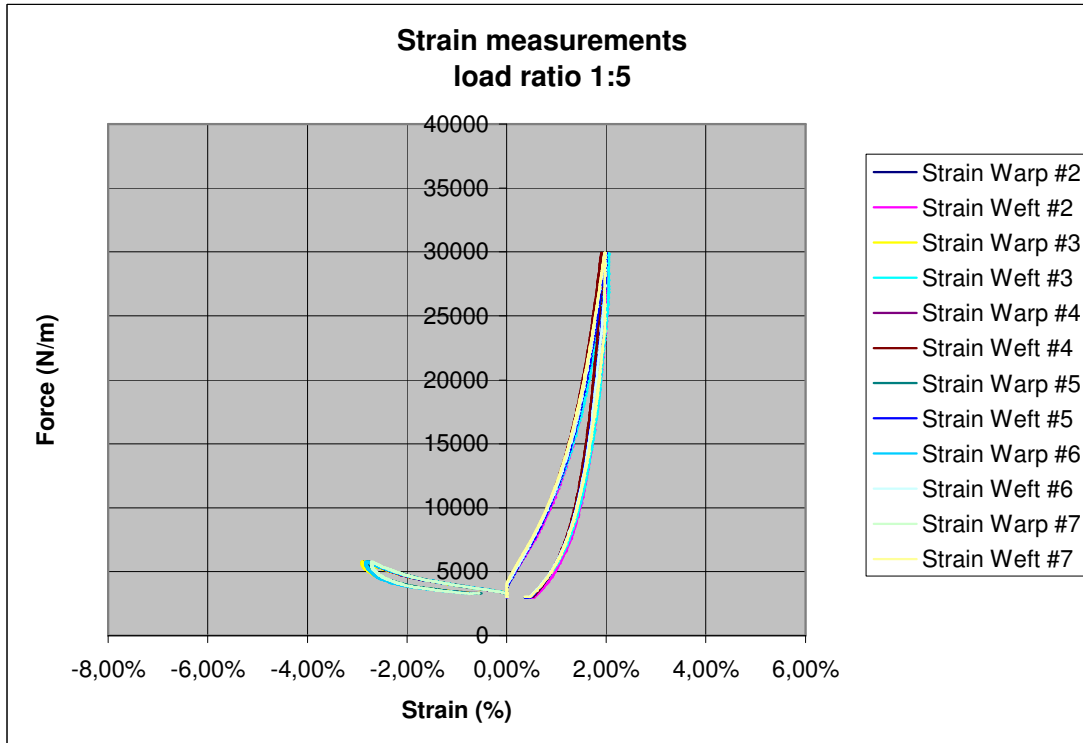


Figure 50: Strain measurements for load ratio 1:5

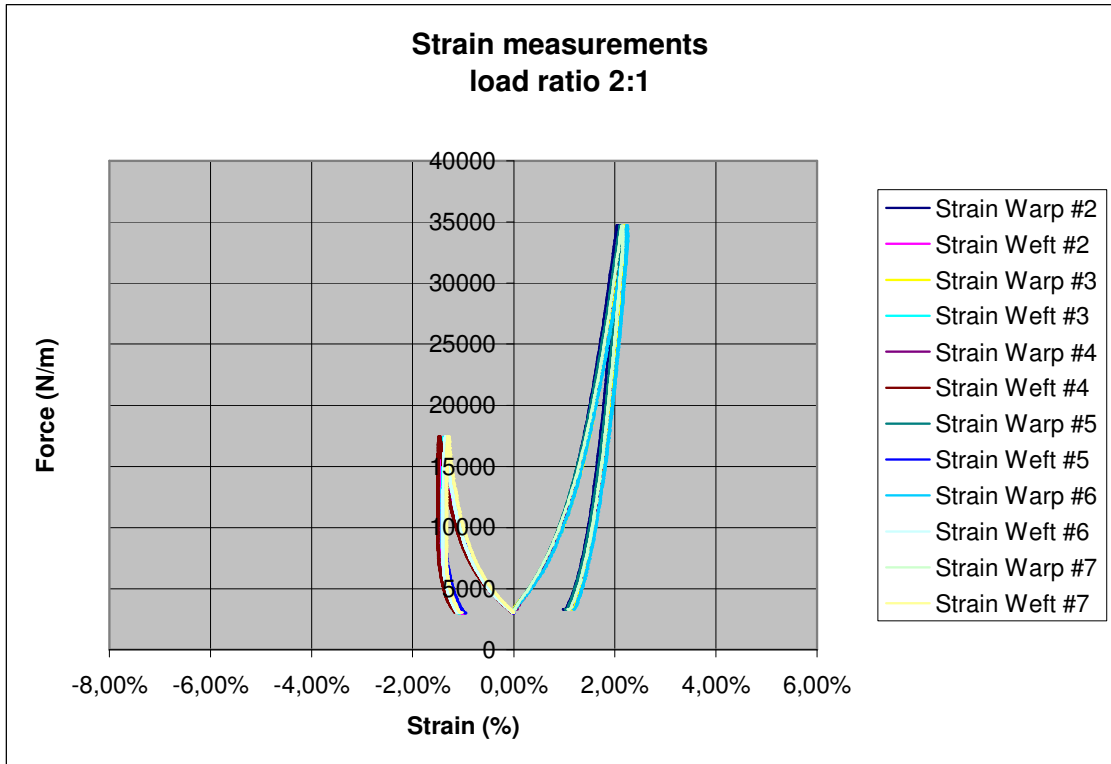


Figure 51: Strain measurements for load ratio 2:1

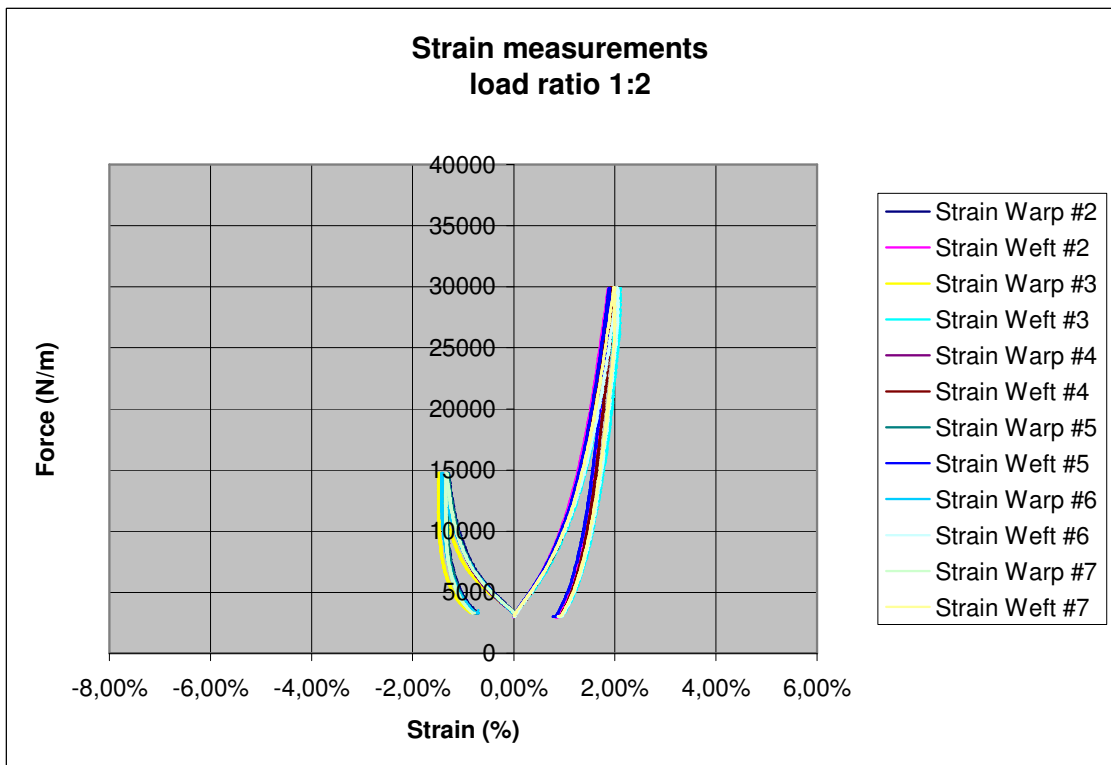


Figure 52: Strain measurements for load ratio 1:2

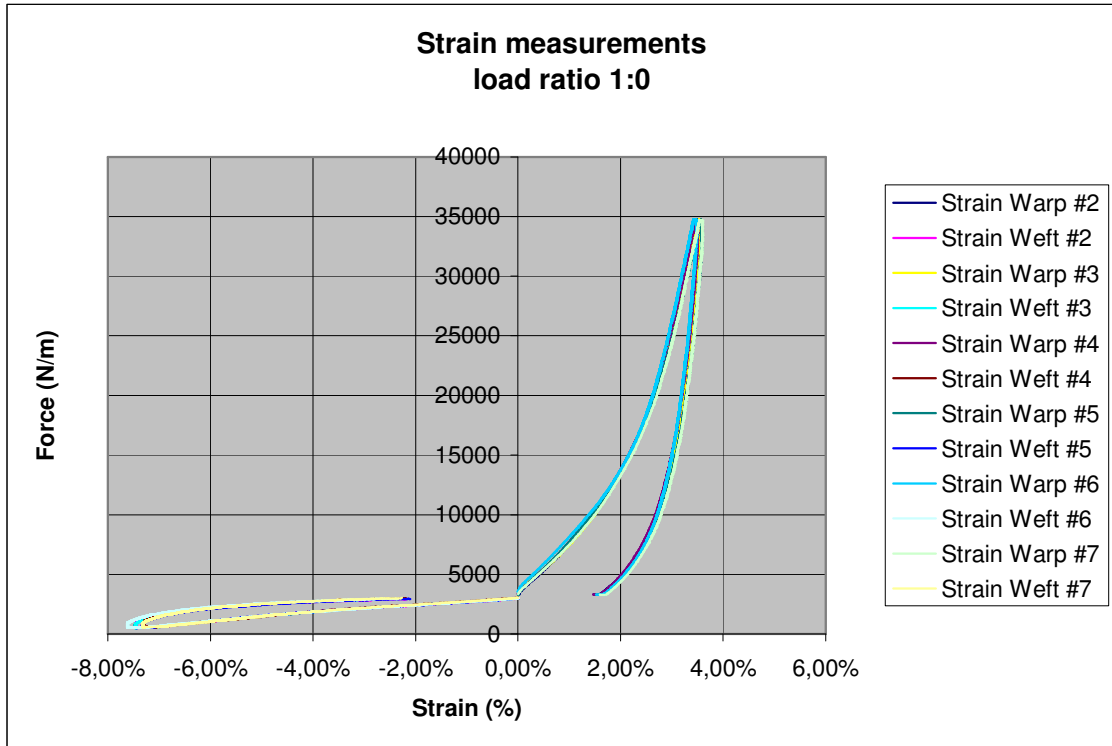


Figure 53: Strain measurements for load ratio 1:0

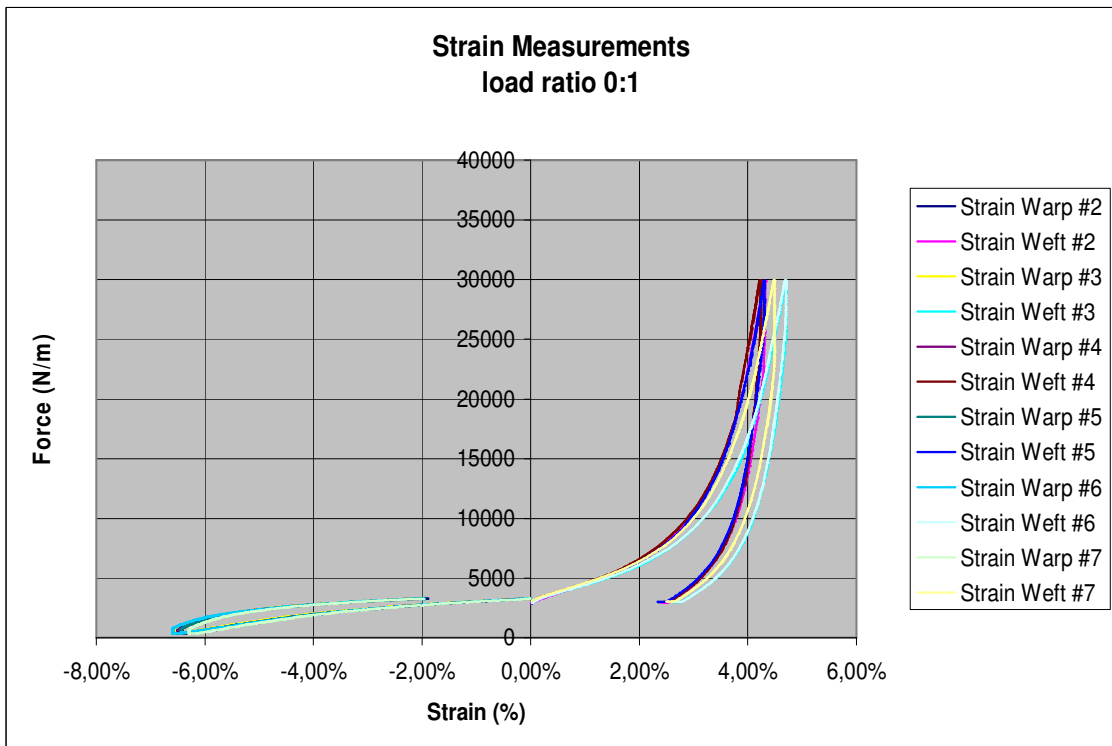


Figure 54: Strain measurements for load ratio 0:1

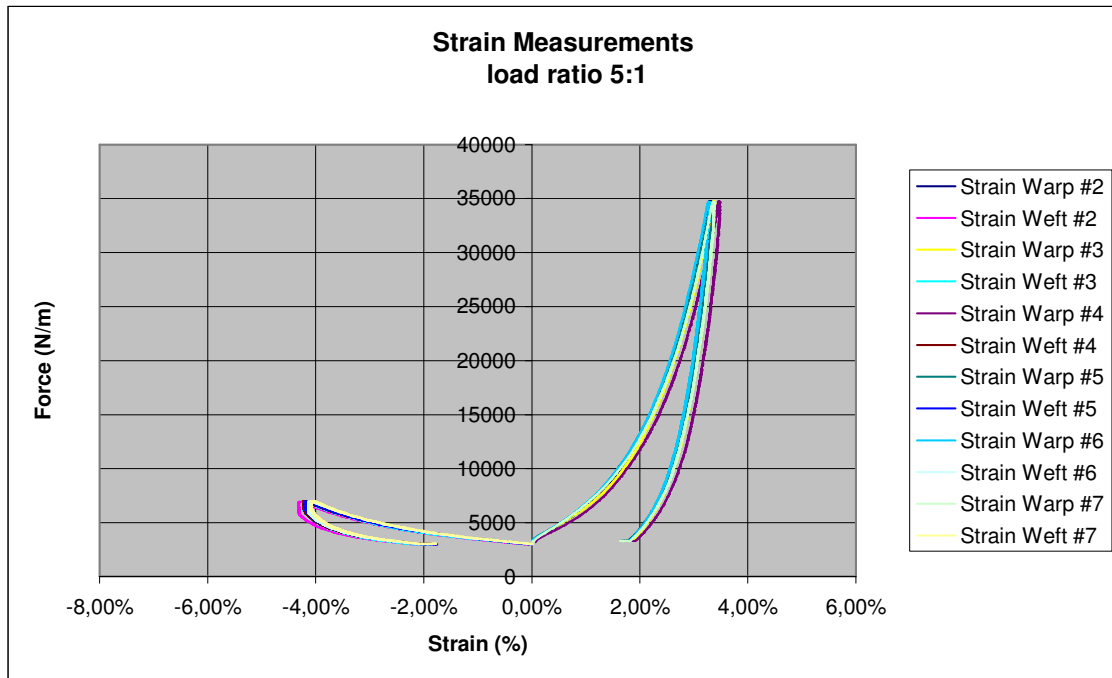


Figure 55: Strain measurements for load ratio 5:1

From the results it becomes clear that the fabric shows non-linear strain behaviour. In addition to the nonlinear strain, the plots also show the biaxial interaction, causing different strain behaviour for various stress ratios. These results confirm the statement that fabric behaviour can not be described by a linear stress-strain relation, using a single Young's modulus for all stress ratios.

The plots show that for a number of stress ratios, permanent strain is present in the fabric. For modeling purposes these strains must be deducted from the strain results. The fabric shows a difference in loading and unloading strain behaviour. This hysteresis effect results in both a loading response and an unloading response. This effect needs to be taken into account when modeling the fabric behaviour, see Section 7.3.

The plots show a certain deviation, which must be taken into account. Apparently there is a certain variation in the fabric properties along the length and width of a role of fabric. In order for the material model to be appropriate for all fabric samples, the spreading and deviation must be taken into account, when modeling the fabric properties.

7.3 Material representation

In order to use the acquired material data as an effective tool for a structural analysis, the data will be put in a model. The model contains information on the strain of the fabric, as well as on the stress acting in the fabric. Each of these parameters has both a warp and a weft component.

From a structural analysis in a finite element program (Ansys in this case), it is possible to acquire the strains that act in the different elements. From that point it is possible to feed the strains in both fibre directions (warp and weft) to the model, and get the corresponding stresses in return. These stresses are on their turn linked to the elements, after which the geometry is updated. In an iterative way, this process is looped until the elements reach their equilibrium state. This equilibrium state means

that the internal element stresses equal the external applied load, such as wind or snow load.

From the experiments a wide set of data is gathered, corresponding with various stress states. The stress states in between the data must be interpolated in order to create a complete data set. The stress states that have been tested are warp:weft 1:1, 1:0, 0:1, 1:2, 2:1, 1:5, 5:1. Stress states such as 1,3:1 or 1,7:1 must be found by interpolating the existing data.

The data consists out of four variables, namely stresses and strains in both warp and weft direction. These variables can be represented by $\epsilon_w, \epsilon_f, \sigma_w, \sigma_f$, where ϵ represents the strain and σ represents the stress. Index w represents the warp direction of the fabric, and index f the fill direction (fill is also called weft). The data with these four variables can best be represented in two three-dimensional graphs, creating surfaces from connected data points. The strains of the fabric can be plotted on the x and y axis, while the corresponding warp or weft stress can be plotted on the z axis.

The material model consists of a set of mathematical formulas that describe the relation between the fabric stresses and strains. For a given strain, the material model can calculate the corresponding material stresses. In order for the finite element program to be able to communicate with the model, the model must be written in FORTRAN and stored in a *User Supplied Subroutine*. The general form is shown in Figure 56.

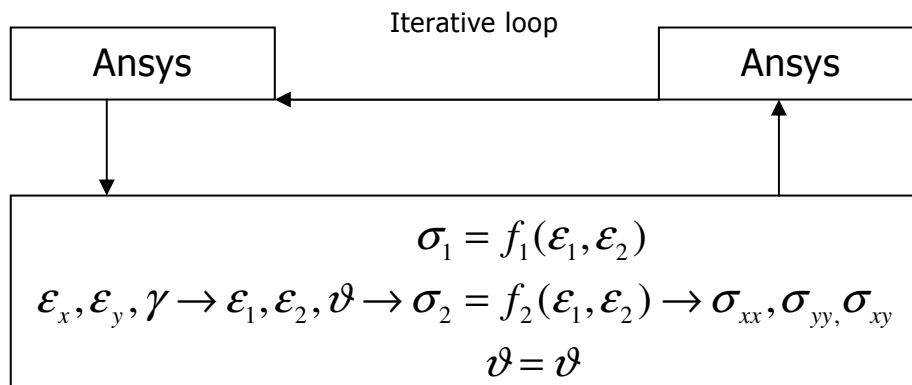


Figure 56: General form of the fabric material model

In the finite element analysis the warp direction will coincide with the first principal direction and the weft direction will coincide with the second principal direction. In a good design this will be approximately the case, however, for some designs and some load cases it will not.

It would be too much work to develop a general material model that can also describe shear in the warp and weft directions. Surely, the effect of this assumption needs to be investigated in a follow up project, see Section 11.2 Recommendations.

The assumption gives a substantial advantage for design in that the warp and weft directions do not need to be specified in the finite element model, which would be very time consuming.

8. Material model

In Chapter 7 the results from the experiments are presented. These results are presented in 2-dimensional graphs, which are suitable for comparing test results from different fabric samples. However, understanding and interpreting the complete fabric behaviour over the complete range of force ratios asks for a 3-dimensional way of presenting the test results. In this chapter the test results are analyzed. By applying various techniques, a model is created that describes the fabric behaviour.

8.1 What to represent in the model ?

Before creating any model, it must be clear what the model needs to represent. In addition, also the purpose of the model must be defined in order to use the data properly.

The model of the fabric behaviour is the link between the calculated material strains, and the corresponding material stresses. The finite element program will introduce strains in the elements, after which the model can return the corresponding stresses. The finite element program checks if the internal stresses are in equilibrium with the externally applied loading on the fabric. If not, the strain will be adjusted, until an equilibrium situation is reached. This iterative process is repeated multiple times until the solution meets the accuracy that is demanded.

This iterative process that is described above was already mentioned in Chapter 7. This process is illustrated in a flowchart in Figure 57. The chart shows how the strains in two directions are input to the model. The model converts these strains in the strain of the main fibre directions of the fabric, the warp and weft direction. By using a mathematical formula, representing the stress-strain relations of both fibre directions, the corresponding stresses can be computed. These stresses in turn are returned to the finite element program, Ansys. The elements are recalculated with these updated element stresses. An equilibrium situation in the fabric is reached as soon as the internal stresses equal the external applied load. The process will be repeated until this situation of equilibrium is reached.

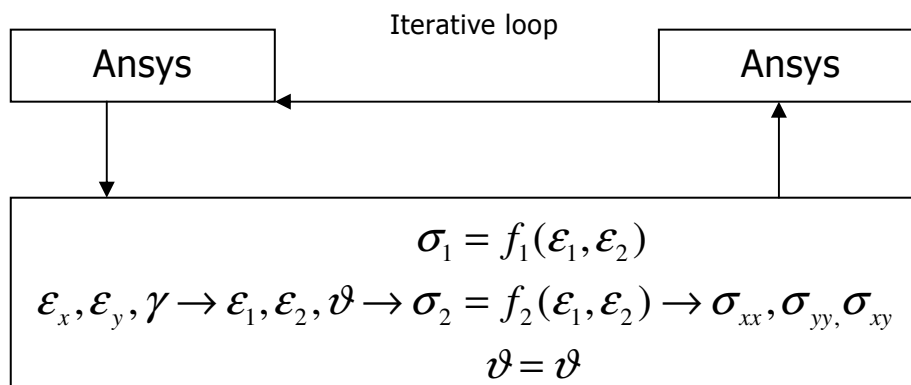


Figure 57: Iterative process to reach equilibrium situation in the structure

From the test results presented in Chapter 7 it becomes clear that there is a certain hysteresis effect in the fabric. This hysteresis effect means that the fabric does not return to its original strains after unloading the fabric. A certain amount of strain is still present in the fabric after unloading. The test protocol has been designed in such way, that these effects are kept at a minimum. It is important to explain how these effects need to be taken in account when creating a material model.

The purpose of this material model is to determine stresses and deflections in the fabric, when external loads are applied on the fabric. In an iterative way the elements in the finite element model will change their strains, and thus their stresses, in order to obtain an equilibrium situation with internal stresses and external applied loads. From this point, two different directions can be chosen with respect to the choice of data for the model.

On one hand, in the iterative process, the changing strains in the elements can be seen as loading and unloading behaviour of the fabric, corresponding to two different loading and unloading curves. An increasing strain would follow the path for loading, while a decreasing strain would follow the unloading path. This would mean that if an element would change from increasing strain to decreasing strain, the response behaviour would lie somewhere between these two loading and unloading curves. With other words, the response would lie in the volume, created by the upper loading curve, and the lower unloading curve.

This interpretation would result in two response surfaces (3 dimensional) and the volume that is included between these surfaces. The exact behaviour within this volume is uncertain, since it has not been tested. Therefore an average surface, the mean from loading and unloading, can be created in order to use just one surface. This solution simplifies the complex behaviour in the response volume by using just one surface.

On the other hand, the iterative process can be interpreted as a numerical process and not as a physical process. The increasing and decreasing of strains in the elements during the calculation process is the result of the iterative way of finding an equilibrium situation. It is not an actual physical process in the fabric. The physical process would be the fabric going straight to its equilibrium situation after applying an external load. This behaviour is included in the loading curve of the fabric response. The only way the fabric will unload, is when the fabric loses its prestress. Even that behaviour is included in the loading curve. For reference, see Section 5.4 'Test procedure'.

With this interpretation it would mean that the response surface can be created by using only the loading data from the experiments. The unloading data can be ignored, and is only useful for purposes in the field of analysis of residual strains after loading.

The purpose of the material model was described earlier. The material model is the link between the calculated fabric strains and the corresponding fabric stresses. The material model must provide material stresses when a stressed membrane structure is analyzed by applying external loads such as wind loads or snow loads. As a result of these applied loads, the structural analysis must provide information on material stresses and deflections. Therefore the model will be based on the loading data only. In that way the model will serve the purpose stated earlier.

In future studies, a more complex material behaviour may be described in order to predict material behaviour on repetitive loading cycles. In that case the unloading data must be included, and possible the volume created by these two loading and unloading curves.

8.2 Stress-stress-strain relation

One way of representing the test data is by using stress-stress-strain graphs. In this type of 3D graphs, both warp and weft stresses are plotted on the x and y axis, while the corresponding strain, in either warp or weft direction of the fabric, is plotted on the z axis. This results in 2 different graphs, one for warp strain and one for weft strain.

Since the fabric stresses are depending on both warp and weft strains due to the biaxial interchange between the fibres, it is essential to include both warp and weft stresses in

the plots. In other words, the fabric strain is depending on two independent variables, namely warp stress and weft stress.

Input Data •

(unlicensed copy)

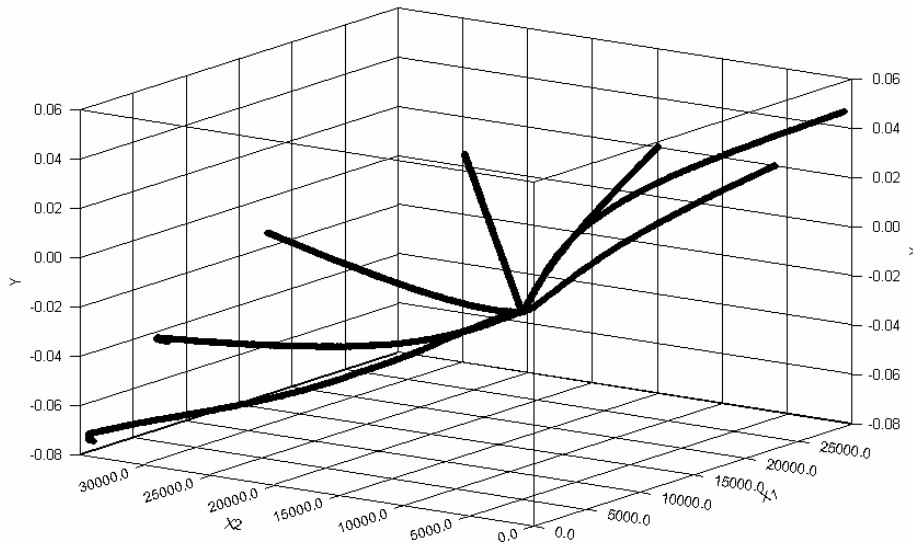


Figure 58: Stress-Stress-Strain (x,y,z) data for weft fibre direction

In Figure 58 the strain response in weft direction is shown, as a function of both warp and weft stresses. The strain curves all have their origin at zero strain. This does not mean a physical zero strain, but this reference level is the prestress level of the fabric. In Chapter 5 this was already discussed. In this way the additional strain, or deflection, can easily be calculated in a structural analysis, based on the reference zero strain.

From Figure 58, the biaxial interchange between both fibre directions becomes visible. A horizontal imaginary surface would indicate that there is no interchange between both fibre directions. However, when looking at Figure 58, it becomes clear that there is a clear dependency between both fibre directions. An imaginary surface through the curves would result in a tilted surface, indicating an interchange between the two fibre directions.

From the figure it becomes also clear that there is a non-linearity in the stress-strain behaviour. This conclusion is not only drawn based on this figure, this was already clear from the test results presented in 2D plots in Chapter 7. See Section 7.2.

By using a curve fitting technique it is possible to create a surface that fits the available data. With this surface it is possible to predict material response for untested areas. Since all experiments cover a wide range of possible warp-weft ratios, the global shape of a surface through this data does not indicate any sudden changes in the surface steepness. Therefore it is assumed that the surface has a gradual slope, and fits all available data.

By using a software tool called DataFit, it is possible to fit a surface through the available data using non-linear regression techniques. To illustrate this, two plots are created from both warp as weft strain.

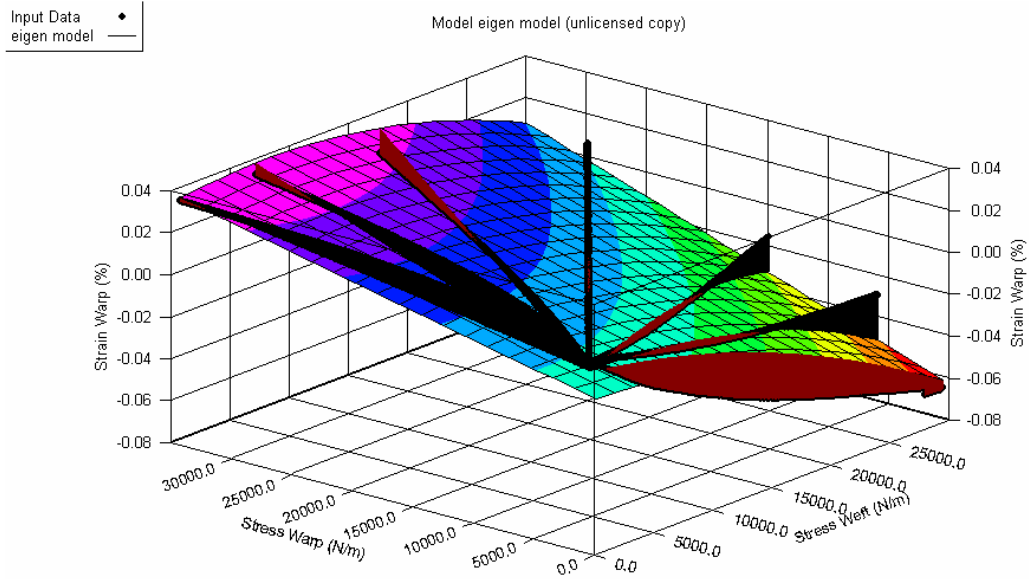


Figure 59: Fitted surface for Warp strain

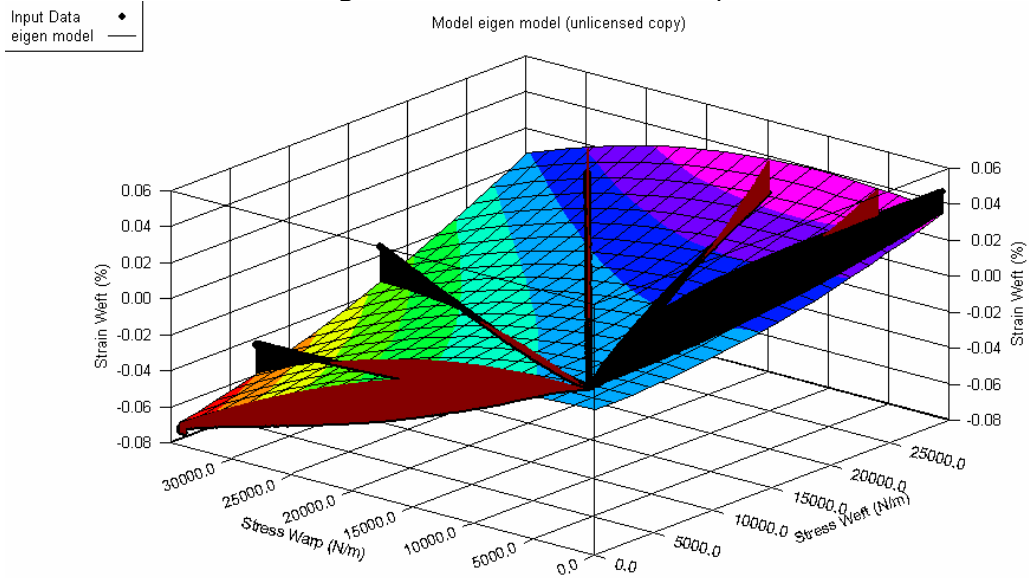


Figure 60: Fitted surface for Weft strain

The first impressions of these plots illustrate the characteristic behaviour of the fabric material. The non-linear stress-strain relation, combined with the interchange of the fibres is clearly visible in these plots. The fits of the surfaces are not optimized yet. The brown and black areas in the surface indicate the difference between the data and the created surface. On black areas, the data lies above the created surface, while on the brown areas the data lies below the surface.

One important disadvantage of representing the data in stress-stress-strain surfaces is that it is not useable in combination with the finite element program. The finite element program calculates material strains in the elements, and uses the material model to relate the corresponding material stresses to the element. With this way of representing the data this is not possible. Therefore the data should be plotted in strain-strain-stress plots. This requires some modification of the experimental data.

Since this way of representing the behaviour cannot be used for modelling , it will not be discussed in detail.

8.3 Strain-strain-stress relation

In Section 8.1 it was explained that in general the finite element program calculates with element strains, and finds the corresponding element stresses based on a known stress-strain relation. For example, when a material has a Hookean stress strain relation, this can be described by the equation:

$$\sigma = E * \varepsilon \quad (8.1)$$

where σ =stress, E =modulus of elasticity and ε =strain. For a given element strain, the finite element program can easily derive the element stress, by using the Hookean stress strain relation. However, the fabric material tested for this thesis does not follow the Hookean law, due to the complex non-linear stress-strain behaviour, and the biaxial interchange between the two fibre directions.

Therefore, the stress-strain relation must be described by an equation, where the *warp strain* and *weft strain* are the independent variables of a function of either *warp stress* or *weft stress*. The general form of this equation can be described as:

$$\begin{aligned} \sigma_{warp} &= f(\varepsilon_1, \varepsilon_2) \\ \sigma_{weft} &= f(\varepsilon_1, \varepsilon_2) \end{aligned} \quad (8.2)$$

The specific equation that describes the stress-strain relation can be found by using the curve fitting technique, which was already used in Section 8.2. After rearranging the data, the experimental data can be visualized in 3D strain-strain-stress plots. The Datafit software then computes in an iterative way the function description of the surface that fits the experimental data.

The experimental data can be plotted in a 3D strain-strain-stress plot.

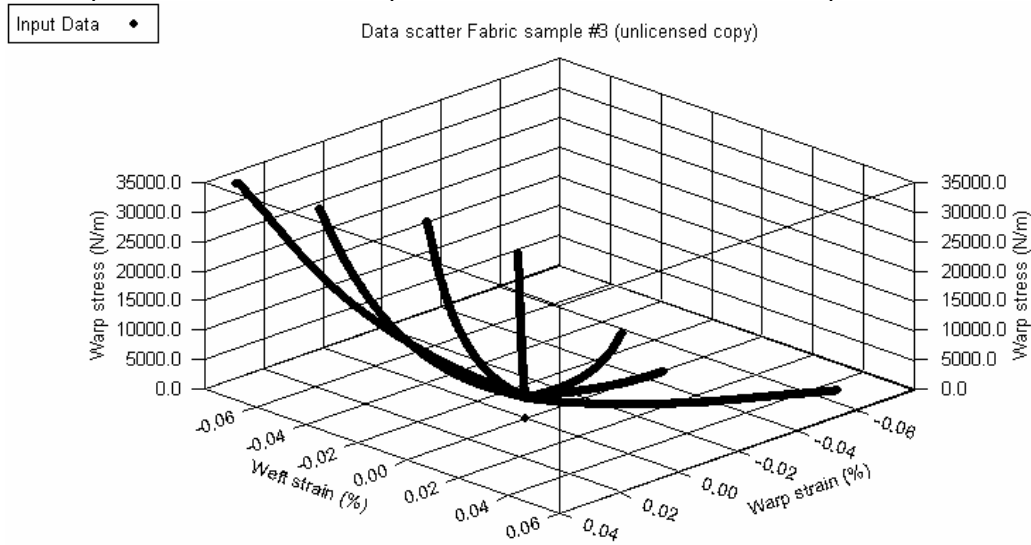


Figure 61: Plot data scatter warp stresses

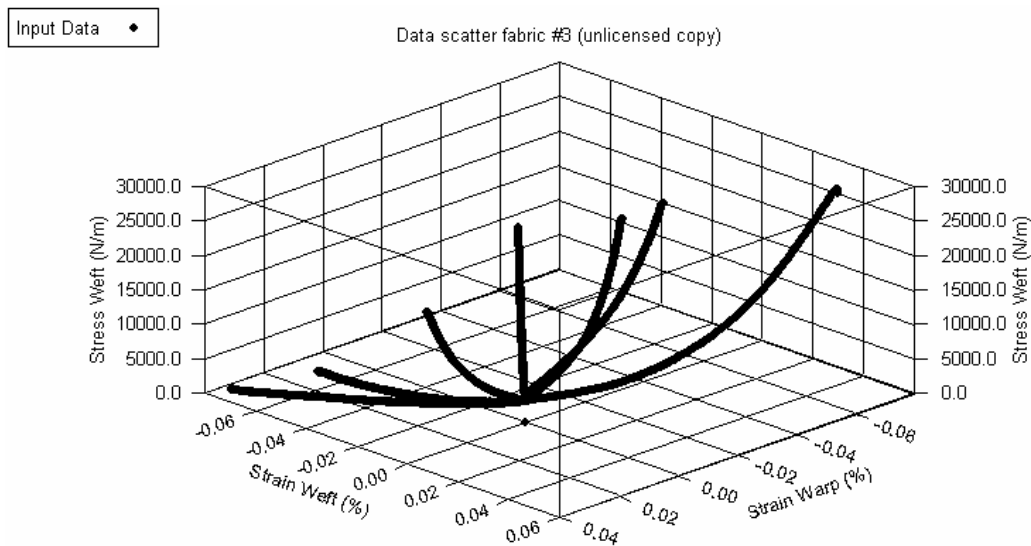


Figure 62: Plot data scatter weft stresses

From these plots it is difficult to interpret the directions of the data lines. Therefore two plots are created from a different view point, giving an indication of spread of the experimental data.

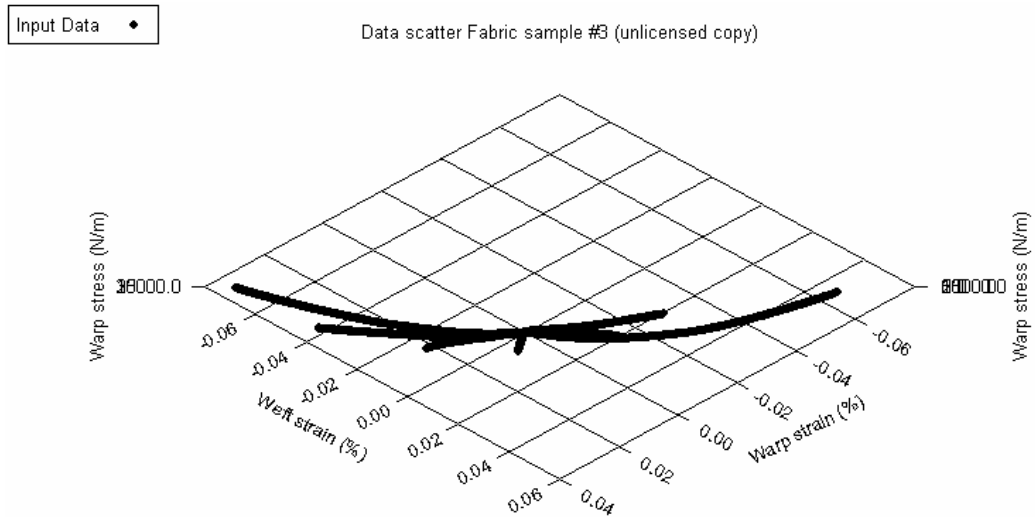


Figure 63: Plot data scatter warp stresses top view

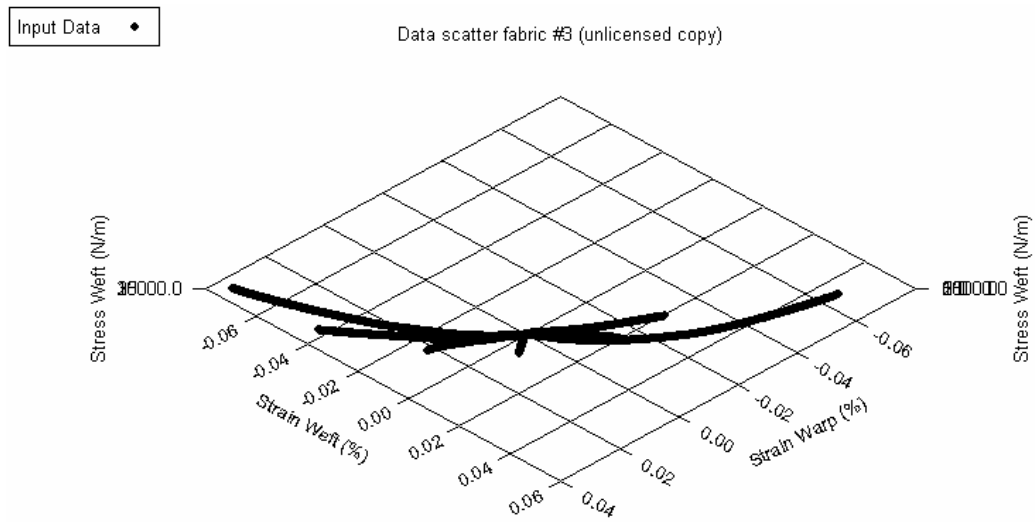


Figure 64: Plot data scatter weft stresses top view

These plots (Figures 63,64) show how the data curves lie in the x,y plane. Combined with the plots from Figures 61 and 62 this gives a good view of the spread of the data. Something that is remarkable is the steepness of the imaginary surface through the data. From this point it is possible to find a surface that fits the data of the experiments. The general form of the equation in which the Datafit software will find a solution must be provided.

This approach to directly fit a surface through the complete dataset did not result in useable results. The mathematic description of the surface could not be found. The approximations of the response surface showed large amounts of errors, making this method not suitable for representing the material behaviour.

8.3.1 Plane stress, isotropic

A first simple model of the strains-strain-stress relation can be made by using a reduced dataset. By doing so, a linear fit can be made through this data. Fitting a surface through the data sets of all six fabric samples, will provide an overview of the spread of the data.

The datasets are reduced up to 1% strain in both warp and weft directions, and in combined warp-weft direction. In Figure 65 and 66, two examples of these plots are shown.

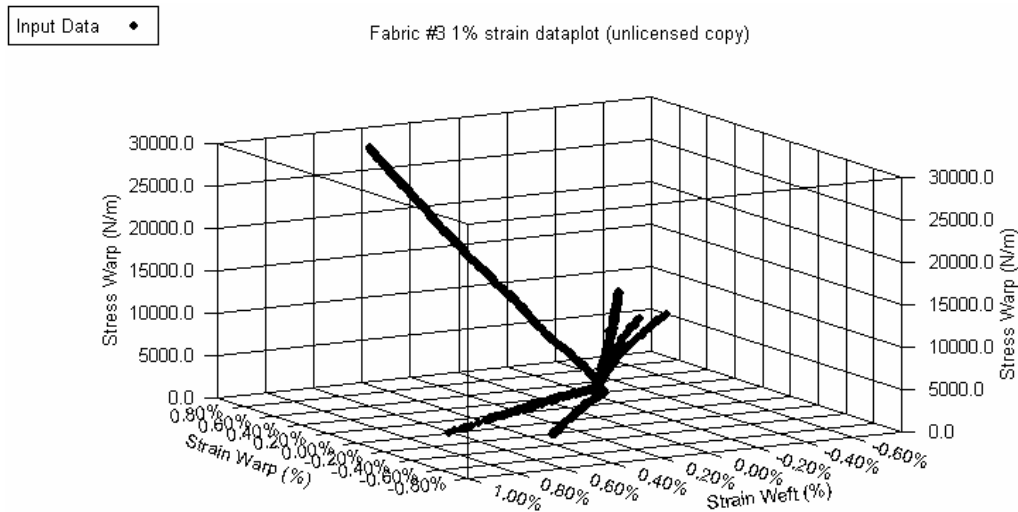


Figure 65: Reduced data plot strain warp, fabric sample #3

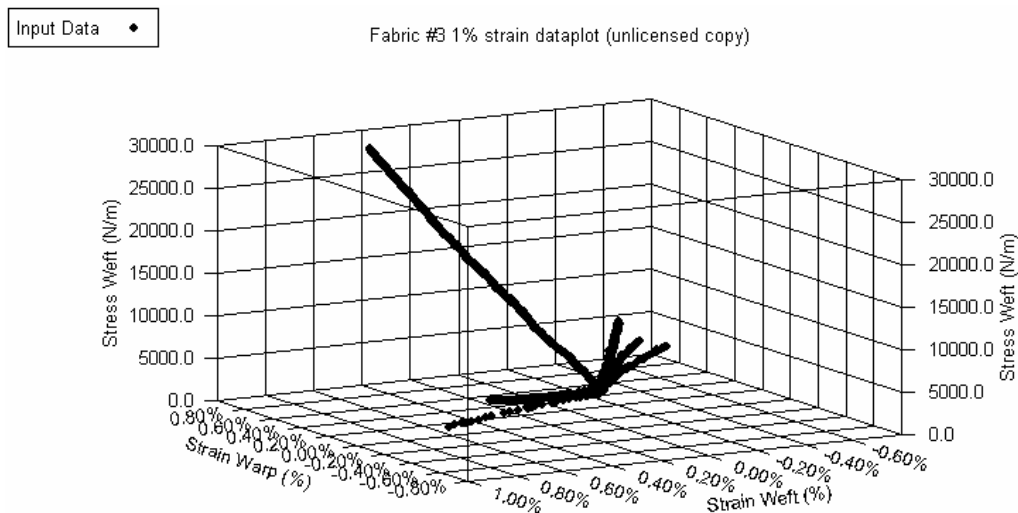


Figure 66: Reduced data plot strain weft, fabric sample #3

Using the DataFit tool, a surface can be fitted through the data. Due to the reduced range of the datasets, up to 1% strain in both and combined direction, a linear relation between strain and stress can be recognized in the data. Therefore a plane with two independent variables can be fitted. The general form of this plane is:

$$\sigma_{warp} = a_1 * \epsilon_{warp} + b_1 * \epsilon_{weft} + c_1 \quad (8.3)$$

$$\sigma_{weft} = a_2 * \epsilon_{warp} + b_2 * \epsilon_{weft} + c_2 \quad (8.4)$$

(σ = stress, ϵ = strain)

Two solutions for the fitted planes are shown in Figures 67 and 68.

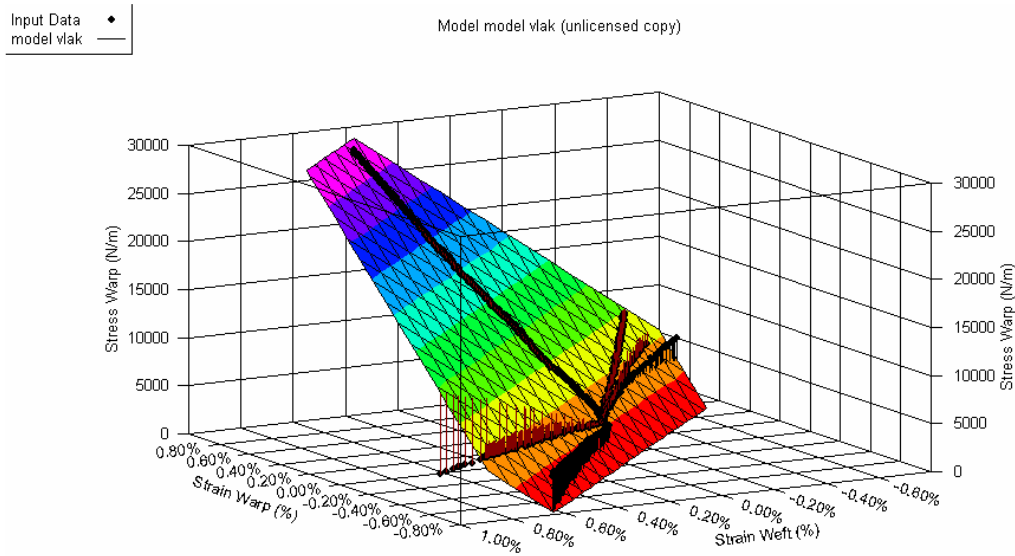


Figure 67: Fitted solution for warp direction, fabric sample #3

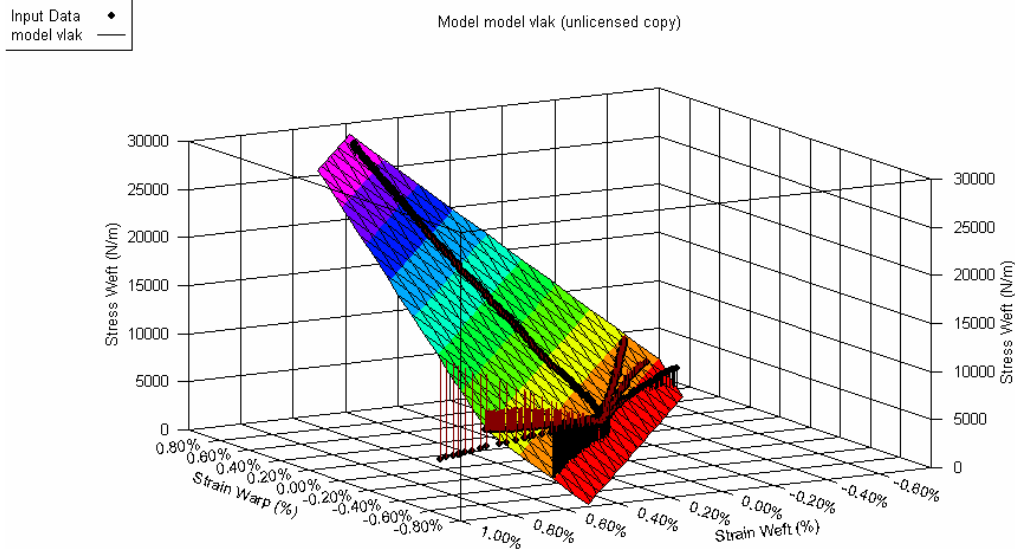


Figure 68: Fitted solution for weft direction, fabric sample #3

For each of the datasets of the six fabric samples a linear fit is performed. This results in six equations for warp, and six equations for weft. In other words, this results in the solutions for

the parameters a_1, b_1, c_1 for the warp plane, and a_2, b_2, c_2 for the weft plane. These parameters are averaged, and for each parameter the relative error between the calculated parameter and average value of the parameter is calculated. These relative errors are shown in Tables 1 and 2.

Table 4: Parameters and errors warp

warp	Fabric 2	Fabric 3	Fabric 4	Fabric 5	Fabric 6	Fabric 7	Average
a1	2578785	2074667	2466363	2338280	2098727	2213385	2295035
b1	2356112	2012140	2387478	2189482	1925193	2095757	2161027
c1	2618	3394	3128	3322	2980	3352	3132

error %	Fabric 2	Fabric 3	Fabric 4	Fabric 5	Fabric 6	Fabric 7
a1	12,36%	-9,60%	7,47%	1,88%	-8,55%	-3,56%
b1	9,03%	-6,89%	10,48%	1,32%	-10,91%	-3,02%
c1	-16,42%	8,35%	-0,14%	6,06%	-4,86%	7,01%

Table 5: Parameters and errors weft

weft	Fabric 2	Fabric 3	Fabric 4	Fabric 5	Fabric 6	Fabric 7	Average
a2	2155101	1891641	2295072	2160015	1986547	2016504	2084147
b2	2370422	2278025	2660019	2494112	2263573	2375988	2407023
c2	2710	3281	3139	3209	2873	3293	3084

error %	Fabric 2	Fabric 3	Fabric 4	Fabric 5	Fabric 6	Fabric 7
a2	3,40%	-9,24%	10,12%	3,64%	-4,68%	-3,25%
b2	-1,52%	-5,36%	10,51%	3,62%	-5,96%	-1,29%
c2	-12,13%	6,38%	1,78%	4,05%	-6,85%	6,77%

From Table 1 and 2, it can be concluded that the spread in the solutions of the parameters of the planes is smaller than 10 %. One exception is fabric #2, where a larger relative error is found. This can be explained by the fact that a mistake was made during testing. Therefore the load ratio 1:1 contains a divergent data. Due to the fact that the 1:1 load ratio has a major influence on the dataset, and therefore also on the solution of the fitted plane, this could be the cause of the relative error up to 16%.

The reduced dataset, only valid for small fabric strains up to 1%, can now be researched if it fits the plane stress theory with isotropic material properties. In Section 4.2 a summary was given about various attempts of fitting the data into a system of Young moduli and interaction moduli. Bridgens (2005), as well as Nederpelt (2004) concluded that the laws of homogenous material do not hold for woven fabric. However, the results of the experiments for this thesis tend to prove the opposite. Therefore the data will be used in the plane stress laws, in order to derive the modulus of elasticity and the Poisson's ratio for the fabric.

The laws for plane stress, and isotropic material are:

$$\begin{aligned}\sigma_{xx} &= \frac{E}{1-\nu^2} (\varepsilon_{xx} + \nu \varepsilon_{yy}) \\ \sigma_{yy} &= \frac{E}{1-\nu^2} (\varepsilon_{yy} + \nu \varepsilon_{xx}) \\ \sigma_{xy} &= G \gamma_{xy}\end{aligned}\tag{8.5}$$

, with σ_{xx} = stresses in warp direction

σ_{yy} = stresses in weft direction

ε_{xx} = strains in warp direction

ε_{yy} = strains in weft direction

σ_{xy} = shear stresses

E = Young modulus

ν = Poisson ratio

When rearranging these equations, the following is acquired:

$$\begin{aligned}\sigma_{xx} &= \frac{E}{1-\nu^2} \varepsilon_{xx} + \frac{\nu E}{1-\nu^2} \varepsilon_{yy} \\ \sigma_{yy} &= \frac{\nu E}{1-\nu^2} \varepsilon_{xx} + \frac{E}{1-\nu^2} \varepsilon_{yy} \\ \sigma_{xy} &= G \gamma_{xy}\end{aligned}\tag{8.6}$$

These equations are now comparable with the equations found in the surface fitting procedure.

$$\sigma_{warp} = a_1 \varepsilon_{warp} + b_1 \varepsilon_{weft} + c_1\tag{8.7}$$

$$\sigma_{weft} = a_2 \varepsilon_{warp} + b_2 \varepsilon_{weft} + c_2\tag{8.8}$$

Combining these equations result in two equations and two unknown variables, modulus of elasticity E and Poisson's ratio ν .

$$\begin{aligned}a_1 &= b_2 = \frac{E}{1-\nu^2} \\ a_2 &= b_1 = \frac{\nu E}{1-\nu^2}\end{aligned}\tag{8.9}$$

The values for the known parameters a_1, a_2, b_1, b_2 are derived from Table 1 and 2. The values are averaged, due to slight differences in the values of the parameters, see Table 3.

Table 6: Averaged values for parameters

a1	b2	Average (a1+b2)	% error
2295035	2407023	2351029	± 2,4%

a2	b1	Average (a2+b1)	% error
2084147	2161027	2122587	± 1,8%

Solving the two equations with the two unknown variables result in a modulus of elasticity E and a Poisson's ratio ν .

Table 7: Solutions for elastic constants, isotropic

			Mean	St. Dev
Poisson's ratio	0,90		0,902	0,0079
Modulus of elasticity	434561	N/m	434560,9	16640

Note that in fabric material the modulus of elasticity E is always expressed as a unit per length.

It is remarkable that the Poisson's ratio is 0,90, this is physical not a valid value for a Poisson's ratio. The Poisson's ratio is normally a value between -1 and 0,5. A Poisson's ratio expresses the amount of strain that occurs in the material, perpendicular to the direction in which the force is applied on the material. In a formula this can be expressed as:

$$\nu = -\frac{\epsilon_{yy}}{\epsilon_{xx}} \quad (8.10)$$

where ϵ_{xx} is the strain in the pulling direction and ϵ_{yy} is the strain in the perpendicular direction. A Poisson's ratio of 0,90 indicates that there are large negative strains in the opposite directions of the pulling directions. Large is in this case almost a 1:1 ratio. This phenomenon can easily be explained with the mechanism of the woven fibres. It was already discussed in Section 3.5 (Crimp Interchange) that straightening one fibre direction increases the crimps in the opposite direction, causing large negative strains in that direction.

Apparently for small fabric strains (up to 1%), this high Poisson's ratio is valid. It is expected that for higher fabric strains, this will not be valid. The straightening of the yarn crimps is then minor to the actual stretching of the yarns.

The equations for the planes, describing a linear relation between warp and weft, can already be used in a structural analysis. The equations can be put in a subroutine, where fabric strains are used to calculate the corresponding fabric stress. However, the model will only be valid for small fabric strains, up to 1%. Therefore this model only covers a limited range of possible fabric strains. Besides a limited range of use, the model is a linear simplification of a fabric behaviour that is in fact non-linear. However, when looking at a small range of a non-linear surface, it can be approximated by a linear surface.

Note that possible stresses are positive only. Negative stresses would result in wrinkles in the fabric, and are therefore not desirable. These conditions should be included in the model, to assure proper outputs.

8.3.2 Plane stress, Orthotropic

In Section 8.3.1 the theory of plane stress on an isotropic material is applied. In an isotropic material the modulus of elasticity is independent of the direction in the material. For the woven fabric this would mean that the elastic behaviour of the yarns for both warp and weft direction would be equal. Although the test results show that there is a difference in elastic behaviour, the differences are small. For the isotropic model, these differences have been averaged in order to derive the elastic constants for the model.

However, when the differences in warp and weft behaviour are not ignored, a model for orthotropic materials can be applied. Orthotropic materials have orthogonal planes of symmetry for which different elastic constants are valid. In the woven fabric, there are

two planes of symmetry, namely the warp and weft direction of the yarns. In case of an infinite number of symmetry planes, the rules for an isotropic material are valid.

The constitutive relation for orthotropic materials is :

$$\begin{aligned}\sigma_{xx} &= \frac{E_x}{1-\nu_x\nu_y}\epsilon_{xx} + \frac{\nu_x E_y}{1-\nu_x\nu_y}\epsilon_{yy} \\ \sigma_{yy} &= \frac{\nu_y E_x}{1-\nu_x\nu_y}\epsilon_{xx} + \frac{E_y}{1-\nu_x\nu_y}\epsilon_{yy}\end{aligned}\quad (8.11)$$

where xx denotes warp *and* yy denotes weft. Due to required symmetry in the stiffness matrix, an additional condition must be set:

$$\nu_x E_y = \nu_y E_x \quad (8.12)$$

The equations for the fitted surfaces are:

$$\sigma_{warp} = a_1 * \epsilon_{warp} + b_1 * \epsilon_{weft} + c_1 \quad (8.13)$$

$$\sigma_{weft} = a_2 * \epsilon_{warp} + b_2 * \epsilon_{weft} + c_2 \quad (8.14)$$

where c_1 and c_2 are offsets.

Using Maple, these equations can be solved in order to derive the elastic constants $E_x = E_{warp}$ and $E_y = E_{weft}$, and the Poisson's ratios $\nu_x = \nu_{warp}$ and $\nu_y = \nu_{weft}$.

Table 8: Solutions for elastic constants, orthotropic

Poisson's ratio	warp	0,88	
	weft	0,92	
Modulus of elasticity	warp	423272	N/m
	weft	443926	N/m

The solutions for the elastic constants for the orthotropic constitutive law differ only slightly from the isotropic laws. From a designer's point of view, the fabric can therefore be handled as an isotropic material. For fabric stresses up to 1% in warp and weft directions, the simplified isotropic material properties can be used in structural analysis. A limitation of this approximation is the limited validity. It can only be used on small fabric strains, up to 1% from pre-stress level.

It was already stated in Section 4.2 Material representation that linearization of non-linear strain behaviour may be justified in case of rough calculations. However, this method does not cover the complex non-linear strain behaviour of the fabric. The scope of this thesis is to develop a model which includes the complex behaviour. Therefore a model will be described in Section 8.3.3 which describes the complex nonlinear behaviour, without limitations on the strain range.

8.3.3 Non-linear model including fibre interaction

The material model in Sections 8.3.1 and 8.3.2 were highly simplified models. The strain range was decreased to a certain extend, in order to be able to model non-linear behaviour as linear behaviour. These simplifications are justified, but are not useable in the industry. However, it does give insight in the fabric behaviour around the prestress

level. A more usable model, which includes the nonlinear behaviour and fibre interaction, can be made by using a large set of equations. These equations describe the fibre interaction as well as the fibre elongation, and combine these strains as a total fabric strain. This theory is invented by Hoogenboom (2007).

In this theory equal fibre properties for warp as weft are assumed. The theory is based on the fibre interaction mechanism, as shown in Figure 69.

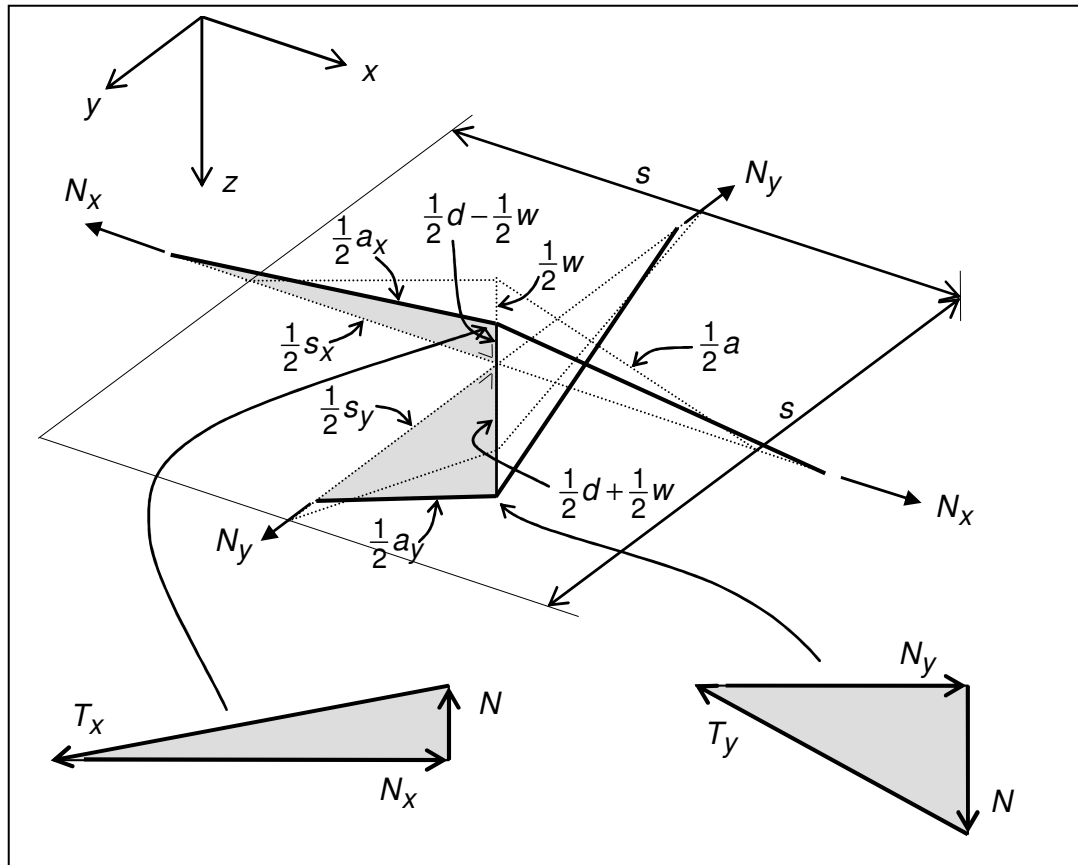


Figure 69: Theory of fibre interaction (Hoogenboom, 2007)

The fibres have a diameter d and a spacing s . The spacing is a measure for the distance between the fibres in the plane of the fabric. The distance between the fibres at the point of crossing over is also called d and is derived from the sum of the distance between both centre lines of the fibres. The displacement of this crossing over point due to straightening of a fibre is called w .

The original length of the fibre is called a , while the length of a stretched fibre is called a_x or a_y . The projection of a_x and a_y on the plane of the fabric is called s_x or s_y . Using these parameters, the following kinematic equations are observed in Figure 69:

$$\epsilon_{xx} = \frac{s_x - s}{s} \quad (8.15)$$

$$\epsilon_{yy} = \frac{s_y - s}{s}$$

$$a^2 = s^2 + d^2 \quad (8.16)$$

$$a_x^2 = s_x^2 + (d - w)^2$$

$$a_y^2 = s_y^2 + (d + w)^2$$

The following constitutive equations can be defined:

$$\begin{aligned}
 T_x &= EA \frac{a_x - a}{a} \\
 T_y &= EA \frac{a_y - a}{a} \\
 A &= \frac{1}{4} \pi d^2
 \end{aligned}
 \tag{8.17}$$

The following equilibrium equations can be observed in Figure 69:

$$\begin{aligned}
 \frac{T_x}{N} &= \frac{a_x}{d - w} \\
 \frac{T_y}{N} &= \frac{a_y}{d + w} \\
 \frac{N_x}{T_x} &= \frac{s_x}{a_x} \\
 \frac{N_y}{T_y} &= \frac{s_y}{a_y} \\
 n_{xx} &= \frac{N_x}{s} \\
 n_{yy} &= \frac{N_y}{s}
 \end{aligned}
 \tag{8.18}$$

A program assists in calculating the fabric stresses at a given pair of fabric strains. The strain in the fabric results in a change in the values of s_x and s_y . From these strains the value for w is computed by varying this value, until the out of balance force R in the force N is smaller than a preset criterium. This is an iterative process. When w is calculated, the strains of the fabric can be computed. The exact code is included in the Usermat, see Appendix C1.

This theory can be used to compute fabric stresses, as a function of fabric strain. It appears that the response of this theory shows the same trend as found in the experiments. Therefore it is a matter of configuring the parameters E , s and d in order to acquire the equations that describe the experimental fabric behaviour.

After calibrating the model, it appears that the parameters for E , s and d must be set as following:

$$\begin{aligned}
 E &= 77500 \text{ N/mm} \\
 s &= 0.9 \text{ mm} \\
 d &= 0,18 \text{ mm}
 \end{aligned}$$

These values for the parameters correspond to estimations of these properties based on the datasheet of the fabric. The Young Modulus corresponds to the Young Modulus of glass. The geometric parameters are realistic, based on the fabric thickness and fibre density.

Calculations and error estimations are put in the Appendix C2. For each fabric, two data points from each of the loading 'spokes' is chosen (arbitrarily). Each fabric has 7 loading spokes, namely 1:1, 1:2, 2:1, 1:5, 5:1, 1:0 and 0:1. For each fabric sample, 14 data points are checked. Six samples have been tested in the lab, which means that 84 data points are included in the parameter calibration and error analysis. This should give an adequate error estimation.

A script written in Visual Basic assists in configuring the parameters. By a method of trial and error the parameters are changed while the script automatically calculates the model stresses at the given experimental strain data points. The model factors are determined, as well as a mean and standard deviance of the model factor. A mean model factor of 1,0 indicates an optimum of the chosen parameters.

The determination of the parameters has not been checked on sensitivity. The data points included in the parameter determination sheet are picked arbitrarily. Due to the smoothness of the dataset it is expected that a second arbitrarily chosen dataset will not result in large errors in the model factors.

9. Ansys User Programmable Feature (UPF)

After creating the theoretical model, the equations for the fabric stress-strain relation are included in a user programmable feature (UPF). This UPF is an external script which is linked to the Ansys software. In the calculation process, Ansys uses the UPF to convert element strains into element stresses by using the constitutive and kinematic equations from the theoretical model. In this chapter it is explained how the UPF is coded, and linked to the Ansys software in order to perform structural analyses on fabric structures.

9.1 Theory of the UPF 'usermat'

A material model contains the constitutive laws for a material. For each load step in de calculation, Ansys inputs a strain increment $\Delta\epsilon$ in the model. Based on the current element strain, an updated strain is calculated:

$$\epsilon_{updated} = \epsilon_{current} + \Delta\epsilon$$

The updated element strain $\epsilon_{updated}$ is then used to calculate the new element stresses, based on a relation between stress and strain:

$$\begin{aligned}\sigma_{updated,warp} &= f(\epsilon_{updated,warp}, \epsilon_{updated,weft}) \\ \sigma_{updated,weft} &= f(\epsilon_{updated,warp}, \epsilon_{updated,weft})\end{aligned}$$

The user material model must be supplied with a particular input, and will deliver a particular output. The input for the model is the current strain of the elements. The output is the updated strain of the elements, the updated stress state of the elements, and a Jacobian matrix. This matrix is only used for convergence matters. Since the fabric has a variable Young's modulus, it will be too time consuming and complex to create proper Jacobians. However, the matrix is only used to assist in fast convergence. Therefore, it does not need to be the exact matrix, but can be a general matrix. The convergence will be slower as a result of this concession.

The Usermat is programmed in the FORTRAN language. Ansys compiles the FORTRAN files and relinks it in order to create a customized Ansys executable. The general structure of a subroutine written in FORTRAN has the following form:

```
Subroutine name (arguments)
Declarations
Statements
```

The statements cover the constitutive laws for the material. In the declarations constants are given values. Some values may be acquired from the input file, such as Young's modulus, Poison's ratio and other properties. This may be useful in order to facilitate quick material adaptations, without recompiling the Usermat.

9.2 Setting up a UPF in Ansys

The user supplied subroutine is called an UPF in Ansys. The particular UPF describing the material properties (constitutive laws) is called USERMAT. In this section the

procedure is described for configuring Ansys, in order for Ansys to be able to call the USERMAT.

- First an UPF must be created. Ansys supplies numerous examples of UPF's. They are intended to be used and edited by users. The right type of UPF must be selected, and edited. The UPF's already have simple functionality. It is preferred to add small changes at a time, to keep insight in the procedures.
- After creating an UPF, it must be compiled and linked to Ansys. This procedure is embedded in the Ansys software. Ansys compiles all FORTRAN files that are located in a specified folder. The edited UPF must be placed in this folder first, before Ansys is able to compile the file. A suitable version of Intel FORTRAN Compiler is required for this operation. In the case of Ansys v10.0 an Intel Fortran Compiler v8.1 is required. Newer versions of the compiler cause errors.
- While compiling and relinking, Ansys creates a custom executable to run Ansys with the custom material model. This new executable can be selected by running the Ansys Product Launcher. After Ansys is started up, the new material model will not yet be available for Ansys.
- The new material model can be activated by issuing the command ***tb, user*** in the input file. The customized material is not accessible through the GUI in Ansys. The user supplied material can only be applied in a limited amount of element types, namely the *18x family*. This contains the elements LINK180, Shell181, Plane182, Plane4 183, Solid 185, Solid 186, Solid187, Beam188 and Beam 189. Instead of using the GUI, the input is supplied in a text file. In this input file some material properties can be assigned, such as Young's Modulus and Poisson's ratio. These material properties are used in the user material model. It is up to the creator of the material model which properties can be assigned through the input file.

9.3 UPF Usermat for PTFE coated fibre glass

The UPF consists out of two parts, calculating the updated stresses based on the strain increment, and computing a Jacobian matrix. The UPF starts with some general commands in order to declare some of the used variables. After the declarations the actual calculation starts.

In this model, a plane strain situation is assumed, where the modeled fabric will be in a 2D plane. Therefore a 3x3 Jacobian matrix will be created. Ansys uses a stiffness matrix for convergence matters only. Normally this matrix is also used to compute stresses, but by using the non linear fibre interaction model (Hoogenboom, 2007), stresses are computed without using a Jacobian matrix, see Section 8.3.3.

In the Usermat a Jacobian matrix is constructed. In order to create an estimation of the exact Jacobian, a small routine is included in the Usermat. The Jacobian contains the steepness of the stress-strain surface, at the point of interest. For linear elastic material there is a direct relation between the Young Modulus and the steepness of the response surface. However, for this highly non linear PTFE coated fiberglass, there is no constant Young modulus. An estimation is calculated by determining the stress j at strain i as well as stress $j+\Delta j$ at strain $i+\Delta i$. The difference between these two point, divided by the increments gives an estimation of the steepness of the response curve.

After constructing the Jacobian, the usermat calculates the material stresses, corresponding with the strain increment for the current load step. Stresses are stored in a vector with three arguments. The strain vector is updated with the strain increment. The result is also stored in a vector with three arguments.

$$\begin{bmatrix} \Delta\sigma_{xx} \\ \Delta\sigma_{yy} \\ \Delta\sigma_{xy} \end{bmatrix} = [J] \begin{bmatrix} \Delta\epsilon_{xx} \\ \Delta\epsilon_{yy} \\ \Delta\epsilon_{xy} \end{bmatrix}$$

The arguments concerning the material properties must be declared in the input file. This enhances the usability of the Usermat model. Variation in material properties from the fabric do not result in the need of editing and recompiling of the Usermat. The properties that must be declared in the input file are:

Young's Modulus	[N/mm]
Diameter of fibre	[mm]
Spacing between fibres	[mm]

10. Subroutine testing

Building and using a user supplied subroutine in Ansys requires some caution in using the subroutine in FE analysis. Due to the customized version of Ansys, some testing is necessary to prove the soundness of the routine. In simple test cases, the behaviour of the routine can be monitored.

10.1 Single element, homogenous stress

A single element, with no mesh, is loaded with a uniform biaxial stress. Two adjacent sides are constraint, while the opposite sides are loaded. The expected results can be calculated by running the model script in either Maple or Visual Basic (VB).

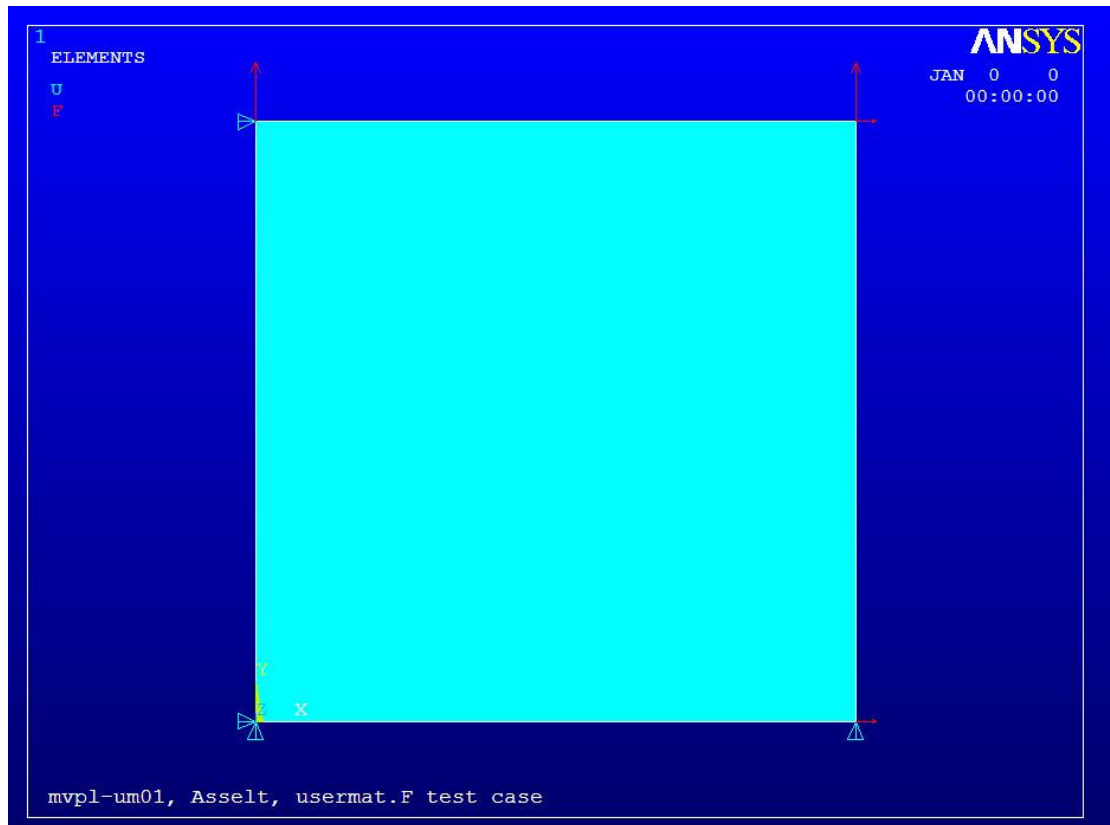


Figure 70: Model single element, no mesh, homogenous stress

Results from the Ansys calculation can be compared with the results from the script running in Visual Basic. Note that this verification of results can be done in this way only, when the stress distribution in the modeled fabric is uniformly distributed.

	Applied loading	Actual loading		Strain Model	Strain Theory
<i>F_x</i>	8 N/mm	7,99 N/mm	epsilon xx	3,42%	3,56%
<i>F_y</i>	4 N/mm	4,00 N/mm	epsilon yy	-4,27%	-4,54%

A slight difference occurs between the model strain and the theoretical strain. This is probably due to convergence criteria. Tighter criteria result in a non converging solution, which means that the applied criteria results in the optimum solution for this situation.

10.2 Multiple elements, homogenous stress

A model containing more than one element is tested to check on the ability of transferring loads between the different elements. Again a homogenous stress is applied to the model. Figure 71 shows the model with the applied boundary conditions and loading.

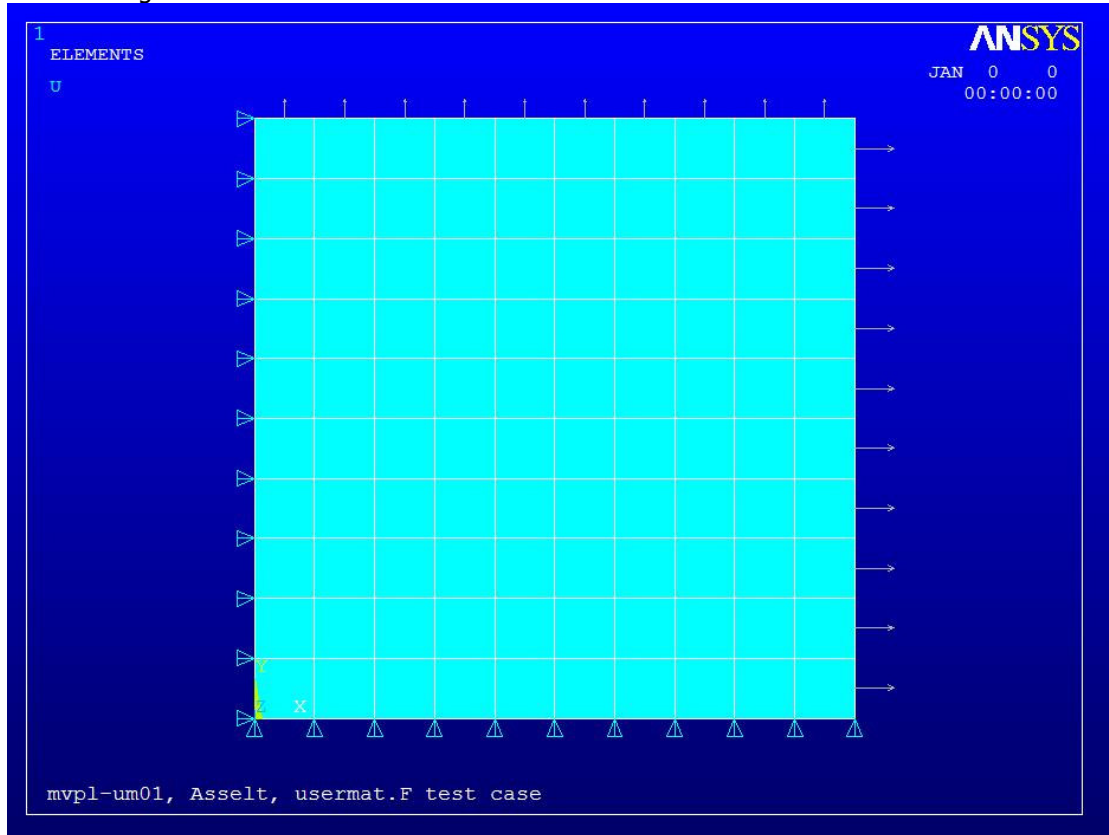


Figure 71: Model multi element, meshed, homogenous stress

It is expected that when loaded similarly to the one-element case, the strains are comparable. The differences between model strain and theoretical strain are of the same magnitude as in the single element case.

	Applied loading	Actual loading		Strain Model	Strain Theory
<i>F_x</i>	8 N/mm	8,02 N/mm	epsilon xx	3,37%	3,62%
<i>F_y</i>	4 N/mm	3,96 N/mm	epsilon yy	-4,16%	-4,65%

10.3 Multiple elements, non-homogenous stress

Load cases with uniformly distributed stress such as in Section 10.1 and 10.2 can be verified with the experimental data. However, non-uniform stresses can not be verified because the experiments are based on uniform stress distributions only.

In Figure 72 the model is shown with a non-uniform stress distribution. The stress in Y -direction is uniformly distributed (4 N/mm) while the stress in X -direction varies from 6 to 8 N/mm.

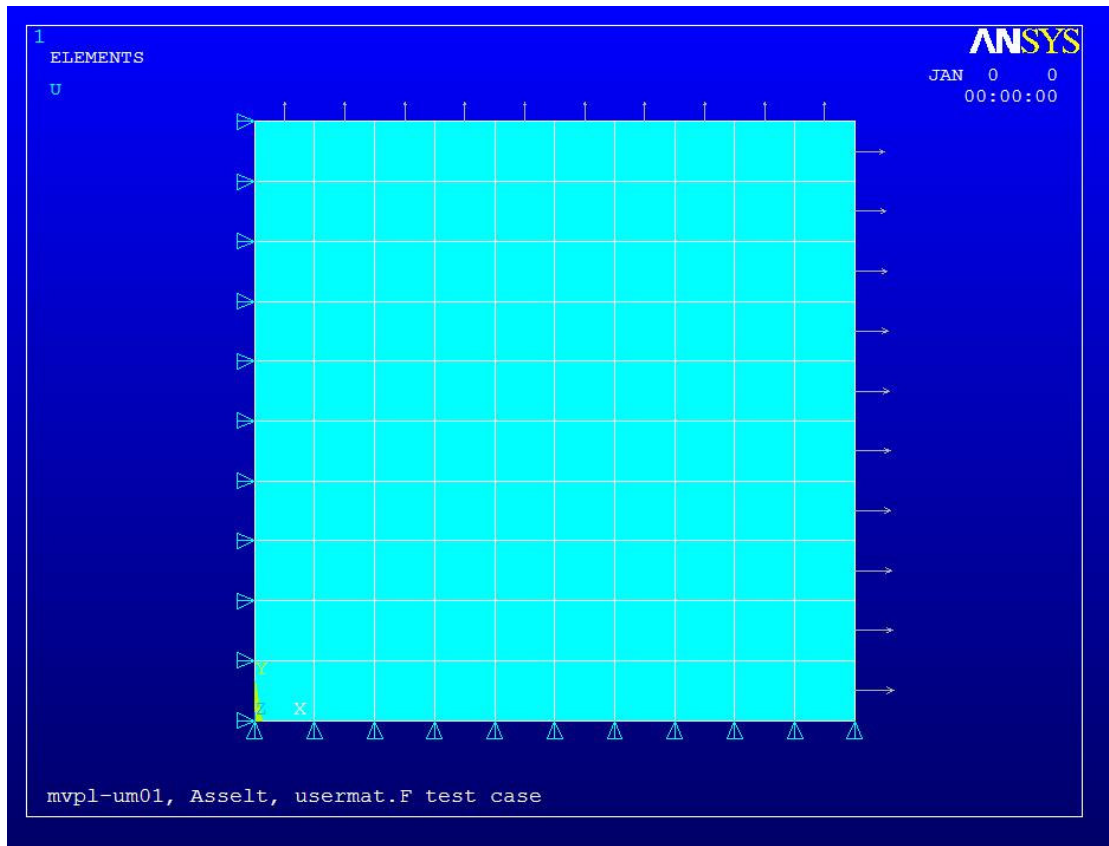


Figure 72: Model multi element, meshed, non uniform stress distribution

This non uniform stress distribution results in the following plot as shown in Figure 73. This plot shows the stress distribution in x direction. It is expected that stresses at the sides vary between 6 and 8 N/mm and this is exactly as shown in the plot. Therefore it can be concluded that the elements are capable of transferring loads between the elements.

A plot in y direction is not shown. A uniform distributed stress is applied, and this results in a uniform distributed stress in the model.

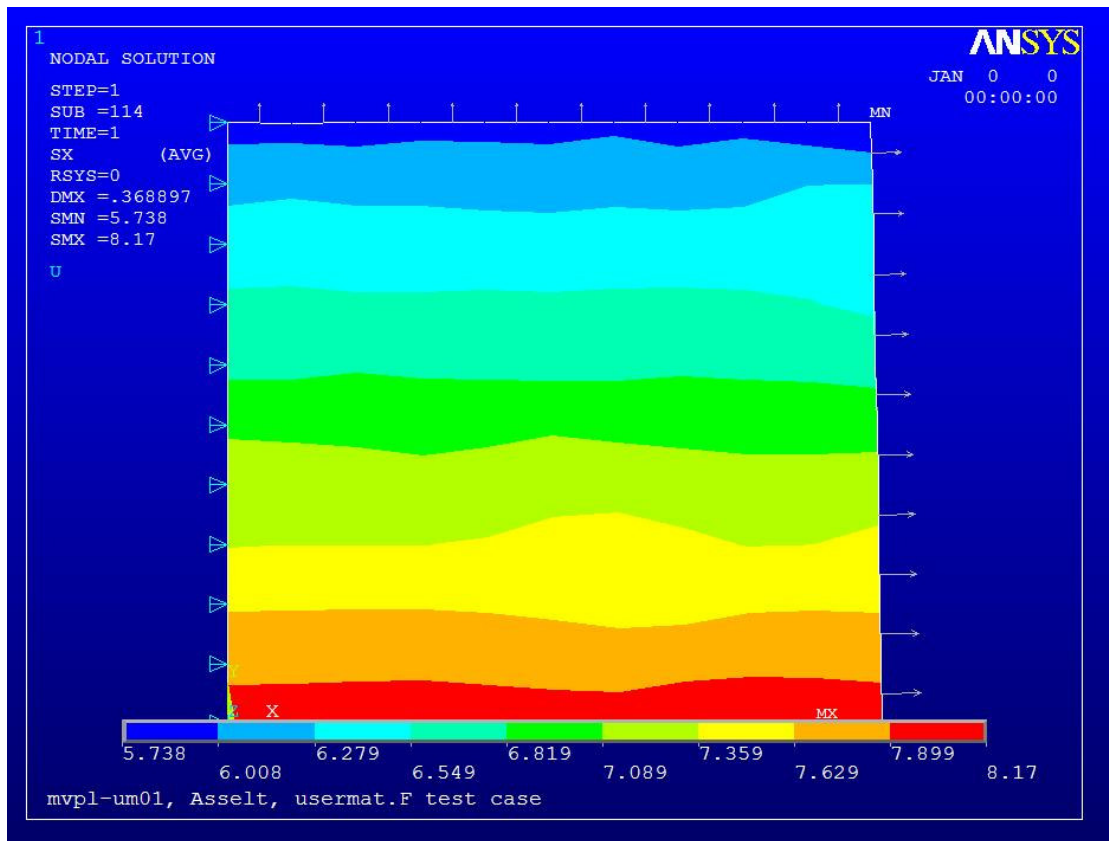


Figure 73: Stress distribution in x direction

10.4 Membrane action

With the previous shown tests with in-plane loading, it has been shown that the model is capable of calculating stresses based on uniform and non-uniform strains. It is interesting to introduce a load perpendicular to the stressed membrane. This will result in membrane action.

This test case is more challenging for the FE program, due to both nonlinear material behaviour as well as geometrical nonlinear behaviour of the structure. Eventually, this type of complexity of calculations is comparable with the calculations on stressed membranes performed in the design process of stressed membrane structures.

The test setup is a square piece of fabric, restrained at two sides and stressed in-plane at two sides, see Figure 74. A load perpendicular to the plane is applied in the centre of the fabric sample. The geometric nonlinear option must be enabled in Ansys, in order to include the change of geometry due to the large displacements. Also, the membrane option of the elements must be enabled, in order to eliminate the possibility of transferring bending moments in the elements.

The displacements are magnified by factor 3, in order to show the effect.

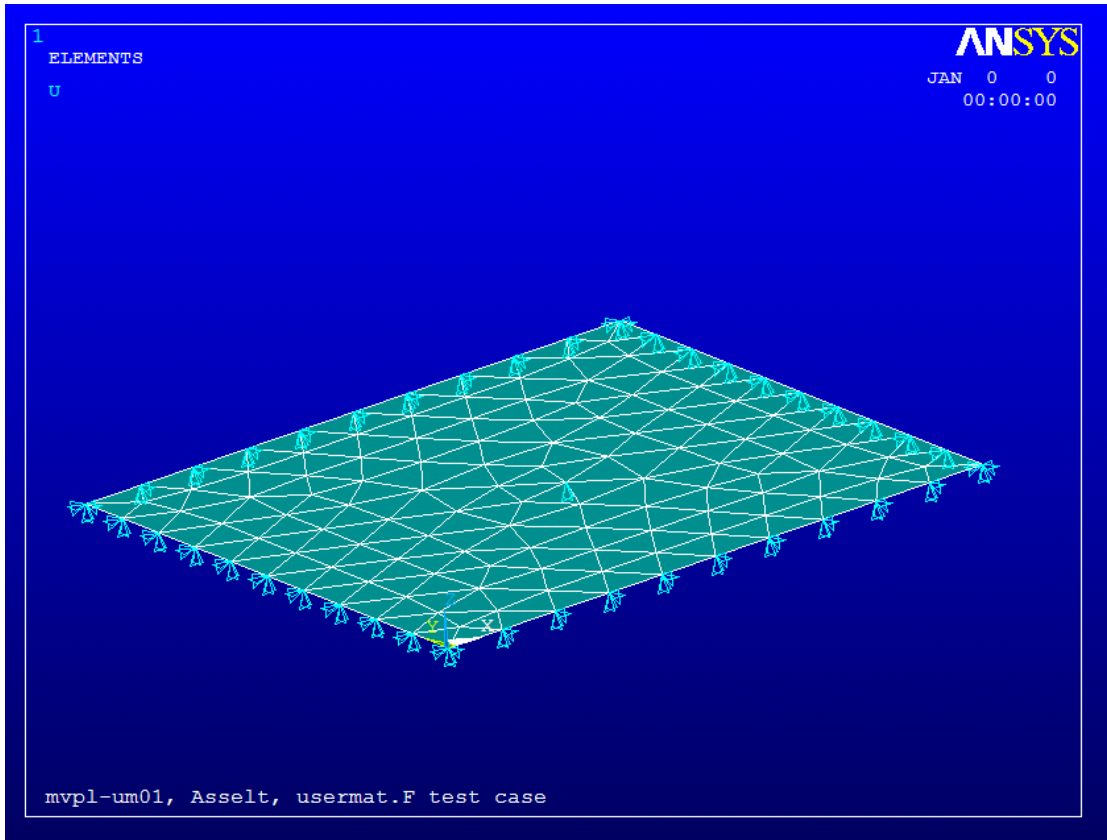


Figure 74: Square sample of fabric, restrained at two sides, and stressed at two sides

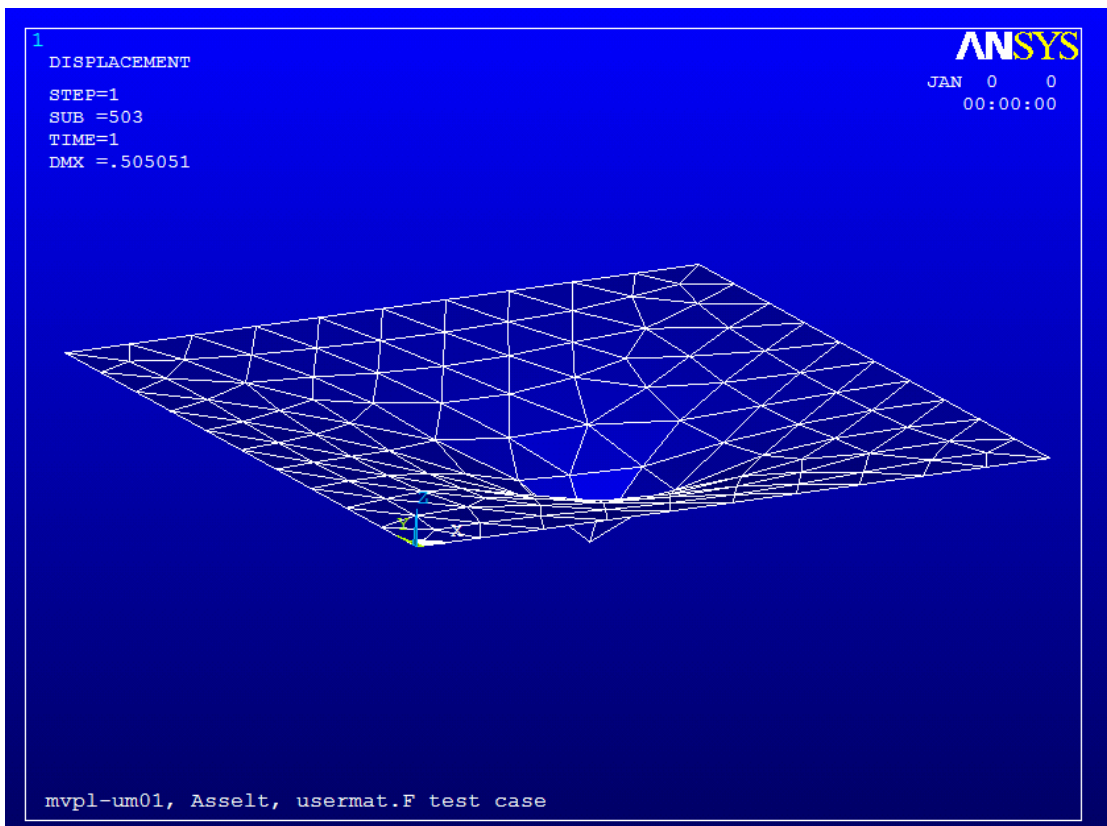


Figure 75: Displacements due to perpendicular load

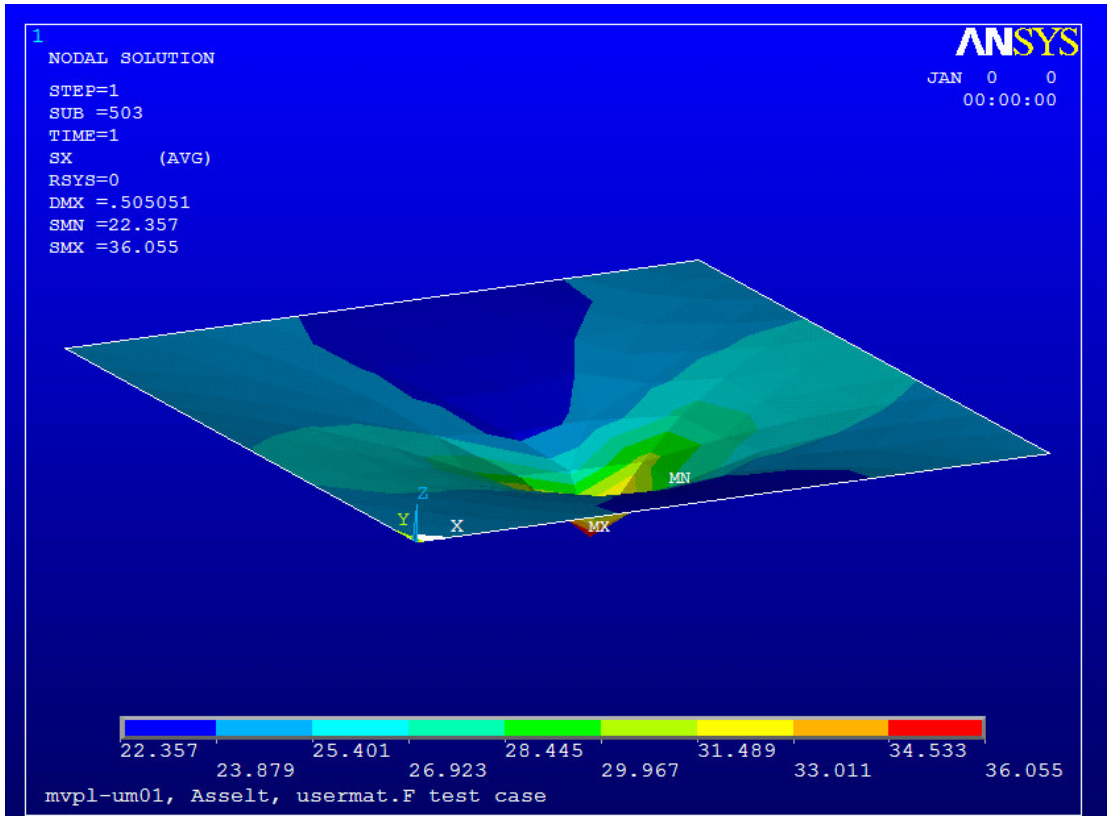


Figure 76: Stresses in the fabric in x direction

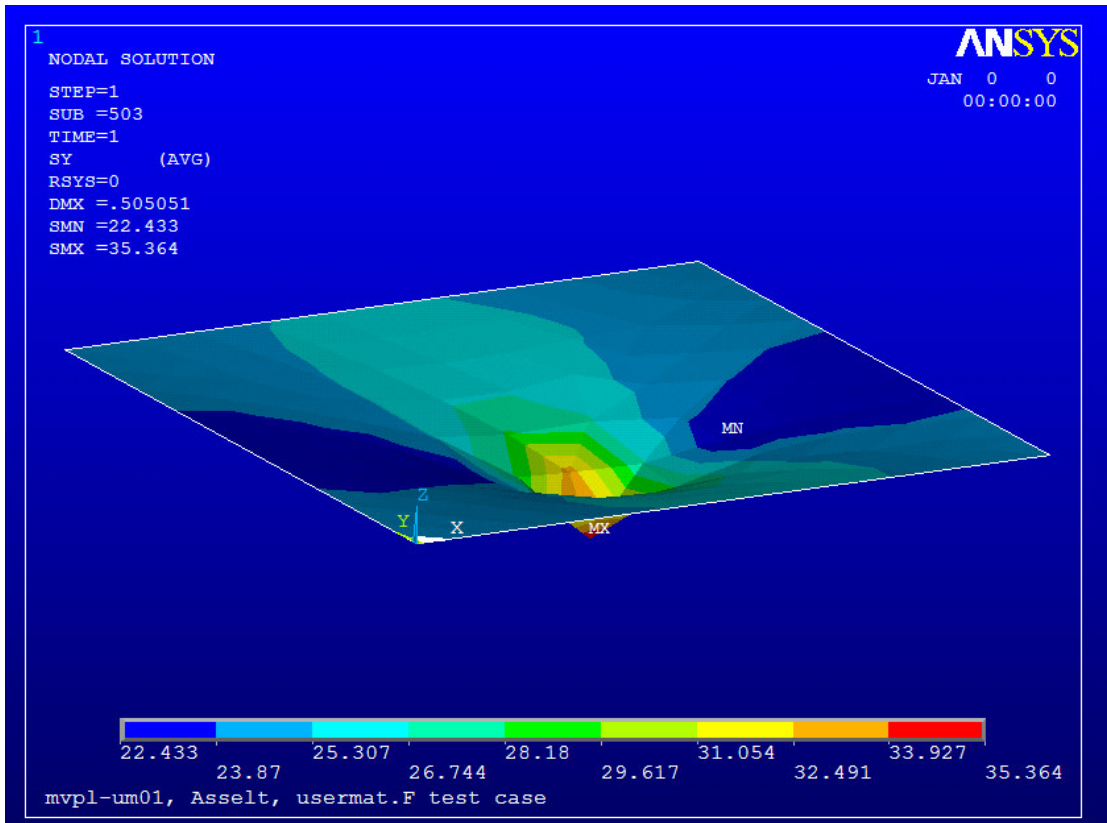


Figure 77: Stresses in y direction

11. Conclusions and recommendations

11.1 Conclusions

Testing

- The bracings with an added stiffness brace are usable for testing PTFE coated fibre glass. Slipping of the fabric is reduced to a minimum by reinforcing the braces with an extra steel strip.
- The new developed displacement measuring devices give accurate measurements during testing. The low amount of internal friction in the devices results in smooth displacement measurements.
- The hydraulic actuators are over dimensioned for the range of loadings that are applied during the experiments. Fine tuning these actuators on a small range is difficult, and could be improved by using smaller actuators (recommendation).
- Using a mould results in fabric samples with equivalent dimensions. This makes comparing of the results of the different samples feasible.
- The software MeetPC, which drives the actuators and stores the measurement data, is suitable for this particular way of testing PTFE coated fibre glass. Individual loading programs for both actuators can be realized by the use of this software.

Modeling

- Representing fabric stress-strain relation by Hooks law, using a modulus of elasticity and Poisson's ratio is not accurate at all. This holds for both isotropic as orthotropic assumptions.
- Representing the stress-strain data by using a response surface obtained by a DataFit tool does not result in sufficiently accurate results. Despite considerable effort a mathematical formula that describes the particular surface accurately has not been determined.
- Representing the stress-strain relation by using a descriptive model, using the fibers' geometry, results in a reasonable accuracy for biaxial stress situations. However, for uniaxial stress situations a poor accuracy has been found.
- Ansys is capable of performing membrane calculations, using a fabric material model. However, complex models of membrane structures, involving large numbers of elements, still cause convergence problems.

This approach of modeling the highly non linear material behaviour contributes to the second generation of structural analysis software of stressed membrane structures. The objective of this thesis is achieved, and the material model is capable of determining fabric strains and stresses in structural analysis.

11.2 Recommendations

Testing

- For future testing, smaller hydraulic actuators may be applied. This improves the possibility for adjusting and fine tuning the actuators. The size of the hydraulic valve (in combination with the condition of the valve) must be adjusted to the size of the actuator.
- Applying actuators driven by an electric engine might improve the accuracy of the actuator, due to the direct response of electrical driven engines.
- Actuators driven by an electric engine are suitable for both short as long-term loadings on the fabric. Long term loadings are not part of the scope of this thesis, but may contribute to the applicability of the material model.

-
- Current tests give insight in the fabric response at a number of given stress ratios (1:1, 1:2, 2:1, 1:5, 5:1, 1:0, 0:1). In order to have a better estimation of the model accuracy (model factor), additional tests can be performed at ratios other than the previous mentioned ones, e.g. 1:3, 3:1, 2:3, 3:2, 1:4, 4:1, 3:4 and 4:3.
 - The data management software MeetPC was configured in such way, that too many data point were recorded. It would have been sufficient to record less data points and still acquire usable data from the tests.
 - No tests have been performed to measure the shear stiffness properties of the fabric. In the material model, a low value for the shear stiffness is assumed. Testing the fabric for shear stiffness is recommended to quantify this unknown fabric property.

Modelling

- The material's Jacobian in the material model is an approximation of the exact Jacobian. Since the creation of the exact Jacobian is a time consuming and complex task, the approximation is sufficient for the test cases presented in this thesis. However, for more complex models of membrane structures a more accurate Jacobian must be supplied.
- The descriptive model is based on non compressibility of the fibres in the lateral direction, while this assumption may not be representing the actual fibre properties. This fibre compressibility can be added to the model, which may possibly improve the performance and accuracy of the model.
- In the descriptive model, it is assumed that the properties for both warp as weft fibres are equivalent. There might be a slight difference in spacing and elastic properties of the fibres in both main directions. Research in these aspects may supply information which can improve the quality of the model.
- A batch of PTFE coated fabric of a lighter quality is still available for research. A series of tests, comparable with the tests for this thesis, can be performed in order to gather a new dataset. It is then possible to research whether the model can be calibrated to the new dataset. The parameters that determine the model calibration are fibre spacing (mm), fibre diameter (mm) and Young's modulus of the glass fibres (N/mm^2). Theoretically, the first guess for the values of the parameters can be made based on the datasheet supplied by the manufacturer.

11.3 Future developments

After creating and testing the material model it is important to indicate where developments can improve the applicability of the model. Besides applicability it is important to indicate what this model's opportunities are for the industry. The industry is the collection of fabric manufacturers, engineers and other professionals that are active in the field of membrane engineering.

In the current state of the model, the convergence issues cause a large calculation time. It is expected that these problems can be solved by programming a script which can determine current Young's modulus for each sub step in the calculation. This script could make the calculation process less time consuming. In that way the material model can be used as an engineers' desktop tool.

The model based on fibre geometry, as presented in Section 8.3.3, shows good similarities with the experimental data for biaxial stresses. However, stresses that tend to be uni-axial, can not yet be represented in the model. Model improvements

concerning fibre lateral compressibility and differences in yarn spacing between warp and weft may add to a wider range of similarities with the experimental data.

The current model is based on relatively short term loadings. The loading is applied in a short amount of time, namely 60 seconds. When loadings would be applied (increased) in a much longer time, comparable with for example the accumulation of snow load during several hours, it would probably show a different response. The fabric would have more time to creep, resulting in a larger fabric strain. A possibility would be to make a distinction between quickly applied loading and slowly applied loading.

Another aspect, which can improve the value of the model, is the inclusion of relaxation of the fabric due to creep of the glass fibres. This has not been tested in the experiments for this thesis, but it will benefit to the applicability of the model. Testing this phenomenon will cost some time, because it is a time-dependant process. A different type of actuator is necessary when performing these experiments. Hydraulic actuators are not suitable for long-term loading.

11.4 Opportunities

Applicability of the model in the industry of tensile structures is an important aspect which determines the value of the end product. It is essential that it is an improvement on the current situation, or at least a step forward in the development of a product which will finally lead to the intended end product.

Currently, the industry uses linear elastic material models to design tensile structures. In the experiments, it has been shown that the material behaviour is highly non-linear due to the stress ratio dependant strain behaviour. The material model created in this thesis incorporates this nonlinear material behaviour. By using this model in the structural design of tensile structures, a more realistic prediction can be made of the acting fabric stresses and strains in the actual structure.

The model's performance must be improved in order to make it a useful tool for the engineer. Calculation times exceed the acceptable time in order to make it practical for desktop use. With improvements on the convergence this calculation time can be reduced.

Further tests on fabric with various qualities must demonstrate whether the model can be easily calibrated for other types of fabric, purely based on the fibres' geometry and Young's modulus of the particular fibre material. Fibre spacing, fibre diameter and Young's modulus of the fibre material are the three parameters which calibrate the material model. If this can be shown, it would mean that the designer is able to select various types of fabric quality, simply by changing the three parameters in the model.

In the current state the material model is not yet applicable for the industry. Further research on convergence issues, model accuracy and the adaptability to other fabric qualities may lead to improvements of the model. The model has potential to contribute to the development of industrially applicable nonlinear material models for architectural fabrics.

Literature and references

- [1] Materials for membrane structures, R. Houtman M. Orpana, Bauen mit Textilien Heft 4/2000
- [2] Leicht und Weit, R. Blum, 1990
- [3] Coated textiles, principles and applications, A.K. Sen, 2001
- [4] Tensile foil, ETFE foil as membrane construction material, J.W.J. de Vries, 2003
- [5] Silicon coated fibreglass for architectural structures, C.A.G. Nederpelt, 2004
- [6] Membrane material behaviour: concept, practise & developments, Bridgens et al, 2004
- [7] Stress-strain equations for non-linear behaviour of coated woven fabrics, A.S. Day, IASS, Osaka, 1986
- [8] Tension Structures, Form and behaviour, W.J. Lewis, 2003
- [9] The design of membrane and lightweight structures, M. Mollaert (ed.), Proceedings of the symposium at the Vrije Universiteit Brussel 2000, 2002.
- [10] http://www.ae.msstate.edu/vlsm/materials/strength_chars/secant.htm (January 25th, 2007)
- [11] Direct stress-strain representation for coated woven fabrics, B. Bridgens and P. Gosling, 2004
- [12] Non-linear material models for coated woven fabrics, Ove Arup & Partners, date unknown
- [13] Architectural fabric properties: determination, representation & prediction, Chapter 3, B.N. Bridgens, 2005
- [14] Structural Model for Textile, Hoogenboom, P.C.J. ,internal report Delft University of Technology, June 2007, online www.mechanics.citg.tudelft.nl/~pierre/publications.html ,August 2007

List of Figures

Figure 2: Millennium Dome, Greenwich (www.burohappold.com)	5
Figure 3: Detail of roof Millennium Dome, (www.greatbuildings.com)	5
Figure 4 : Burj al-Arab hotel, Bubai(www.wikipedia.org).....	6
Figure 5: Two different configurations of a weave (Houtman,2000).....	7
Figure 6: Application of PTFE onto the glass fibers (Mollaert,2002)	7
Figure 7: Fabric shows non-linear force-strain behaviour	8
Figure 8: Fabric response is depending on the fiber orientation	9
Figure 9: The fabric shows a non-elastic response under repeated loading	9
Figure 10: Cross section on a PTFE coated fiberglass fabric and a PVC coated polyester fabric (Bridgens et al, 2004)	10
Figure 11: Schematic representation of the crimp interchange effect in a fabric (Bridgens et al, 2004).....	11
Figure 12: Example of a geometric nonlinear two-bar system (Lewis, 2004)	13
Figure 13: Example of a cable structure with unknown coordinates for node 5 (Lewis, 2003) ...	16
Figure 14: Principle of determining the secant modulus [10]	19
Figure 15: Response surface created by Minami (Bridgens et al, 2004)	20
Figure 16: Cylinder test (Nederpelt, 2004)	23
Figure 17: Plain bi-axial test	24
Figure 18: PTFE coated fiber glass, initial behaviour and a decreasing additional strain.....	25
Figure 19: Conditioning process to prepare the fabric sample for testing (Bridgens, 2004).....	26
Figure 20: Different load paths in preset warp-weft ratios produce a wide range of stress states of the fabric	27
Figure 21: Test rig for bi-axial testing	28
Figure 22: Four different configurations for slits in the cruciform sample (Bridgens, 2004).....	29
Figure 23: Clamping the sample (Nederpelt, 2004)	30
Figure 24: Enforcement on the clamp	30
Figure 25: Example of the data gathered from the experiments	31
Figure 26: Conditioning program (Bridgens, 2005).....	32
Figure 27: Testing program with applied load in both warp and weft direction	33
Figure 29: Dimensions of the cruciform sample.....	34
Figure 30: Stresses in x -direction in the sample	35
Figure 31: Stress distribution on the central square	37
Figure 32: Stress distribution on a wider area than the central square.....	38
Figure 33: Sample with 10 slits in the cruciform arms	39
Figure 34: Potentiometers on the measuring area	40
Figure 35: A medical needle ensures a fixed position of the potentiometer	41
Figure 36: Potentiometer with rolling supports.....	42
Figure 37: Parallel setup of the potentiometers.....	43
Figure 38: Loading program for repeated tests	44
Figure 39: Force strain results for 5th test	44
Figure 40: Young's moduli categorized	45
Figure 41: Strain measurements	46
Figure 42: Strain measurements with potentiometers replaced	46
Figure 43: Fabric codes.....	48
Figure 44: Example of 17 hours prestress	49
Figure 45: Conditioning program (two cycles)	50
Figure 46: Conditioning fabric 7	50
Figure 47: Theoretical load paths for fabric quality B18089.....	51
Figure 48: Actual load paths performed during testing	52
Figure 49: Strain measurements for load ratio 1:1.....	53
Figure 50: Strain measurements for load ratio 1:5.....	53
Figure 51: Strain measurements for load ratio 2:1.....	54
Figure 52: Strain measurements for load ratio 1:2.....	54
Figure 53: Strain measurements for load ratio 1:0.....	55
Figure 54: Strain measurements for load ratio 0:1.....	55
Figure 55: Strain measurements for load ratio 5:1.....	56
Figure 58: Stress-Stress-Strain (x,y,z) data for weft fibre direction	60
Figure 59: Fitted surface for Warp strain.....	61
Figure 60: Fitted surface for Weft strain	61
Figure 61: Plot data scatter warp stresses.....	63

Figure 62: Plot data scatter weft stresses	63
Figure 63: Plot data scatter warp stresses top view	64
Figure 64: Plot data scatter weft stresses top view	64
Figure 65: Reduced data plot strain warp, fabric sample #3.....	65
Figure 66: Reduced data plot strain weft, fabric sample #3	65
Figure 67: Fitted solution for warp direction, fabric sample #3	66
Figure 68: Fitted solution for weft direction, fabric sample #3.....	66
Figure 70: Model single element, no mesh, homogenous stress	77
Figure 71: Model multi element, meshed, homogenous stress	78
Figure 72: Model multi element, meshed, non uniform stress distribution.....	79
Figure 73: stress distribution in x direction.....	80
Figure 74: Square sample of fabric, restrained at two sides, and stressed at two sides.....	81
Figure 75: Displacements due to perpendicular load	81
Figure 76: Stresses in the fabric in x direction	82
Figure 77: Stresses in y direction.....	82

List of tables

Table 1: Conditioning program	32
Table 2: Test characteristics	43
Table 3: Conditioning procedure.....	49
Table 4: Parameters and errors warp	67
Table 5: Parameters and errors weft	67
Table 6: Averaged values for parameters	68
Table 7: Solutions for elastic constants, isotropic	69
Table 8: Solutions for elastic constants, orthotropic.....	70

Appendices

General

- A0 Student info
- A1 Committee members

Testing

- B1 Datasheet Verseidag B18089
- B2 Manual for testing
- B3 Potentiometer calibration
- B4 Sample preparation
- B5 Modifying the biaxial test bench for PTFE coated fibre glass testing

Modeling

- C1 Usermat code
- C2 Determination of model factor
- C3 CD Rom contents

A0 Student info

Name: P.H. van Asselt (Peter)
Address: Boerderijstraat 8
Zip code: 2623 AT
City: Delft

Student number: 1004212

Mobile Phone: 06 48 15 28 22
Email: p.h.vanasselt@student.tudelft.nl

Room: 0.72 BG CiTG, Stevinweg 1, Delft

A1 Committee members

Name: **Prof.dipl.ing. J.N.J.A. Vambersky** (Chairman)
Email: J.N.J.A.Vambersky@tudelft.nl
Telephone: +31 (0)15 27 85488
Faculty: Civiele Techniek & Geowetenschappen
Section: Sectie Gebouwen & Civieltechnische Constructies
Address: Stevinweg 1
Room: 1.53ST2
Zip code: 2628CN
Place: Delft

Name: **ir. J.L. Coenders** (daily supervisor)
Email: J.L.Coenders@tudelft.nl
Telephone: +31 (0)15 27 85711
Faculty: Civiele Techniek & Geowetenschappen
Section: Sectie Gebouwen & Civieltechnische Constructies, Structural Design Lab
Address: Stevinweg 1
Room: 1.60ST2
Zip code: 2628CN
Place: Delft

Name: **ir. R. Houtman**
Email: Rogier@tentech.nl
Telephone: +31 (0)30 252 1869
Company: Tentech
Section: nvt
Address: Rotsoord 13E
Room: nvt
Zip code: 3523 CL
Place: Utrecht

Name: **dr. ir. P.C.J. Hoogenboom**
Email: P.C.J.Hoogenboom@tudelft.nl
Telephone: +31 (0)15 27 88 081
Faculty: Civiele Techniek & Geowetenschappen
Section: Department Structural Mechanics
Address: Stevinweg 1
Room: 6.48
Zip code: 2628CN
Place: Delft

Name: **Ir. P.A. de Vries** (experimental support)
Email: P.A.deVries@tudelft.nl
Telephone: +31 (0)15 27 84 034
Faculty: Civiele Techniek & Geowetenschappen
Section: Department Structural Mechanics
Address: Stevinweg 1
Room: 2.56ST2
Zip code: 2628CN
Place: Delft

B1 Datasheet Verseidag B18089

Quality: B 18089 GF

Type III

Date: Sep 03

Properties	Test Standards		Values	Units
Fibre Type of the Base Fabric Faserstoff des Trägergewebes Tissu Support	(DIN 60001)		Glass EC 3/4	
Yarn Count Fadendichte Nombre de Fil	(DIN EN 1049)	warp weft	10 11	yarn/cm
Titer of Yarn Garn Titer Târes du fil		warp weft	33x2x3 33x2x3	tex
Weave Style Bindung Armure	(DIN ISO 9354)		L 1/1	
Weight per Unit Area of Base Fabric Flächenbezogene Masse des Gewebes Poids du Tissu Support	(DIN EN 12127)		450	g/m ²
Base Coat Beschichtungsart Nature de l'Énduit			PTFE	
Total Mass per Unit Area Flächenbezogene Gesamtmasse Masse Totale	(DIN EN ISO 2286-2)		1150	g/m ²
Total thickness Gesamtdicke épaisseur total	(DIN EN ISO 2286-3)		0,7	mm
Tensile Strength Höchstzugkraft Resistance à la Rupture en chaîne/en trame	(DIN 53354)	warp weft	7000 6000	N/5cm
Tear Resistance Weißerißkraft Resistance à la Déchirure en chaîne/en trame	(DIN53363)	warp weft	500 500	N
Adhesion Haftung Adhesion	(DIN 53357)		80	N/5cm
Translucency at 550 nm Transluzenz bei translucidité	(DIN 5036)		12 - 14	%
Fire behaviour according to Brandverhalten entspricht ignifuge selon	DIN 4102 Part 1 B1, NFPA 92503 M1, BS 476 Part ,4,6,7,11 ASTM E 84, ASTM E 108, ASTM E 136 (fabric), NFPA 701 small scale, CL 2			

B2 Manual for testing

Important note

In this thesis the B18089 has been tested. The intention was to test the B18089 as well as the B18039. However, due to time constraints the research is limited to the B18089. The procedure for testing the B18039 is still included in this testing manual, in case this fabric is tested for follow up research.

Analysis of tent structures

Implementation of non-linear material behaviour in structural analysis

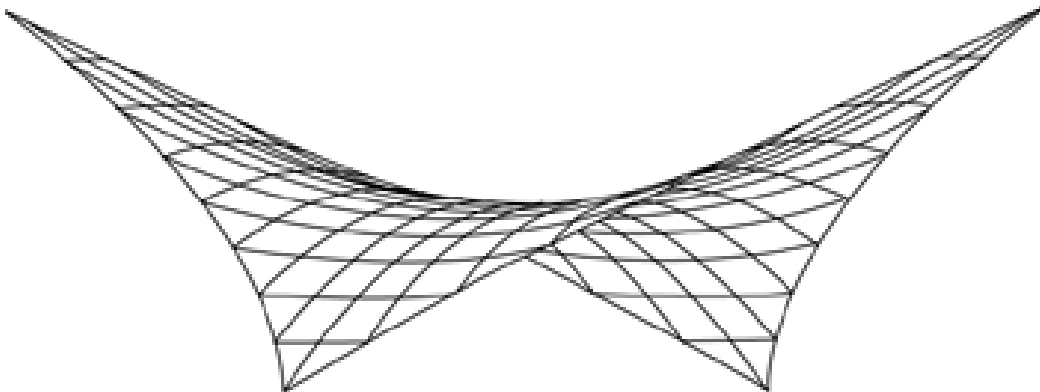


Table of contents

Analysis of tent structures
Table of contents	1
1. Introduction	2
2. Material	3
3. Testing.....	4
3.1 Test piece.....	4
3.2 Prestress	5
3.3 Conditioning.....	5
3.4 Testing.....	6
3.5 Expected results	8
Appendix	10
Measuring points B18039	11
Measuring points B18089	12
Datasheet B18039	13
Datasheet B18089	14

1. Introduction

In the Masters' Thesis "Analysis of tent structures – *Implementation of non-linear material behaviour in structural analysis*" research will be done to the biaxial nonlinear behaviour of architectural textile. By describing the nonlinear stress-strain relation of the fabric, a more detailed and accurate structural analysis of a tent structure can be made.

In current practice various software packages are available for analyzing membrane structures. The material properties are represented by a simplification of the actual properties. The non-linear stress-strain relation is linearized, in order to derive a constant E-modulus from the stress-strain relation. The structural analysis of the tent structure is based on the constant E modulus.

This method will provide an approximation of the actual material behaviour. The actual behaviour is non-linear, where the fabric becomes stiffer on higher stress states. This stiffening behaviour is caused by the woven glass fibre base of the fabric. The fibres tend to rearrange themselves under tension. This causes large strains in the fabric. After straightening and rearranging the fabric strain is caused by elongation of the glass fibres. The elongation of the fibres causes less strain than the process of rearranging.

Due to the configuration of the fibres, an interaction between the fibres causes a stress ratio dependant strain behaviour. Each ratio of stresses in the two main directions results in a unique strain behaviour.

In order to obtain a stress-strain relation of the fabric, biaxial tests will be performed. By tensioning the fabric at various stress ratios, a complete response will be generated of the fabric behaviour.

The results of the biaxial tests is a complete set of data representing the stress-strain behaviour of the fabric. Based on this data set, a model can be produced. This model can link a stress state to a given strain rate. When analyzing a tent structure, the strains caused by external loadings can be calculated. The model can return the stress state of the fabric, when given the strain rate.

In this manual a test procedure will be described, in order to obtain data that is useable for the model. Due to a absence of a national code, this method is developed by a British Phd student, who researched architectural textiles.

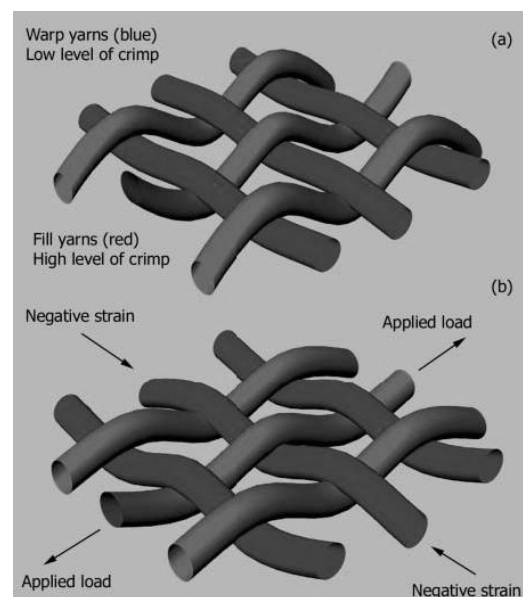


Figure 78: Interaction between the yarns (Bridgens, 2004)

2. Material

The material to be tested in this Thesis has been provided by Verseidag (Germany). The researched fabric is PTFE coated fiberglass. PTFE is an industrial name for Teflon. This fabric is produced in various quality types. In this thesis only two quality types will be researched. This will make it possible to compare results of different tests. Technical data of the fabrics are included in the appendix.

The choice for this material has been advised by Mr R. Houtman, from TenTech bv. This fabric is a widely used material in the membrane industry. Due to the non-forgiveness of the material, knowledge and insight in material behaviour of this type is desired. Due to time constraints it is not possible to test other types of fabric.

3. Testing

In this chapter the test protocol will be described. Backgrounds and motivation for different actions are described in short. More detailed information can be found in the literature study of the thesis.

3.1 Test piece

The test specimen will be cut out of the roles of fabric provided by Verseidag. The dimensions of the sample are given in figure 2.

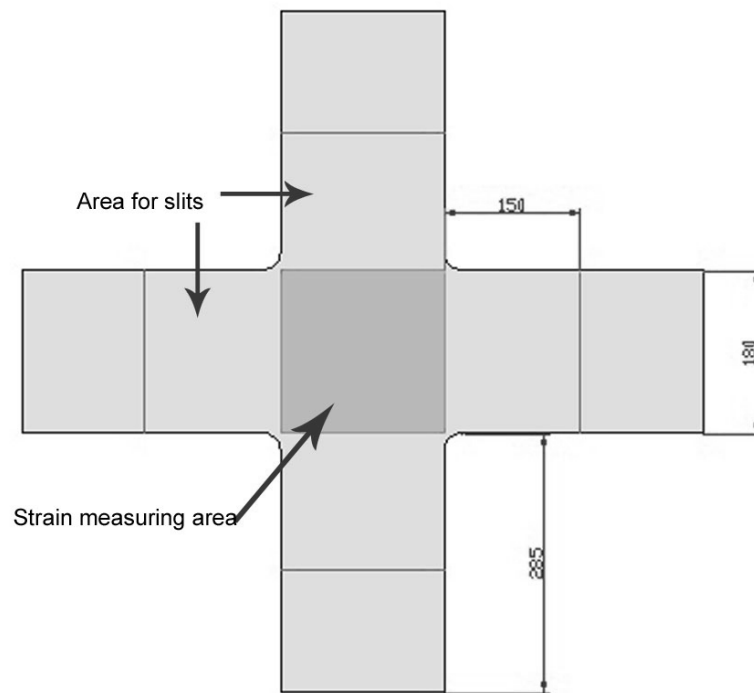


Figure 79: Dimensions of the test specimen

In Figure 2, four different areas are pointed out that will be carried out with slits. Due to the monoaxial forces in the arms of the sample, lateral contraction will cause a constraint of the central measuring area. Because this constraint is undesired, slits in the arms will prevent the fabric from contracting. An analysis in Ansys will provide the optimal configuration of the slits.

The grey area is the central measuring area. Small potentiometers will record the displacement of the sample. By using the original distance of the potentiometers, and the recorded displacement, the strain of the material can be calculated.

On the samples, the warp and weft direction must be indicated with a marker. This is necessary due a different ultimate stress for both directions. Besides the warp and weft directions, the origin of the location of the sample must be recorded. A possible variation of fabric quality along the width of the role can then be identified. The lighter fabric quality is provided in two different batches, from different parts along the length of the role. Therefore the batchnumber must be recorded as well.

3.2 Prestress

In order to prepare the test sample for testing, a **17 hour** prestress state must be applied to the sample. This is necessary to remove permanent strain from the sample. The fabric shows large initial and permanent strains. After removing these strains, the fabric shows almost elastic behaviour. Repetitive tests then provide similar results. The prestress will be at a stress level that is comparable with the stress level that is applied in membrane structures.

The prestress level is expressed as a percentage of the ultimate tensile strength of a strip of fabric (UTS). The UTS is the breaking strength of the fabric when loaded uniaxial. For both warp and weft directions the UTS is given on the manufacturer's data sheet, see Appendix. The prestress level is set at 2,5% of the UTS. In Table 1 the prestress levels are indicated. These values are given in a force per width unit. In Table 2, the prestress values are calculated for the 180mm sample width.

Table 9: Prestress levels

	UTS (N/5cm)	UTS (N/5cm)	Pretension 2,5%UTS(N/5cm)	Pretension 2,5%UTS (N/5cm)
	Warp	Weft	Warp	weft
B18039	4200	4000	105	100
B18089	7000	6000	175	150

The sample width is 180mm. The values for prestress for 180mm are calculated in Table 2.

Table 10: Prestress levels per sample arm

	Pretension (N)	Pretension (N)
	warp	weft
B18039	378	360
B18089	630	540

3.3 Conditioning

After a 17 hour during period of prestress, the fabric will be conditioned in order to remove large initial strains from the fabric. The fabric is stressed in a cycle of loadings. The fibres will rearrange and cause large permanent strains in the fabric. After repeating these loading cycles the additional strain will eventually become negligibly small.

The loading cycles are shown in Table 3. The prestress level is shown in Table 2. The conditioning load is set at 25% of the ultimate tensile strength, as provided by the fabric's manufacturer. These values are shown in Table 4. From experience of Bridgens, it appeared that 3 cycles are sufficient in order to prepare the test sample for testing. Three cycles take up to **1,5 hours**

Table 11: Program for conditioning (one cycle)

Time (minutes)	Warp	Weft
0-5	prestress	Prestress
5-10	Conditioning Load	Conditioning Load
10-15	Prestress	Prestress
15-20	Conditioning Load	Prestress
20-25	Prestress	Prestress
25-30	Prestress	Conditioning Load

Table 12: Conditioning loads, as stated in table 3

	Conditioning load (N)	Conditioning load (N)
	Warp	Weft
B18039	3780	3600
B18089	6300	5400

The conditioning process can be illustrated as shown in Figure 3, where the applied stress is plotted against the time.

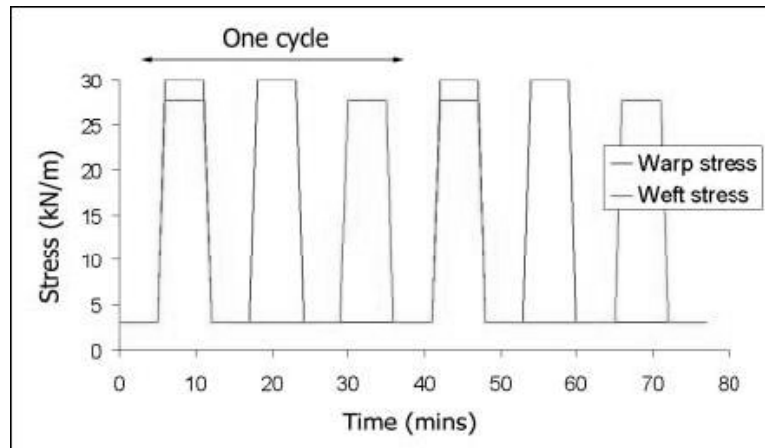


Figure 80: Conditioning program (Bridgens, 2004)

3.4 Testing

After conditioning the sample, the sample is ready for testing. A complete set of tests can be performed on the same sample of fabric. The ultimate load that will be applied will not exceed 25% of the ultimate tensile strength. Tearing of the fabric will not occur therefore.

The tests will be performed at a series of preset load ratios. The starting point of each load ratio is the prestress situation. From that point different paths will be followed, maintaining the preset ratio between the two forces. Each path contains a number of measuring points, at which the stress situation is kept constant for the duration of 1 minute. During this minute, measurements of strain are taken every 5 seconds. Similarly, strain measurements are taken on the other points of the load path.

A load path contains a loading and unloading path. Due to a non-coinciding loading and unloading behaviour, measurements must be taken on both the loading as well as on the unloading path. The end of the unloading path returns at the point of prestress.

For both fabric qualities an individual loading program is designed. These are given in Figures 4 and 5.

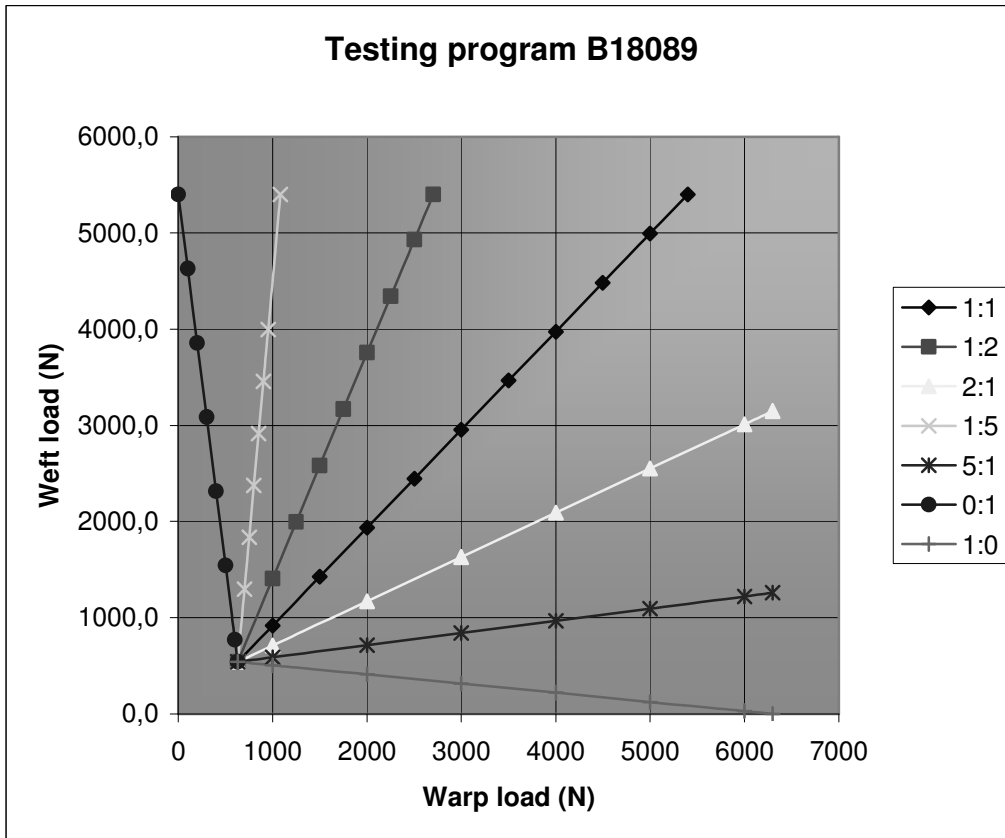


Figure 81: Testing program for fabric quality B18089

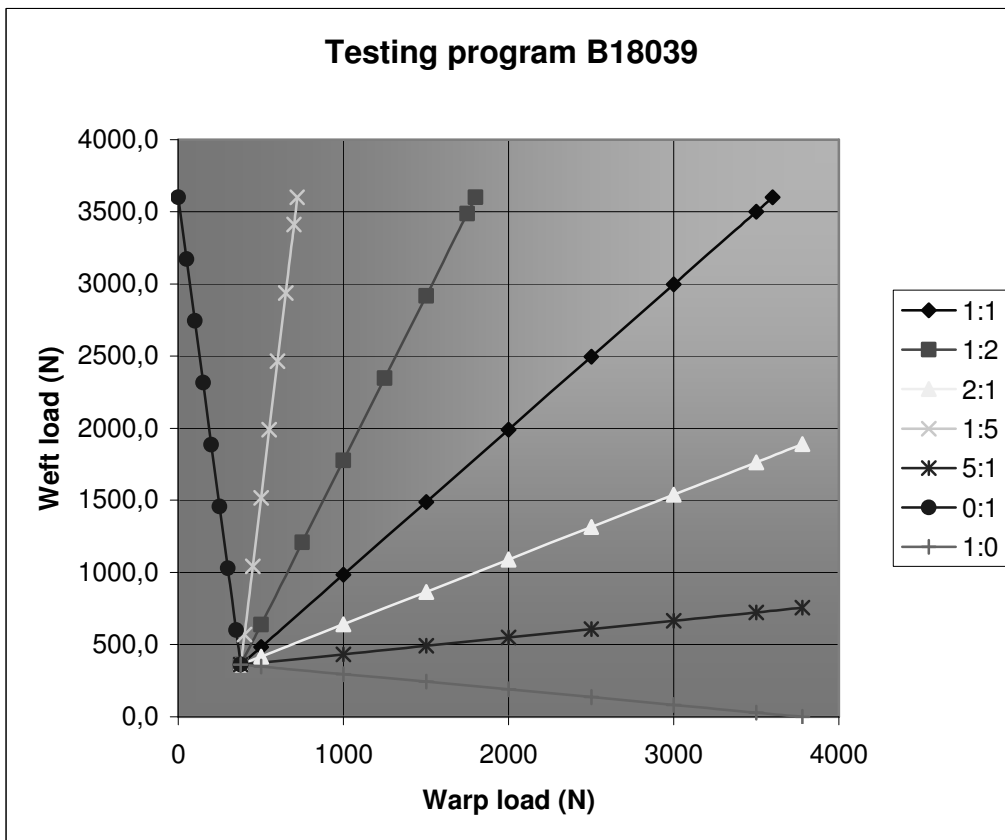


Figure 82: Testing quality for fabric quality B18039

The measuring points are included in the appendix. At these points, the particular load ratio is kept constant, while logging the strain data from the potentiometers every 5 seconds.

The order of applying the load paths is not arbitrary. The history of loading has a certain influence on the strain response of the fabric. Therefore the order as stated in table 5 must be followed when performing the tests.

Table 13: Order of testing loadpaths

Order	Warp:weft ratio
1	1:1
2	1:5
3	2:1
4	1:2
5	1:0
6	0:1
7	5:1

3.5 Expected results

In order to use measuring devices with an appropriate range, the expected results for stress and strain are stated below.

Based on the maximum load that will be applied during the tests, a loadcell with the proper range can be selected. For both fabric qualities, the maximum load to be applied is stated in Table 6.

Table 14: Maximum load per fabric quality, in N per arm

Fabric quality	Maximum load warp (N)	Maximum load weft (N)
B18039	3780	3600
B18089	6300	5400

The range for the displacement measuring devices depends on the expected strain of the fabric. The total testing process can be divided into three different stages: prestress, conditioning and testing. Based on results from Bridgens (Architectural fabric properties, 2005) the expected strains after each stage are stated in Table 7. No data is available for the lighter fabric quality, but expected is that the strains will be in the same range.

Table 15: Strains in the fabric, measured after each stage of the testing process

Fabric quality	Prestress		Conditioning		Testing	
	Warp strain (%)	Weft strain (%)	Warp strain (%)	Weft strain (%)	Warp strain (%)	Weft strain (%)
B18039						
B18089	1.15	2.85	-1.19	13.85	0.25	12.61

Besides permanent strains measured after testing, the elastic strain during testing must also be considered. Test results from Bridgens show that strains up to 12% occur during testing.

Strains are measured as a percentage of the original measuring distance. The totals expected strain is approximately 25%. When measuring over a distance of 80 to 100mm, the required measuring range of the devices must be up to 25mm.

It must be noticed that negative strains also occur during testing. The measuring device must be able to detect negative strains as well.

Appendices

Measuring points B18039

Measuring points for fabric quality B18039. Loads are given in couples, one for the warp direction and one for the weft direction.

	1:1		1:2		2:1		1:5	
warp (N)	weft (N)							
378	360,0	378	360,0	378	360,0	378	360	
500	482,7	500	638,0	500	414,9	400	568,4	
1000	985,5	750	1207,6	1000	639,7	450	1042,1	
1500	1488,3	1000	1777,2	1500	864,6	500	1515,8	
2000	1991,1	1250	2346,8	2000	1089,5	550	1989,5	
2500	2493,9	1500	2916,5	2500	1314,3	600	2463,2	
3000	2996,6	1750	3486,1	3000	1539,2	650	2936,8	
3500	3499,4	1800	3600,0	3500	1764,1	700	3410,5	
3600	3600,0			3780	1890,0	720	3600	

	5:1		0:1		1:0	
warp (N)	weft (N)	warp (N)	weft (N)	warp (N)	weft (N)	
378	360,0	378	360,0	378	360,0	
1000	432,4	350	600,0	500	347,1	
1500	490,6	300	1028,6	1000	294,2	
2000	548,8	250	1457,1	1500	241,3	
2500	607,0	200	1885,7	2000	188,4	
3000	665,2	150	2314,3	2500	135,4	
3500	723,4	100	2742,9	3000	82,5	
3780	756,0	50	3171,4	3500	29,6	
		0	3600,0	3780	0,0	

Measuring points B18089

Measuring points for fabric quality B18039. Loads are given in couples, one for the warp direction and one for the weft direction.

	1:1		1:2		2:1		1:5	
warp (N)	weft (N)							
630	540,0	630	540,0	630	540,0	630	540	
1000	917,0	1000	1408,7	1000	710,3	700	1296	
1500	1426,4	1250	1995,7	2000	1170,6	750	1836	
2000	1935,8	1500	2582,6	3000	1631,0	800	2376	
2500	2445,3	1750	3169,6	4000	2091,3	850	2916	
3000	2954,7	2000	3756,5	5000	2551,6	900	3456	
3500	3464,2	2250	4343,5	6000	3011,9	950	3996	
4000	3973,6	2500	4930,4	6300	3150,0	1080	5400	
4500	4483,0	2700	5400,0					
5000	4992,5							
5400	5400,0							

	5:1		0:1		1:0	
warp (N)	weft (N)	warp (N)	weft (N)	warp (N)	weft (N)	
630	540,0	630	540,0	630	540,0	
1000	587,0	600	771,4	1000	504,8	
2000	714,0	500	1542,9	2000	409,5	
3000	841,0	400	2314,3	3000	314,3	
4000	967,9	300	3085,7	4000	219,0	
5000	1094,9	200	3857,1	5000	123,8	
6000	1221,9	100	4628,6	6000	28,6	
6300	1260,0	0	5400,0	6300	0,0	

Datasheet B18039

Quality: B 18039 GF

Type II

Date: Sep 03

Properties	Test Standards		Values	Units
Fibre Type of the Base Fabric Faserstoff des Trägergewebes Tissu Support	(DIN 60001)		Glass EC 3/4	
Yarn Count Fadendichte Nombre de Fil	(DIN EN 1049)	warp weft	13 13	yarn/cm
Titer of Yarn Garn Titer Titres du fil		warp weft	33x2x2 33x2x2	tex
Weave Style Bindung Armure	(DIN ISO 9354)		L 1/1	
Weight per Unit Area of Base Fabric Flächenbezogene Masse des Gewebes Poids du Tissu Support	(DIN EN 12127)		365	g/m ²
Base Coat Beschichtungsart Nature de l'Énduit			PTFE	
Total Mass per Unit Area Flächenbezogene Gesamtmasse Masse Totale	(DIN EN ISO 2286-2)		800	g/m ²
Total thickness Gesamtdicke épaisseur total	(DIN EN ISO 2286-3)		0,5	mm
Tensile Strength Höchstzugkraft Resistance à la Rupture en chaîne/en trame	(DIN 53354)	warp weft	4200 4000	N/5cm
Tear Resistance Weißerißkraft Resistance à la Déchirure en chaîne/en trame	(DIN53363)	warp weft	300 300	N
Adhesion Haftung Adhesion	(DIN 53357)		60	N/5cm
Translucency at 550 nm Transluzenz bei translucidité	(DIN 5036)		15-17	%
Fire behaviour according to Brandverhalten entspricht ignifuge selon	DIN 4102 Part 1 A2, NFPA 92503 M1, BS 476 Part 3,4,5,6,7, ASTM E 84, ASTM E 108, ASTM E 136 (fabric), NFPA 701 small scale			

Datasheet B18089

Quality: B 18089 GF

Type III

Date: Sep 03

Properties	Test Standards		Values	Units
Fibre Type of the Base Fabric Faserstoff des Trägergewebes Tissu Support	(DIN 60001)		Glass EC 3/4	
Yarn Count Fadendichte Nombre de Fil	(DIN EN 1049)	warp weft	10 11	yarn/cm
Titer of Yarn Garn Titer Titres du fil		warp weft	33x2x3 33x2x3	tex
Weave Style Bindung Armure	(DIN ISO 9354)		L 1/1	
Weight per Unit Area of Base Fabric Flächenbezogene Masse des Gewebes Poids du Tissu Support	(DIN EN 12127)		450	g/m ²
Base Coat Beschichtungsart Nature de l'Énduit			PTFE	
Total Mass per Unit Area Flächenbezogene Gesamtmasse Masse Totale	(DIN EN ISO 2286-2)		1150	g/m ²
Total thickness Gesamtdicke épaisseur total	(DIN EN ISO 2286-3)		0,7	mm
Tensile Strength Höchstzugkraft Resistance à la Rupture en chaîne/en trame	(DIN 53354)	warp weft	7000 6000	N/5cm
Tear Resistance Weißerißkraft Resistance à la Déchirure en chaîne/en trame	(DIN53363)	warp weft	500 500	N
Adhesion Haftung Adhesion	(DIN 53357)		80	N/5cm
Translucency at 550 nm Transluzenz bei translucidité	(DIN 5036)		12 - 14	%
Fire behaviour according to Brandverhalten entspricht ignifuge selon	DIN 4102 Part 1 B1, NFPA 92503 M1, BS 476 Part ,4,6,7,11 ASTM E 84, ASTM E 108, ASTM E 136 (fabric), NFPA 701 small scale, CL 2			

B3 Potentiometer calibration

Potentiometers are used to measure the fabric displacements. In order for the potentiometers to display displacements, instead of units, they must be calibrated. The calibration process will also show if the potentiometers have a linear range. Besides that, calibration will also show non-recording areas of the potentiometers. These 'dead zones' must be blocked with mechanical devices to prevent them from entering these zones.

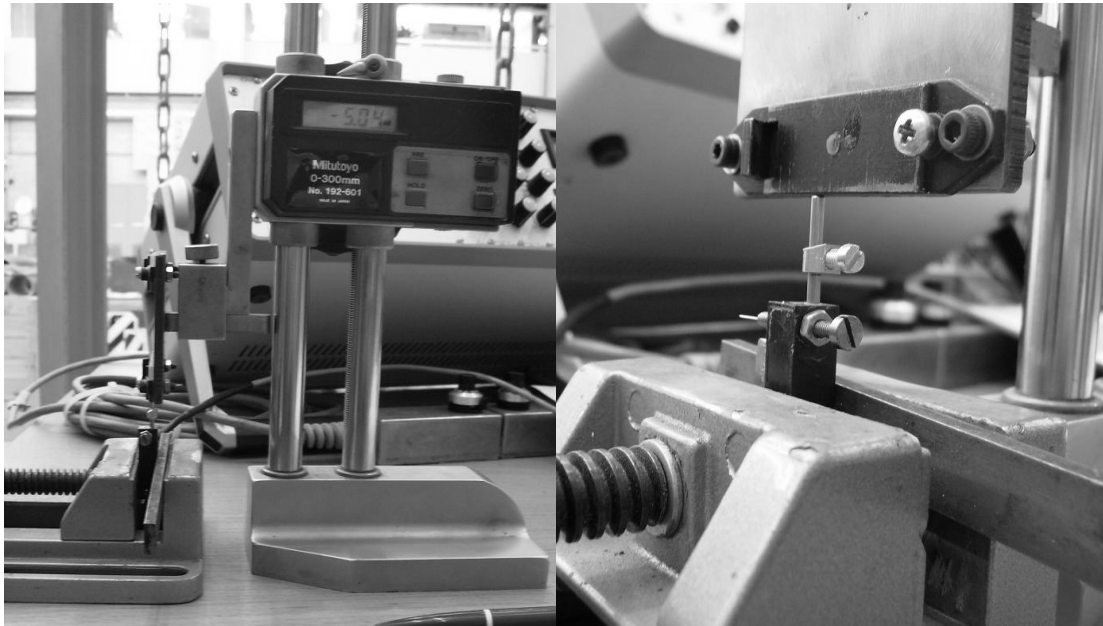


Figure 83: Calibration of potentiometer by using a digital height meter

Calibrating the potentiometers is done by using a digital height meter. The potentiometers are clamped in a vertical direction. Initially the calibration factor is set at 0. By applying a known displacement on various points on the range of the potentiometer, the output can be recorded. Plotting the displacements over the recorded outputs result in the plots shown in Figure 31.

The plots show that the potentiometers have a linear range. The mechanical devices are applied on the potentiometer to prevent it from entering the non-recording zones. From the plots it becomes clear that there are no non-recording zones in the range of the tested displacements.

The software used to log the experimental data is the in-house software from the Delft University of Technology. The software is called BFG and is designed by ir. C. van Beek.

The used formula to represent the displacements is:

$$\text{Monitor Value} = \text{units (units)} \times \text{scale factor (mm/unit)}$$

The PC-card measures in *units*, while the desired output is in *mm*. Therefore a scale factor must be used. This scale factor (in *mm/unit*) can be derived from the calibration plots. The slope of these plots is the scale factor. For each potentiometer the following scale factors are derived from the plots.

Table 16: Scale Factor for the potentiometers

Set	Channel	Scale Factor
B-set	Channel 8	0.0026377
B-set	Channel 9	0.0026518
A-set	Channel 10	0.0026499
A-set	Channel 11	0.0026033

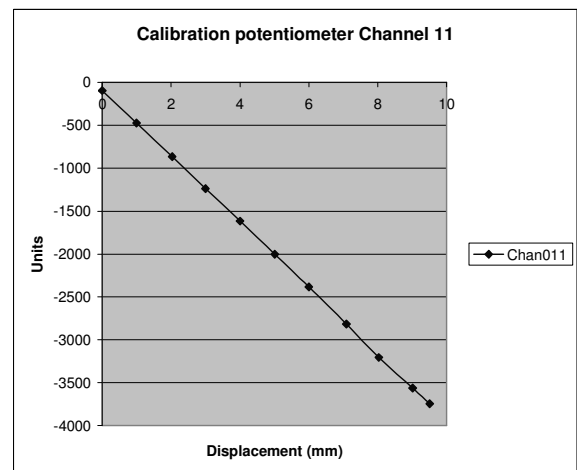
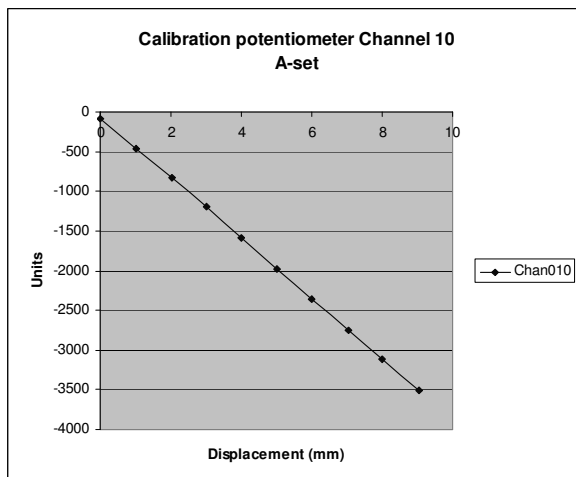
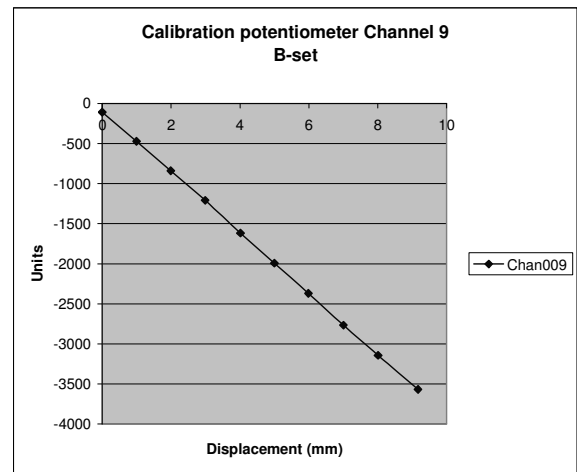
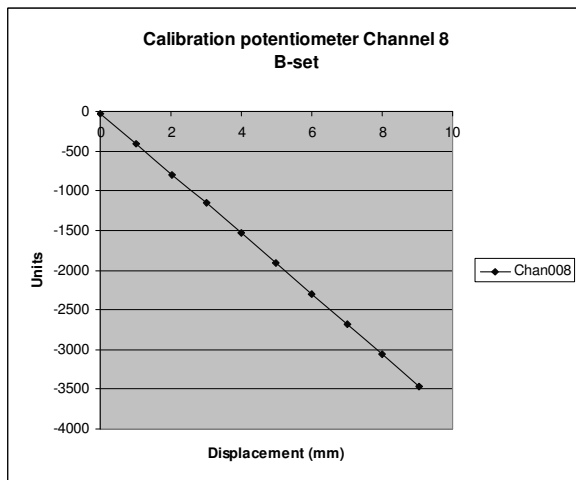


Figure 84: Calibration of potentiometers

B4 Sample preparation

The PTFE coated fibreglass is supplied on rolls with a width of 2450mm. A procedure is designed to create the cruciform test samples from the roll. Creating a sample takes approximately 2 hours. It is necessary to include a high level of detail in creating the samples, in order to diminish errors in testing due to inaccuracies in the sample geometry.

Step 1 Drawing

Draw the shape of the cruciform sample on the fabric, with the aid of a prefabricated mould. The cruciform arms should have sufficient length in order to secure the fabric in the clamps. In this case, a total length of 1200mm was used. To prevent the corners from tearing, the corner should be a fillet with a radius of approximately 25mm.

In this stage it is useful to apply markings on the central measuring square. Markings such as diagonals and symmetry lines are useful for the positioning of the strain measurement devices.

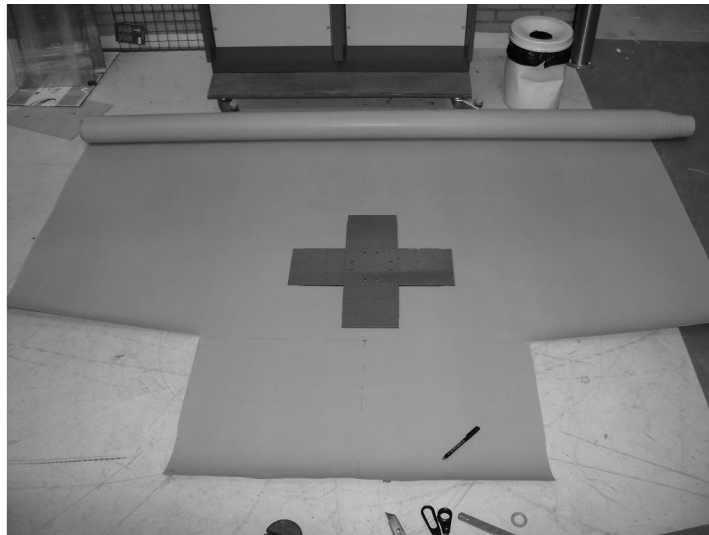


Figure 85: Drawing the shape with the aid of a mould

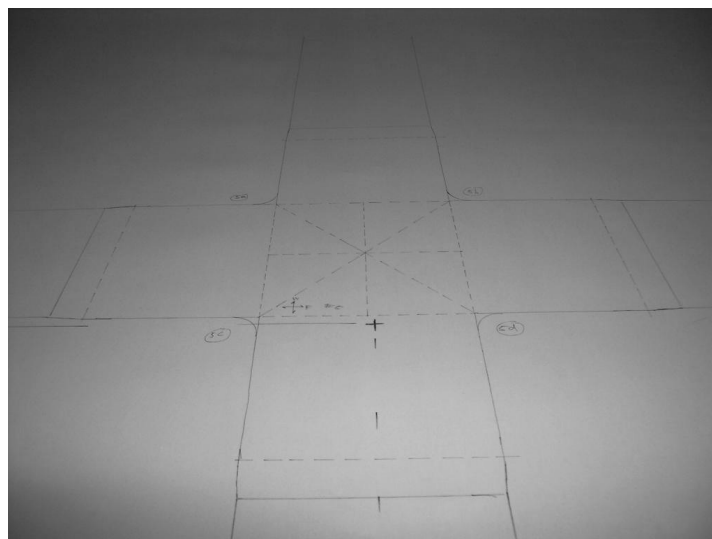


Figure 86: Adding symmetry lines on the central measuring square

Step 2 Cutting

The sample can now be cut out with a pair of scissors. The fillet corner is best cut out with the aid of a sharp knife. It can be recommended to handle the sample with care. Folding may cause internal damage to the glass fibres.

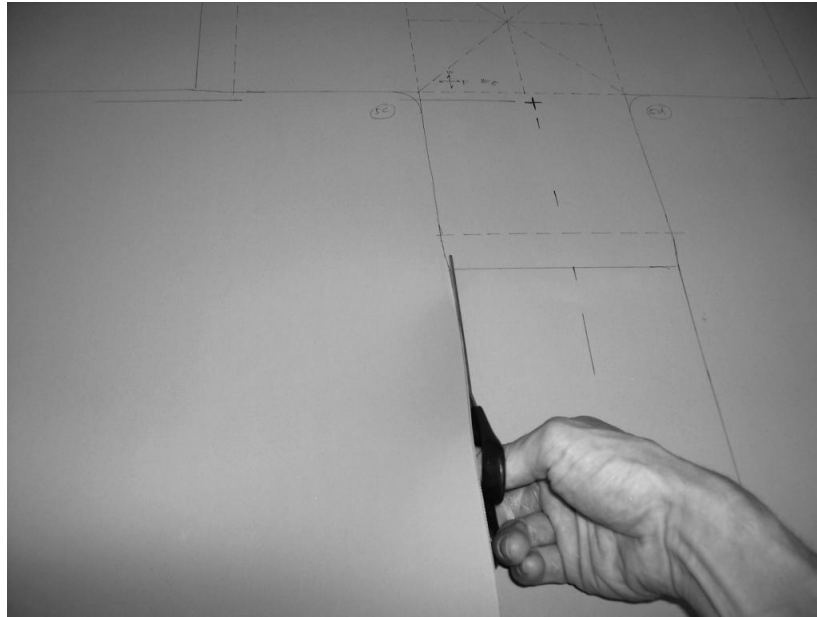


Figure 87: Cutting the sample

Step 3 Finishing

Now the slits can be applied to the sample. Some self made paper rulers which indicate the slit width can help out with cutting the slits. These rulers can be taped on to the fabric. By clamping a large steel ruler on the fabric, lined up with the paper rulers, the slits can be cut in the fabric by using a sharp knife.

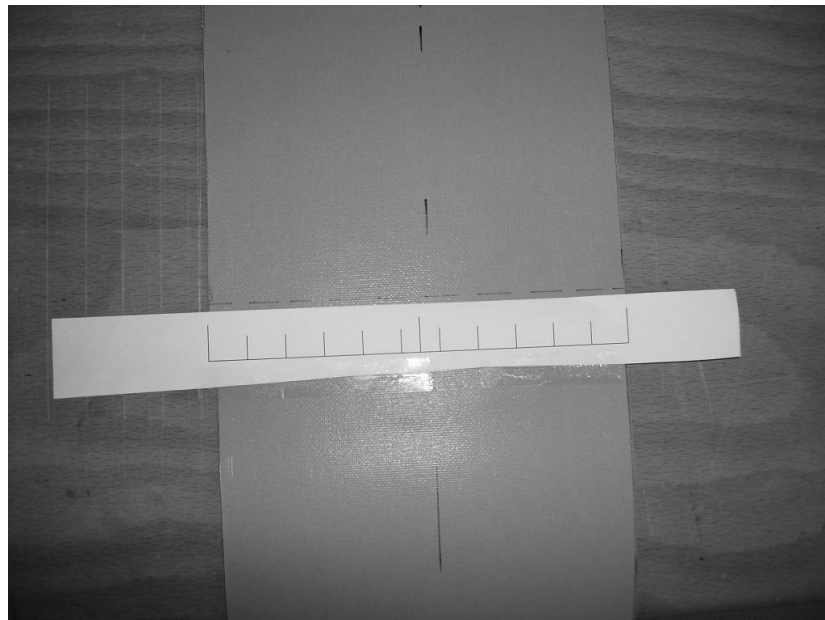


Figure 88: Paper rulers enhance cutting the slits in the fabric

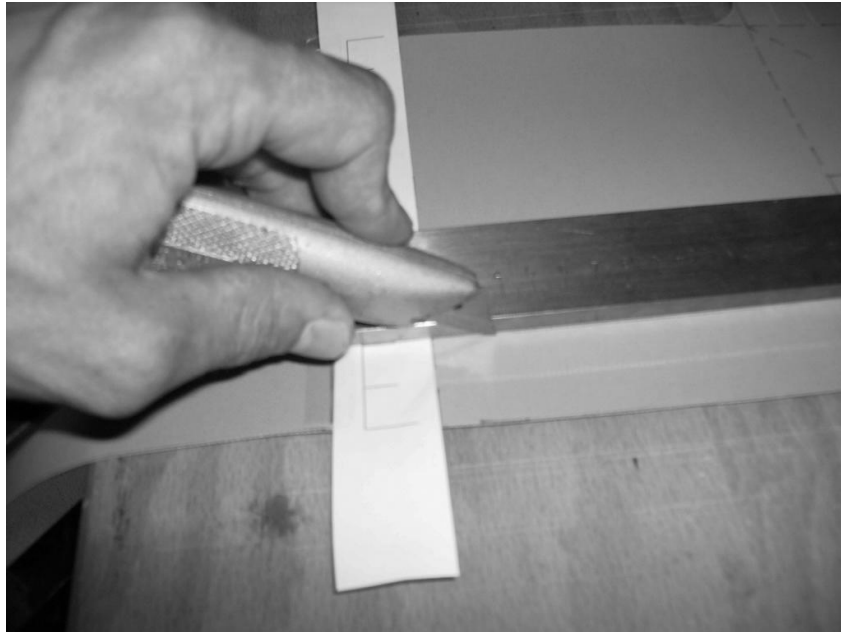


Figure 89: Cutting the slits with a sharp knife

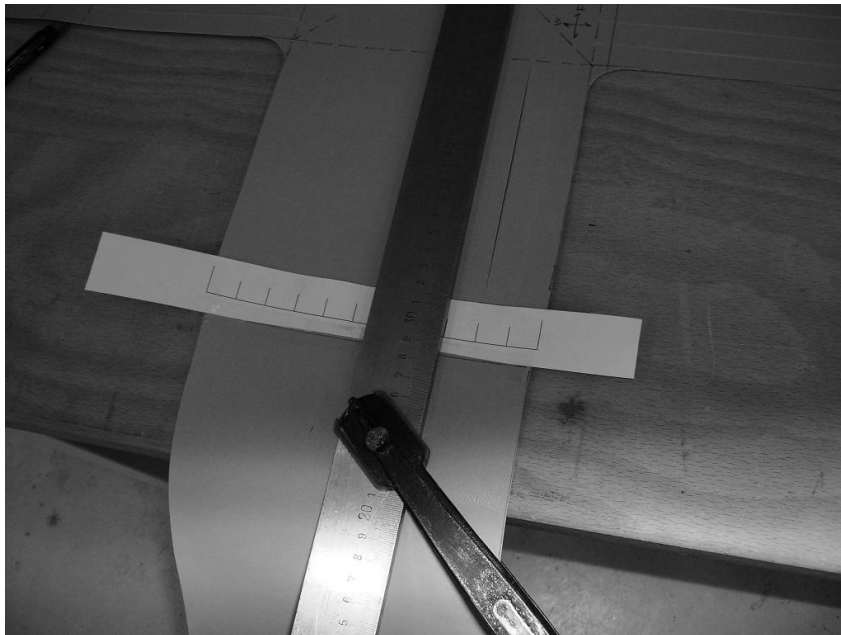


Figure 90: A steel ruler clamped on the fabric lined up with the markers on the paper ruler

B5 Modifying the biaxial test bench for PTFE coated fibre glass testing

The experimental part of the thesis involves a lot of trial-and-error work around finding a suitable way of testing the fabric. The main problem with the test setup is the way of clamping the sample. With clamping the sample, the objective is to prevent the sample from slipping and to ensure a uniform distribution of the applied force into the fabric. Various problems arose in the search of the best way of clamping the sample.

The tube

A PVC tube is used in the clamp to establish friction between the clamp and the fabric. The tube is supposed to be flexible enough to adapt to any irregularities in the fabric surface, but stiff enough to be able to apply a pressure force on the fabric. However, when applying force to the clamps, the fabric slips out of the clamps. The presence of PTFE, or Teflon, as a top layer of the fabric, is not helpful in generating friction between the fabric and the clamp. Therefore a larger force is applied on the tube, to generate friction. Slipping of the fabric now showed up at a higher load. The slipping was a result of plastic deformation of the PVC tube, see Figure 38. The reaction force of the fabric on the tube caused it to deform, see Figure 38. After the deformation of the tube, the friction decreased, causing the fabric to slip.

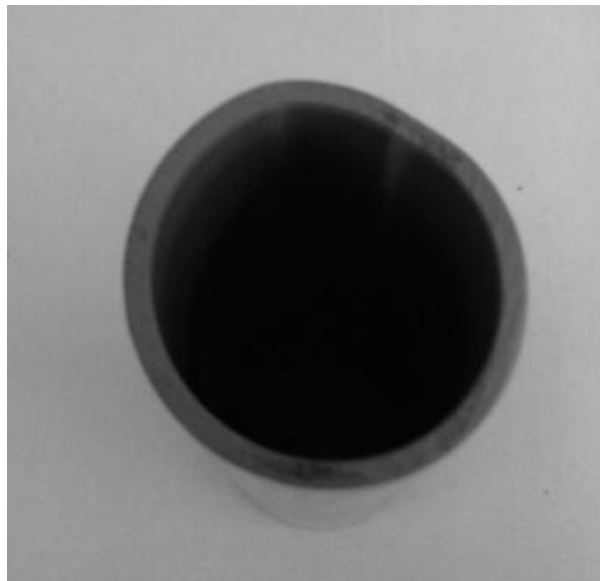


Figure 91: Deformed tube

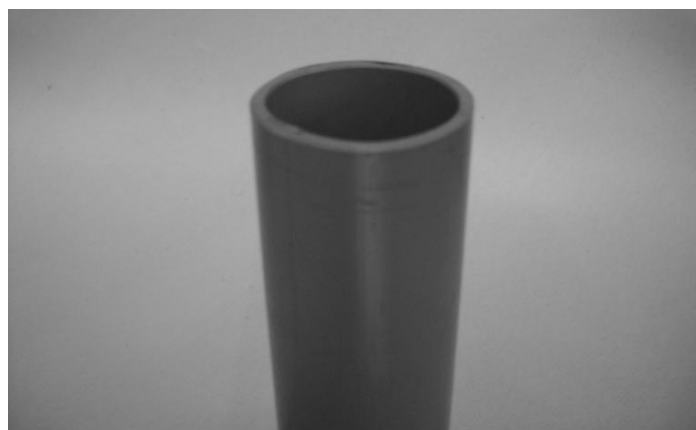


Figure 92: Plastic deformation (white part) of the PVC tube

A solution was found in applying PVC tubes with a larger wall thickness. With the enlarged wall thickness, the stiffness of the tube increased. In this way, a larger load on the tube could be applied.

The bridge

After using the new tube, the bridge on the clamp appeared to be not stiff enough to transfer the applied force in a uniform way. The bridge is attached to the clamp by two bolts on both ends of the bridge. It appeared that the force was transferred properly on the sides on the bridge. However, due to the lack of stiffness, the bridge deformed into an arch shape. This resulted in a release of pressure of the tube on the fabric on the middle part of the bridge. When stressing the fabric, slip occurred in the middle part of the bridge. This was noticeable by the deformation on a straight line that was drawn on the fabric, see Figure 40.

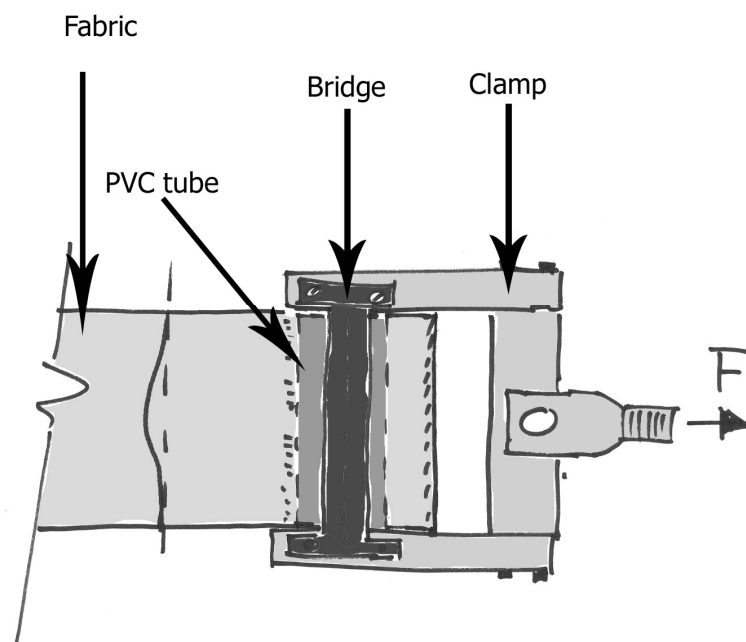


Figure 93: Deformation of the straight line indicates fabric slip

Reverse configuration of the fabric

The fabric was acting in such a way, that the reaction force of the fabric on the tube resulted in a release of clamping pressure. By reversing the configuration of the fabric, the opposite result was achieved. An increasing tension force in the fabric resulted on an increased clamping force. Slip still occurred on the middle part of the fabric.

In addition to the slip, the clamp was forced upwards by the fabric. Normally the clamp is pushed downwards on the supporting table. When reversing the fabric configuration the clamp is pushed upwards. This is an unwanted effect.

Improved bridge

The fabric configuration was then returned to the original setting. In order to achieve a uniform stress introduction, a stiffer bridge was needed. By adding a steel strip on the bridge, additional stiffness was achieved. In this way, the pressure from the bridge could be transferred uniformly to the PVC tube. No slip occurred after this improvement.



Figure 94: Improved bridge with increased stiffness

Potentiometer placement

The potentiometers are equipped with a pointed screw, which is driven just into the fabric to ensure its position. A magnet on the bottom side of the fabric pulls the potentiometer down onto the fabric. The pointed screw pushes the fibres away to make room for the point. However, after tensioning the fabric the fibres tend to push the tapered point upwards and out of the fabric.



Figure 95: Screw with pointed end

A solution is found by using medical needles with a diameter of 0,3mm. Small holes are drilled in the screw, in order to be able to glue the injection needles in place. The needle pierces the fabric, but it is assumed that the needle does not harm any of the fibres. The needle is small enough not to get forced out of the fabric.



Figure 96: Screw with a medical needle

The total view of a potentiometer equipped with the improved screw is shown in Figure 44. The needle is supposed to be driven through the fabric.

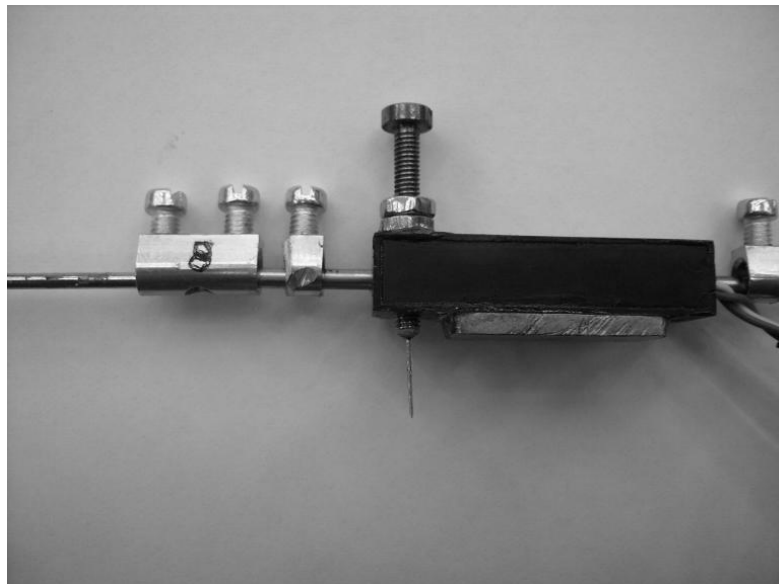


Figure 97: Potentiometer equipped with improved screw

C1 Usermat

```
*deck,usermat parallel user gal
subroutine usermat(
& matId, elemId,kDomIntPt, kLayer, kSectPt,
& ldstep,isubst,keycut,
& nDirect,nShear,ncomp,nStatev,nProp,
& Time,dTime,Temp,dTemp,
& stress,statev,dsdePl, sedEl, sedPl,epseq,
& Strain,dStrain, epsPl, prop
& )

#include "impcom.inc"

INTEGER
& matId, elemId,
& kDomIntPt, kLayer, kSectPt,
& ldstep,isubst,keycut,
& nDirect,nShear,ncomp,nStatev,nProp

DOUBLE PRECISION
& Time, dTime, Temp, dTemp,
& sedEl, sedPl, epseq, epsZZ
DOUBLE PRECISION
& stress (ncomp ), statev (nStatev),
& dsdePl (ncomp,ncomp),
& Strain (ncomp ), dStrain (ncomp ),
& epsPl (ncomp ), prop (nProp )

DOUBLE PRECISION E, G, d, s, epsxx, epsyy, gxy,
& epsxxp, epsyyp, a, Ad, sx, sy, w,
R,
& ax, ay, Tx, Ty, Nx,
Ny,factor,incr,
& nxxp,nyyp,nxyp,nxx,nyy,nxy,epsxxinc,
& epsyyinc

INTEGER i, j
DOUBLE PRECISION twoG,
& young, posn,
& c1, c2, c3,c4, c5

c *** get Young's modulus and Poisson's ratio, initial yield stress
and slope of stress-strain
young = prop(1)
posn = prop(2)
twoG = young / (1.d0+posn)
ncomp = 3
factor = prop(3)

c ***Initialisatie van de routine variabelen
E=young
G=500d0
d=prop(5)
s=prop(6)
```

```

        epsxx=Strain(1)+dStrain(1)
        epsyy=Strain(2)+dStrain(2)
        gxy=Strain(3)+dStrain(3)
        epsxxp=0
        epsyyp=0
        incr=0.1d0
c        epsxxp=prop(3)
c        epsyyp=prop(4)

c ***computation
        a=sqrt(s**2+d**2)
        Ad=0.25d0*3.1415d0*(d**2)
        sx=s*(1.0d0+epsxx+epsxxp)
        sy=s*(1.0d0+epsyy+epsyyp)
        w=0
        R=100.0d0
        do while (abs(R) .gt. 0.0001d0*a*d)
            ax=sqrt(sx**2+(d-w)**2)
            ay=sqrt(sy**2+(d+w)**2)
            Tx=(ax/a-1.0d0)
            Ty=(ay/a-1.0d0)
c            if (Tx<0) Tx=0
c            if (Ty<0) Ty=0
            R=(Tx*ay*(d-w))-Ty*ax*(d+w)
        w=w+R/a
        end do

        Tx=young*Ad*Tx
        Ty=young*Ad*Ty
        Nx=(sx*Tx/ax)
        Ny=(sy*Ty/ay)

        nxxp=Nx/s
        nyyp=Ny/s
        nxyp=G*Strain(3)

c ****Computation of considered point with additional strain
increment in x
c ****Add small increment in x direction
        epsxxinc=epsxx+incr

        a=sqrt(s**2+d**2)
        Ad=0.25d0*3.1415d0*(d**2)
        sx=s*(1.0d0+epsxxinc+epsxxp)
        sy=s*(1.0d0+epsyy+epsyyp)
        w=0
        R=100.0d0
        do while (abs(R) .gt. 0.0001d0*a*d)
            ax=sqrt(sx**2+(d-w)**2)
            ay=sqrt(sy**2+(d+w)**2)
            Tx=(ax/a-1.0d0)
            Ty=(ay/a-1.0d0)
c            if (Tx<0) Tx=0
c            if (Ty<0) Ty=0
            R=(Tx*ay*(d-w))-Ty*ax*(d+w)
        w=w+R/a
        end do
        Tx=young*Ad*Tx
        Ty=young*Ad*Ty

```

```

        Nx=(sx*Tx/ax)
        Ny=(sy*Ty/ay)

nxx=Nx/s
nyy=Ny/s
nxy=G*Strain(3)

dsdePl(1,1)=(nxx-nxxp)/incr
dsdePl(2,1)=(nyy-nyyp)/incr
dsdePl(3,1)=0

c ****Restore the original epsxx and add increment to epsyy
epsyyinc=epsyy+incr

a=sqrt(s**2+d**2)
Ad=0.25d0*3.1415d0*(d**2)
sx=s*(1.0d0+epsxx+epsxxp)
sy=s*(1.0d0+epsyyinc+epsyypp)
w=0
R=100.0d0
do while (abs(R) .gt. 0.0001d0*a*d)
    ax=sqrt(sx**2+(d-w)**2)
    ay=sqrt(sy**2+(d+w)**2)
    Tx=(ax/a-1.0d0)
    Ty=(ay/a-1.0d0)
c     if (Tx<0) Tx=0
c     if (Ty<0) Ty=0
    R=(Tx*ay*(d-w))-Ty*ax*(d+w)
w=w+R/a
end do
Tx=young*Ad*Tx
Ty=young*Ad*Ty
Nx=(sx*Tx/ax)
Ny=(sy*Ty/ay)

nxx=Nx/s
nyy=Ny/s
nxy=G*Strain(3)

dsdePl(1,2)=(nxx-nxxp)/incr
dsdePl(2,2)=(nyy-nyyp)/incr
dsdePl(3,2)=0
dsdePl(2,1)=dsdePl(1,2)
dsdePl(1,3)=0
dsdePl(2,3)=0
dsdePl(3,3)=500

c vul de stress vector met nieuwe waarden
stress(1)=nxxp+3.302
stress(2)=nyyp+2.948
stress(3)=G*Strain(3)

return
end

```

C2 Determination of model factor

Fabric ID	Ratio	warp strain error	weft strain error	Experimental	Experimental	Model	Model	phi warp error	phi weft error
				warp stress error	weft stress error	warp stress error	weft stress error		
Fabric 2	1:1								
	1:1								
	1:2	-0,62%	0,85%	6,01	9,29	6,22	7,35	1,0	1,3
	1:2	-1,13%	1,52%	10,64	20,17	8,50	13,59	1,3	1,5
	2:1	0,88%	-0,67%	9,79	5,90	7,69	5,80	1,3	1,0
	2:1	1,90%	-1,35%	30,43	15,42	18,91	9,55	1,6	1,6
	1:5	-0,80%	0,69%	3,80	8,37	3,67	3,52	1,0	2,4
	1:5	-2,10%	1,55%	4,75	18,46	4,92	7,80	1,0	2,4
	5:1	1,75%	-1,76%	10,61	3,86	13,76	6,84	0,8	0,6
	5:1	3,11%	-3,97%	30,13	6,34	31,80	5,84	0,9	1,1
	0:1	-1,50%	2,09%	2,92	6,72	10,32	20,99	0,3	0,3
	0:1	-4,50%	3,78%	1,62	18,37	5,79	44,28	0,3	0,4
	1:0	1,90%	-2,75%	12,83	2,24	11,42	4,87	1,1	0,5
	1:0	3,20%	-6,27%	29,60	0,94	32,54	1,86	0,9	0,5

Fabric ID	Ratio	warp strain	weft strain	Experimental	Experimental	Model	Model	phi warp	phi weft
				warp stress	weft stress	warp stress	weft stress		
Fabric 3	1:1								
	1:1								
	1:2	0,39%	0,28%	16,81	16,69	10,00	9,46	1,7	1,8
	1:1	0,64%	0,49%	27,18	27,30	14,65	13,88	1,9	2,0
	1:2	-1,10%	1,39%	8,23	14,59	7,72	11,69	1,1	1,2
	1:2	-1,44%	2,00%	13,71	27,45	10,07	19,75	1,4	1,4
	2:1	1,21%	-0,84%	12,94	7,37	11,18	7,45	1,2	1,0
	2:1	1,87%	-1,25%	26,21	13,47	19,03	9,87	1,4	1,4
	1:5	-1,47%	1,18%	4,25	13,09	4,48	5,52	0,9	2,4
	1:5	-2,71%	1,93%	5,48	26,80	5,44	11,82	1,0	2,3
	5:1	2,03%	-2,15%	12,71	4,16	16,70	7,03	0,8	0,6
	5:1	2,95%	-3,56%	25,50	5,78	29,43	6,49	0,9	0,9
	0:1	-3,77%	3,77%	2,12	13,98	7,93	45,10	0,3	0,3
	0:1	-6,34%	4,67%	0,44	29,19	1,10	62,16	0,4	0,5
	1:0	1,93%	-2,73%	12,91	2,24	12,08	5,04	1,1	0,4
	1:0	3,06%	-5,68%	26,18	1,18	29,44	2,75	0,9	0,4

Fabric ID	Ratio	warp strain	weft strain	Experimental	Experimental	Model	Model	phi warp	phi weft
				warp stress	weft stress	warp stress	weft stress		
Fabric 4	1:1								
	1:1								
	1:2	0,19%	0,11%	10,64	10,50	6,29	5,87	1,7	1,8
	1:1	0,52%	0,35%	24,44	24,56	12,07	11,34	2,0	2,2
	1:2	-1,19%	1,61%	10,82	20,76	8,81	14,67	1,2	1,4
	1:2	-1,31%	1,85%	13,68	27,48	9,79	17,95	1,4	1,5
	2:1	1,10%	-0,85%	11,94	6,96	9,42	6,52	1,3	1,1
	2:1	1,88%	-1,37%	27,56	14,18	37,07	33,40	0,7	0,4
	1:5	-1,40%	1,07%	4,19	12,80	3,93	4,25	1,1	3,0
	1:5	-2,69%	1,84%	5,57	27,95	5,08	10,18	1,1	2,7
	5:1	2,25%	-2,24%	14,03	4,33	20,37	7,81	0,7	0,6
	5:1	3,13%	-3,68%	27,00	5,99	32,76	6,59	0,8	0,9
	0:1	-2,48%	2,73%	2,59	9,26	9,38	28,13	0,3	0,3
	0:1	-5,68%	4,04%	0,91	25,21	2,97	49,07	0,3	0,5
	1:0	2,28%	-3,54%	16,07	2,00	16,11	4,83	1,0	0,4
	1:0	3,00%	-5,47%	25,74	1,24	28,20	3,04	0,9	0,4

Fabric ID	Ratio	warp strain	weft strain	Experimental	Experimental	Model	Model	phi warp	phi weft
				warp stress	weft stress	warp stress	weft stress		
Fabric 5	1:1								
	1:1								
	1:2	0,16%	0,09%	9,29	9,08	5,79	5,39	1,6	1,7
	1:1	0,54%	0,36%	23,91	23,97	12,39	11,62	1,9	2,1
	1:2	-0,70%	0,93%	6,28	10,02	6,38	7,80	1,0	1,3
	1:2	-1,28%	1,83%	13,89	27,89	9,81	17,79	1,4	1,6
	2:1	0,92%	-0,66%	10,32	6,19	8,35	6,20	1,2	1,0
	2:1	1,62%	-1,13%	22,08	11,65	15,60	8,84	1,4	1,3
	1:5	-1,01%	0,87%	3,95	10,20	4,08	4,29	1,0	2,4
	1:5	-2,43%	1,77%	5,22	23,97	5,30	10,08	1,0	2,4
	5:1	1,40%	-1,31%	8,79	3,66	10,68	6,40	0,8	0,6
	5:1	2,78%	-3,32%	23,14	5,48	26,65	6,66	0,9	0,8
	0:1	-2,61%	2,92%	2,54	9,85	9,63	31,32	0,3	0,3
	0:1	-5,46%	4,07%	1,06	23,73	3,49	49,67	0,3	0,5
	1:0	1,32%	-1,58%	9,35	2,51	7,43	4,72	1,3	0,5
	1:0	3,10%	-5,73%	26,33	1,18	30,26	2,67	0,9	0,4

Fabric ID	Ratio	warp strain	weft strain	Experimental	Experimental	Model	Model	phi warp	phi weft
				warp stress	weft stress	warp stress	weft stress		
Fabric 6	1:1								
	1:1								
	1:2	0,34%	0,08%	11,23	11,06	7,63	6,98	1,5	1,6
	1:1	0,69%	0,28%	22,88	22,94	13,45	12,09	1,7	1,9
	1:2	-1,03%	1,44%	8,67	15,57	8,46	13,01	1,0	1,2
	1:2	-1,39%	1,99%	13,92	27,98	10,26	19,88	1,4	1,4
	2:1	0,96%	-0,67%	9,88	6,01	8,84	6,48	1,1	0,9
	2:1	1,54%	-1,08%	18,55	9,99	14,63	8,55	1,3	1,2
	1:5	-1,19%	0,96%	4,04	11,23	3,95	4,16	1,0	2,7
	1:5	-2,60%	1,84%	5,42	26,24	5,26	10,59	1,0	2,5
	5:1	1,39%	-1,36%	8,76	3,69	10,16	6,10	0,9	0,6
	5:1	2,74%	-3,23%	23,03	5,48	26,11	6,77	0,9	0,8
	0:1	-2,61%	3,13%	2,54	9,79	10,37	35,40	0,2	0,3
	0:1	-5,35%	4,38%	1,09	23,23	3,81	56,01	0,3	0,4
	1:0	1,12%	-1,35%	8,73	2,57	5,79	4,16	1,5	0,6
	1:0	2,43%	-3,91%	17,54	1,89	18,22	4,64	1,0	0,4

Fabric ID	Ratio	warp strain	weft strain	Experimental	Experimental	Model	Model	phi warp	phi weft
				warp stress	weft stress	warp stress	weft stress		
Fabric 7	1:1								
	1:1								
	1:2	0,11%	0,09%	8,20	8,02	5,28	4,91	1,6	1,6
	1:1	0,37%	0,29%	17,60	17,60	9,87	9,38	1,8	1,9
	1:2	-0,62%	0,88%	5,81	8,99	6,48	7,77	0,9	1,2
	1:2	-1,23%	1,72%	11,59	22,53	9,35	16,25	1,2	1,4
	2:1	0,79%	-0,54%	8,85	5,57	7,57	5,89	1,2	0,9
	2:1	1,83%	-1,18%	26,12	13,50	18,80	9,99	1,4	1,4
	1:5	-0,90%	0,74%	3,86	9,41	3,54	3,34	1,1	2,8
	1:5	-2,48%	1,80%	5,34	25,50	5,33	10,40	1,0	2,5
	5:1	0,60%	-0,47%	5,19	3,73	5,66	4,69	0,9	0,8
	5:1	2,40%	-2,61%	17,04	4,78	21,61	7,29	0,8	0,7
	0:1	-1,85%	2,42%	2,80	7,58	10,50	25,08	0,3	0,3
	0:1	-4,58%	3,95%	1,53	19,02	5,73	47,65	0,3	0,4
	1:0	1,45%	-1,71%	9,70	2,54	8,79	5,14	1,1	0,5
	1:0	2,74%	-4,48%	20,49	1,17	23,54	4,30	0,9	0,3

mean 1,03 1,18
st dev 0,42 0,75

C3 CD Rom contents

A CD Rom is included. This cd contains the following information

- Results from the experiments
- Processed data from experiments
- Pictures taken during experiments
- Interesting topic related articles
- Scans from notes taken during experiments
- Ansys files from sample analysis
- Ansys documentation on UPF's
- Ansys documentation on USERMAT
- Ansys files containing test cases
- This report in PDF